

STATUS OF THESIS

Title of thesis

Modelling of Biomass Gasification for Hydrogen Production Using Computational Fluid Dynamics (CFD)

I ATHIRAH BINTI MOHD TAMIDI

hereby allow my thesis to be placed at the Information Resource Center (IRC) of Universiti Teknologi PETRONAS (UTP) with the following conditions:

1. The thesis becomes the property of UTP
2. The IRC of UTP may make copies of the thesis for academic purposes only.
3. This thesis is classified as

Confidential

Non-confidential

If this thesis is confidential, please state the reason:

The contents of the thesis will remain confidential for _____ years.

Remarks on disclosure:

Endorsed by

Signature of Author

Signature of Supervisor

Permanent address:

24, Jalan Bukit 1,
Kampung Tersusun Bukit Jana,
34600 Kamunting, Perak.

Name of Supervisor

Dr. Ku Zilati Ku Shaari

Date : _____

Date : _____

UNIVERSITI TEKNOLOGI PETRONAS

MODELLING OF BIOMASS GASIFICATION FOR HYDROGEN PRODUCTION
USING COMPUTATIONAL FLUID DYNAMICS (CFD)

by

ATHIRAH BINTI MOHD TAMIDI

The undersigned certify that they have read, and recommend to the Postgraduate Studies Programme for acceptance this thesis for the fulfilment of the requirements for the degree stated.

Signature:

Main Supervisor:

DR. KU ZILATI KU SHAARI

Signature:

Co-Supervisor:

DR. LAU KOK KEONG

Signature:

Head of Department:

ASSOC. PROF. DR. SHUHAIMI MAHADZIR

Date:

MODELLING OF BIOMASS GASIFICATION FOR HYDROGEN PRODUCTION
USING COMPUTATIONAL FLUID DYNAMICS (CFD)

by

ATHIRAH BINTI MOHD TAMIDI

A Thesis

Submitted to the Postgraduate Studies Programme

as a Requirement for the Degree of

MASTER OF SCIENCE

IN CHEMICAL ENGINEERING

UNIVERSITI TEKNOLOGI PETRONAS

BANDAR SERI ISKANDAR

PERAK

AUGUST 2011

DECLARATION OF THESIS

Title of thesis

Modelling of Biomass Gasification for Hydrogen Production Using Computational Fluid Dynamics (CFD)

I ATHIRAH BINTI MOHD TAMIDI

hereby declare that the thesis is based on my original work except for quotations and citations which have been duly acknowledged. I also declare that it has not been previously or concurrently submitted for any other degree at UTP or other institutions.

Witnessed by

Signature of Author

Signature of Supervisor

Permanent address:

24, Jalan Bukit 1,
Kampung Tersusun Bukit Jana,
34600 Kamunting,
Perak.

Name of Supervisor

Dr. Ku Zilati Ku Shaari

Date : _____

Date : _____

ACKNOWLEDGEMENTS

First and foremost, thank you Allah the Almighty, for without his consent, it would be impossible for me to achieve what had been done in this work. Special gratitude and deepest appreciation I would like to dedicate to my wonderful supervisor, Dr. Ku Zilati Ku Shaari for all her dedication, guidance, encouragement and continuous support throughout this research. Without her, I might not be able to complete the entire work successfully. Without doubt she is a great teacher, a caring mother and a close friend of mine. To my co-supervisor, Dr. Lau Kok Keong, your kind support and thoughtful ideas gave me extra motivation to move forward. I'm very thankful to have both of you as my coach in completing my study.

Not forgotten my beloved family who endlessly cared and support me in every ups and downs that I faced during the completion of this work. Thank you for being understanding and for all the sacrifices and love that they gave me all the time without fail. Keeping the thoughts of them in my mind all the time keeps me pursuing my work no matter how many times I should fell. May all the kindness will be blessed by Allah in life and hereafter.

To all my lovely friends especially those in the Biohydrogen team, thank you for your endless guidance, support and thoughts towards the completion of this research. Without you guys, the world would be too lonely and gloomy especially at the isolated Block P Biohydrogen Office and Lab. I will really miss you guys.

And last but not least, special thanks to all the supporting Biohydrogen team members that work their heart out to ensure the research run smoothly and completed as scheduled. Thank you all from the deepest of my heart.

ABSTRACT

Biomass steam gasification process has emerged as a clean and efficient way of producing H₂. However, experimental study of biomass gasification is costly and dangerous to human being. Simulation and modelling approach is expected to be more cost saving, safe and easy to scale up in order to study the biomass gasification process. In this work, computational fluid dynamic (CFD) approach using the commercial CFD software, ANSYS Fluent[®] V6.3 has been utilized in order to study the hydrodynamics and the gasification reactions in the fluidized bed gasifier.

The overall research objective of this work is to obtain the optimum condition for biomass steam gasification process. For this, a hydrodynamics and a steady state reaction models were developed and validated with literature data. The hydrodynamics model was developed in order study the effect of steam inlet velocity, solid particle size and bed height to diameter ratio to the solid fluidization in the fluidized bed gasifier using Eulerian-Eulerian multiphase model coupled with kinetic theory granular flow approach. The reaction model was developed using volumetric reaction model approach in order to predict the H₂ production from the gasifier. The reaction model was used to predict the effect of reaction parameters such as gasification temperature, steam to biomass ratio and adsorbent to biomass ratio to the production of H₂ from biomass gasification process. The findings from the developed hydrodynamics and reaction model were compared with experimental and simulation data from literature and were found to be in good agreement.

Based on the results obtained from the hydrodynamics simulation, steam inlet velocity of 3-3.5 U_{mf} , 250 μm particle size and bed height to diameter ratio of 3 and below are the optimum conditions that gives the best solid fluidization and mixing in the gasifier. From the reaction model, gasification temperature of 850 °C and steam to biomass ratio of 2 gives the highest concentration and yield of H_2 which are 48 mol% and 94.75 g H_2/kg biomass respectively. The addition of CO_2 adsorbent in the gasifier highly improves the H_2 production from the gasifier. At adsorbent to biomass ratio of 1 and at gasification temperature as low as 600-750 °C, high concentration and yield of H_2 could be obtained from the gasifier which are 47 mol% and 195.3 g H_2/kg biomass respectively.

ABSTRAK

Proses gasifikasi biojisim berstim telah muncul sebagai cara yang bersih dan berkesan untuk menghasilkan H_2 . Namun, kajian eksperimen gasifikasi biojisim adalah mahal dan berbahaya untuk manusia. Penggunaan simulasi dan model matematik didapati dapat menjimatkan kos, disamping selamat dan mudah untuk diskala semula bagi mempelajari dan memahami dengan lebih mendalam proses gasifikasi biojisim. Untuk projek ini, kaedah pengkomputeran bendalir dinamik (computational fluid dynamic) menggunakan perisian komersil, ANSYS Fluent[®] V6.3 telah digunakan untuk mengkaji fenomena hidrodinamik dan tindak balas kimia yang berlaku semasa proses gasifikasi di dalam reaktor fluidisasi.

Objektif utama bagi projek ini adalah untuk mendapatkan keadaan paling optimum untuk proses gasifikasi biojisim berstim. Untuk itu, model hidrodinamik dan model tindak balas kimia telah dirangkakan dan dibuktikan dengan data dari kajian-kajian yang telah diterbitkan. Model hidrodinamik yang telah dibuktikan digunakan untuk mengkaji pengaruh kelajuan stim, saiz zarah pepejal dan nisbah tinggi kepada diameter reaktor kepada proses fluidisasi pepejal di dalam reaktor menggunakan model multi-fasa "Eulerian-Eulerian" yang digabungkan dengan teori kinetik aliran granular. Model tindak balas kimia yang telah dirangkakan menggunakan pendekatan model volumetrik digunakan untuk menganggarkan penghasilan H_2 dari proses gasifikasi tersebut. Model tindak balas kimia juga digunakan untuk mengkaji pengaruh keadaan tindak balas seperti suhu gasifikasi, nisbah stim kepada biojisim dan nisbah adsorben kepada biojisim kepada penghasilan H_2 daripada proses gasifikasi biojisim. Penemuan dari model hidrodinamik dan model tindak balas kimia ini telah dibandingkan dengan data eksperimen dan simulasi dari kajian-kajian yang telah diterbitkan dan didapati menunjukkan ada persamaan.

Berdasarkan keputusan yang diperoleh daripada simulasi hidrodinamik, kelajuan stim pada $3-3,5 U_{mf}$, $250 \mu\text{m}$ saiz zarah pepejal dan nisbah tinggi kepada diameter besamaam dengan 3 dan ke bawah adalah kondisi-kondisi optimum yang memberikan fluidisasi dan percampuran terbaik di dalam reaktor. Dari model tindak balas kimia, suhu gasifikasi pada $850 \text{ }^\circ\text{C}$ dan nisbah stim kepada biojisim bersamaan dengan 2 memberikan kepekatan dan penghasilan H_2 yang tertinggi iaitu 48 mol% dan 94.75 g H_2/kg biojisim. Penambahan CO_2 adsorben ke dalam reaktor sangat membantu dalam meningkatkan penghasilan H_2 dari reaktor tersebut. Pada nisbah adsorben kepada biojisim bersamaan dengan 1 dan gasifikasi pada suhu serendah $600-750 \text{ }^\circ\text{C}$, kepekatan dan penghasilah H_2 yang tinggi boleh diperolehi iaitu 47 mol% dan 195.3 g H_2/kg biojisim.

In compliance with the terms of the Copyright Act 1987 and the IP Policy of the university, the copyright of this thesis has been reassigned by the author to the legal entity of the university,

Institute of Technology PETRONAS Sdn Bhd.

Due acknowledgement shall always be made of the use of any material contained in, or derived from, this thesis.

© Athirah Binti Mohd Tamidi, 2011
Institute of Technology PETRONAS Sdn Bhd
All rights reserved.

TABLE OF CONTENTS

APPROVAL PAGE	ii
TITLE PAGE	iii
ACKNOWLEDGEMENTS	v
ABSTRACT	vi
ABSTRAK	viii
COPYRIGHT PAGE	x
LIST OF FIGURES	xiii
LIST OF TABLES	xvi
LIST OF ABBREVIATION	xvii
LIST OF NOMENCLATURE	xviii
CHAPTER 1	1
1.1 BACKGROUND.....	1
1.1.1 Hydrogen from Biomass	1
1.1.2 Biomass Gasification Technologies.....	2
1.1.3 Fluidized Bed Gasifier	5
1.1.4 In-situ CO ₂ adsorption	8
1.1.5 Computational Fluid Dynamic.....	9
1.1.6 Biomass Gasification Modelling Approach.....	10
1.2 PROBLEM STATEMENT	11
1.3 OBJECTIVES OF RESEARCH.....	12
1.4 SCOPE OF RESEARCH	13
CHAPTER 2	15
2.1 HISTORY OF BIOMASS GASIFICATION	15
2.2 BIOMASS GASIFICATION STUDY: EXPERIMENTAL APPROACH.....	18
2.2.1 Hydrodynamics Study.....	18
2.2.2 Reaction Study	21
2.3 BIOMASS GASIFICATION STUDY: MODELLING APPROACH.....	29
2.3.1 Hydrodynamics Study.....	29
2.3.2 Reaction Study	33
CHAPTER 3	39
3.1 COMPUTATIONAL DOMAIN FOR FLUIDIZED BED GASIFIER	39
3.2 GRID GENERATION STUDY.....	41
3.3 HYDRODYNAMICS MODEL DEVELOPMENT AND VALIDATION	43
3.3.1 Minimum fluidization velocity	44
3.3.2 Modelling multiphase flow	45
3.3.3 Hydrodynamics Model Validation.....	49

3.3.4	Hydrodynamics model variables and simulation parameters	50
3.4	REACTION MODEL DEVELOPMENT AND VALIDATION.....	52
3.4.1	Modelling reacting flow.....	52
3.4.2	Modelling Species Transport and Finite-Rate Chemistry.....	56
3.4.3	Defining mixture components and its physical properties.....	60
3.4.4	Defining Reactions.....	61
3.4.5	Reaction model validation	62
3.4.6	Reaction model variables	63
CHAPTER 4	65
4.1	GRID GENERATION STUDY.....	65
4.2	HYDRODYNAMICS MODEL.....	66
4.2.1	Model validation	66
4.2.2	Effect of steam inlet velocity	70
4.2.3	Effect of particle size	75
4.2.4	Effect of height to diameter ratio (H/D)	80
4.3	REACTION MODEL	85
4.3.1	Model validation	85
4.3.2	Effect of reaction temperature	86
4.3.3	Effect of steam to biomass ratio (S/B).....	89
4.3.4	Effect of CO ₂ adsorbent	92
CHAPTER 5	95
5.1	CONCLUSION.....	95
5.2	RECOMMENDATION AND FUTURE WORK	97
REFERENCES	99

LIST OF FIGURES

Figure 1.1: Source of H ₂ production [1, 4]	2
Figure 1.2: Example of biomass	3
Figure 1.3: Types of gasification methods [16]	4
Figure 1.4: Typical Fluidized bed gasifier	6
Figure 1.5: CO ₂ adsorption process by CaO	8
Figure 2.1: Main application of gasification [43]	15
Figure 2.2: Progress of mixing and segregation with the gas velocity [56]	20
Figure 2.3: Effect of gas flow rate on bubble dynamics [23]	20
Figure 2.4: Product gas composition vs. gasification temperature for biomass steam gasification [17]	26
Figure 2.5: Effect of steam to biomass ratio (S/B) on gas composition [61].....	27
Figure 2.6: Effect of Adsorbent to Biomass ratio on product gas composition [62]...	29
Figure 2.7: Multiphase fluid system	30
Figure 2.8: Effect of operating temperature on product gas composition from simulation of biomass air-gasification [36]	37
Figure 2.9: Effect of gasifier temperature on (a) product gas composition (b) H ₂ yield from biomass steam gasification [14]	37
Figure 2.10: Contour of concentration distribution of species in fluidized bed reactor [38].....	38
Figure 3.1: 3D domain of a fluidized bed gasifier	40
Figure 3.2: 2D Axissymmetry plane from the 3D domain	40
Figure 3.3: 2D grid of fluidized bed gasifier	42
Figure 3.4: Flow regions in fluidized bed [20]	43
Figure 3.5: Domain dimension for model validation.....	49
Figure 3.6: Location of solid concentration analysis	51
Figure 3.7 : Reacting particle in particle surface reaction model	54
Figure 4.1 : Flow velocity magnitude for different mesh sizes	66
Figure 4.2 : Contours for solid volume fraction at $U=1.7U_{mf}$; (a) Result obtained from simulation; (b) Result from Busciglio et al., 2009 [30]	68

Figure 4.3 : Comparison of simulation result from Fluent with experimental data and CFX model from Busciglio et al. [30]	69
Figure 4.4: Comparison of instantaneous bed height of 3.4Umf obtained from simulation with other result from literature [30].....	70
Figure 4.5: Contour of solid volume fraction at 3Umf (Case 1).....	71
Figure 4.6: Contour of solid volume fraction at 3.5Umf (Case 2).....	71
Figure 4.7: Contour of solid volume fraction at 4Umf (Case 3).....	72
Figure 4.8: Contour of solid volume fraction at 5Umf (Case 4).....	72
Figure 4.9: Time-weighted average of solid concentration at different steam inlet velocity.....	73
Figure 4.10: Solid concentration profile for different steam inlet velocity	74
Figure 4.11: Contour of solid volume fraction for particle size of 100 μ m (Case 8) ...	75
Figure 4.12: Contour of solid volume fraction for particle size of 250 μ m (Case 2) ...	76
Figure 4.13: Contour of solid volume fraction for particle size of 300 μ m (Case 9) ...	76
Figure 4.14: Contour of solid volume fraction for particle size of 400 μ m (Case 10) .	77
Figure 4.15: Time-weighted average of solid concentration for different particle sizes	77
Figure 4.16: Concentration profile for different particle sizes	79
Figure 4.17: Contour of solid volume fraction for H/D of 2 (Case 2)	80
Figure 4.18: Contour of solid volume fraction for H/D of 3 (Case 5)	81
Figure 4.19: Contour of solid volume fraction for H/D of 4 (Case 6)	81
Figure 4.20: Contour of solid volume fraction for H/D of 5 (Case 7)	82
Figure 4.21: Time-weighted average of solid concentration for different H/D	82
Figure 4.22: Concentration profile for different (H/D).....	84
Figure 4.23: Comparison of H ₂ mol% predicted by model with literature data at 800°C	85
Figure 4.24: Effect of reaction temperature on H ₂ production from biomass gasification.....	86
Figure 4.25: Effect of gasification temperature on product gas composition.....	87
Figure 4.26: Effect of gasification temperature on H ₂ yield.....	88
Figure 4.27: Effect of S/B on product gas composition.....	90
Figure 4.28: Effect of steam to biomass ratio on carbon conversion*	90
Figure 4.29: Effect of steam to biomass ratio on H ₂ yield.....	91

Figure 4.30: Effect of adsorbent to biomass ratio (A/B) on product gas composition	93
Figure 4.31: H ₂ concentration from biomass gasification with and without CO ₂ adsorbent	93
Figure 4.32: Effect of CO ₂ adsorbent on H ₂ yield	94

LIST OF TABLES

Table 1.1: Types of fluidized bed gasifier [8].....	6
Table 1.2: Main Biomass Gasification Reactions.....	7
Table 2.1: Summary of recent experimental study on hydrodynamics	19
Table 2.2: Summary of experimental study on biomass gasification reaction	22
Table 2.3: Summary of hydrodynamics modelling using E-E model and KTGF	32
Table 2.4: Summary of reaction study using modelling approach	34
Table 3.1: Number of cells for each grid size.....	42
Table 3.2: Equation for U_{mf} calculation.....	44
Table 3.3: Multiphase model for Eulerian-Eulerian approach [32].....	45
Table 3.4: Simulation Parameters for model validation	49
Table 3.5: Hydrodynamics model case studies.....	50
Table 3.6 : Simulation Parameters for Biomass Gasifier.....	51
Table 3.7: Chemical Reactions	53
Table 3.8 : Generalized finite-rate model	53
Table 3.9 : Particle surface reaction model.....	55
Table 3.10: Main Biomass Gasification Reactions.....	61
Table 3.11: Kinetic data for reaction model	62
Table 3.12 : Simulation parameters for model validation.....	63
Table 3.13 : Case studies for reaction model.....	63
Table 3.14 : Variable values for in-situ CO_2 adsorption.....	64
Table 4.1: Comparison of simulated H_2 yield with literature data at 850 °C	89

LIST OF ABBREVIATION

A/B	Adsorbent to Biomass Ratio
AER	Adsorbent Enhanced Reforming
CFD	Computational Fluid Dynamic
E-E	Eulerian-Eulerian
E-L	Eulerian-Lagrangian
ER	Equivalence Ratio
H/D	Bed Height to Diameter Ratio
HHV	High Heating Value
KTGF	Kinetic Theory of Granular Flow
MHV	Medium Heating Value
S/B	Steam to Biomass Ratio
VOF	Volume of Fluid

LIST OF NOMENCLATURE

Letter

$\vec{\Gamma}$	Interphase momentum change
$\vec{J}_{i/j}$	Diffusion flux of species i/j
$\hat{R}_{i,r}$	Arrhenius molar rate of creation/destruction of species i in reaction r
$\overline{\overline{S}}$	Stress-strain tensor
$\vec{k}_{b,r/f,r}$	Backward or forward rate constant for reaction r
\vec{s}'	Unit vector in the direction of the incident radiation
h_j^0	Enthalpy of formation of species j
A_r	Pre-exponential factor (constant)
C_d	Drag coefficient
$C_{j,r}$	Molar concentration of species j in reaction r
$D_{i,m}$	Diffusion coefficient for species i in the mixture
E_r	Activation energy for the reaction
\vec{F}	External body force
M_i	Symbol denoting species i
$M_{w,i}$	Molecular weight of species i
R_i	Net rate of production of species i by chemical reaction
R_j	Volumetric rate of creation of species j
S_h	Heat of chemical reaction
S_i	Rate of creation by addition from the dispersed phase plus any user-define sources
S_m	Source term
T_{ref}	Reference temperature : 298.15K
$Y_{i/j}$	Mass fraction of species i/j
d_p	Particle diameter (m)

e	Coefficient of restitution for particle collision
\vec{g}	Gravitational force (m/s^2)
\vec{g}	Gravitational force (m/s^2)
g_0	Radial distribution function
k_{eff}	Effective conductivity
k_r	Radiative conductivity
$k_{\theta i}$	Diffusion coefficient
$n'_{j,r}$	Rate exponent for reactant species j in reaction r
$n''_{j,r}$	Rate exponent for product species j in reaction r
\vec{r}	Position vector
\vec{s}	Unit vector in the direction of scattering
\vec{v}	Velocity (m/s)
\vec{v}	Velocity (m/s)
$v'_{i,r}$	Stoichiometric coefficient for reactant i in reaction r
$v''_{i,r}$	Stoichiometric coefficient for product i in reaction r
$\nabla \vec{v}^T$	Effect of volume dilution
C	Linear-anisotropic phase function coefficient
d	Column diameter (mm)
F	Interphase momentum exchange coefficient
G	Incident radiation
P	Pressure (Pa)
Re	Reynolds number
u	Superficial velocity (m/s)
U_{mf}	Minimum fluidization velocity (m/s)
I	Unit tensor/ Radiation intensity
N	Number of chemical species in the system
R	Universal gas constant
T	Local temperature
a	Absorption coefficient
k	Thermal conductivity
n	Refractive index
p	Static pressure (Pa)

s Path length

t Time

Greek Symbols

$\Upsilon_{j,r}$ Third-body efficiency of the j^{th} species in the r^{th} reaction

Ω' Solid angle

β_r Temperature exponent (dimensionless)

$\gamma_{\theta i}$ Collisional dissipation energy

$\varepsilon_i^{\text{max}}$ Maximum packing limit of species i

θ Granular temperature

μ_g Shear viscosity

σ_s Scattering coefficient

$\bar{\tau}$ Stress tensor

ϕ_{gs} Energy exchange between gas and solid phase

Φ Phase function

ε Volume fraction

μ Molecular viscosity

ρ Density (kg/m^3)

ρ Density (kg/m^3)

σ Stefan-Boltzmann constant ($5.672 \times 10^{-8} \text{ W/m}^2\text{-K}^4$)

Subscripts

g Gas phase

s Solid phase

CHAPTER 1

INTRODUCTION

1.1 Background

1.1.1 Hydrogen from Biomass

It is widely known that combustion of fossil fuels contributes to the build-up of carbon dioxide (CO₂) in the atmosphere, which contributes to the global warming issue all around the world. In 2005, it is reported that the concentration of CO₂ was 379 ppm, approximately 180-300 ppm more than the equilibrium concentration for the last 650 000 years [1]. Hence, the search towards cleaner and renewable alternative energy is attracting more attention.

Hydrogen (H₂) is one of the potential alternative energy that could be used to replace the existing fossil fuels. H₂ is an important material in the chemical, petroleum and energy industries. H₂ is mainly used for the manufacture of ammonia (NH₃) and methanol. It is also widely used in petroleum hydrotreating processes [2]. H₂ is an environmentally clean energy source for the generation of electric power and space heating, thus, it is expected that the demand in H₂ will increase in the near future.

H₂ is expected to become a prominent energy carrier for stationary and mobile power generation applications such as in transport, industrial, commercial and residential applications [1, 3, 4]. Figure 1.1 shows the current source of H₂ production.

All together, 96% source of H₂ production is coming from fossil fuels. H₂, which is produced from fossil fuel sources, may also contribute to the green house gas emission and environmental pollution. Therefore, in order to produce environmental friendly H₂, renewable sources must be used as the main feedstock to produce H₂ [3].

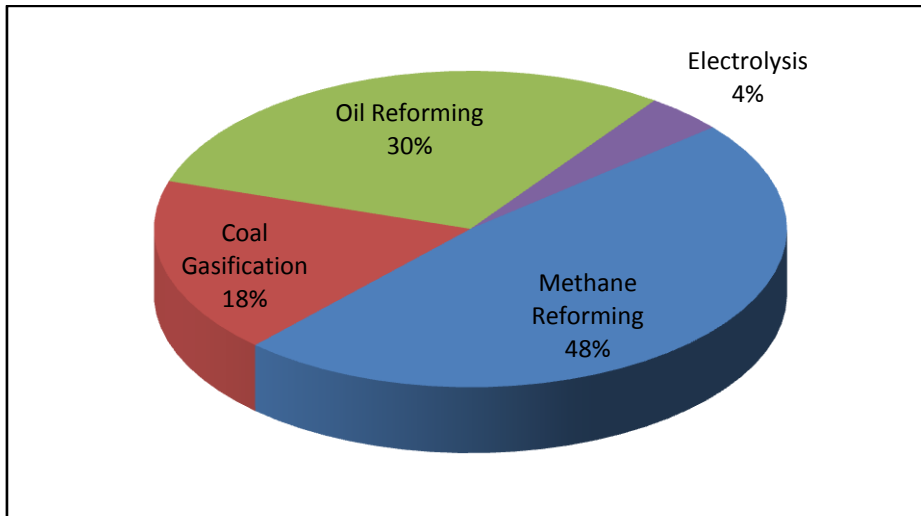


Figure 1.1: Source of H₂ production [1, 4]

Of all renewable sources, biomass has the highest potential to produce H₂ through the gasification process. Biomass is regarded as the ultimate result of the accumulation of solar energy on the earth. It possesses high intrinsic value as a sustainable, worldwide source of energy, and readily available in diverse form [5]. Gasification is the process of converting solid biomass to a gaseous fuel mainly H₂, carbon monoxide (CO), CO₂, methane (CH₄) and light hydrocarbon [6, 7] by heating in a gasification medium such as air, oxygen or steam [8].

1.1.2 Biomass Gasification Technologies

Current energy supplies in the world are dominated by fossil fuel which is around 400 EJ per year [9]. Nevertheless, 10-15% of this demand is covered by biomass resources making biomass by far the most important renewable energy source [9]. The word biomass generally refers to substance that is biological origin for example agricultural products, lumber or plants such as shown in Figure 1.2. Since biomass is produced by solar energy, air, water and soil, it can be produced infinitely as long as these sources are available.

Nowadays there are abundant of biomass that exists in the form of waste [10, 11]. If this biomass waste can be utilized, energy and clean environment can be provided without increasing the concentration of CO₂ in the atmosphere since biomass is grown through the photosynthesis process.



Figure 1.2: Example of biomass

Biomass can be converted into useful forms of energy using gasification process. As a matter of fact, gasification is not a new process. Especially, coal gasification has been used for many decades before improving natural gas. Gasification is the conversion of biomass into a combustible gas mixture via the partial oxidation at high temperature typically from 800-900 °C [12]. Gasification converts biomass into fuel gas mainly methanol, H₂ and Fischer-Tropsch liquids [9].

Furthermore, biomass gasification is greatly appealing for H₂ generation and hot fuel cell application [13]. There are several potential gasifying agents that can be used to gasify biomass which includes air, oxygen-rich air, steam and a mixture of air and steam [14]. The details of different types of gasification process using different types of gasifying medium are shown in Figure 1.3. The use of air results in dilution of product gas with nitrogen. Oxygen-rich air gasification can produce medium heating value (MHV) gas but it needs large investment for oxygen production equipment especially for the process of purifying oxygen from air and this disadvantage impedes its popularization [14-16].

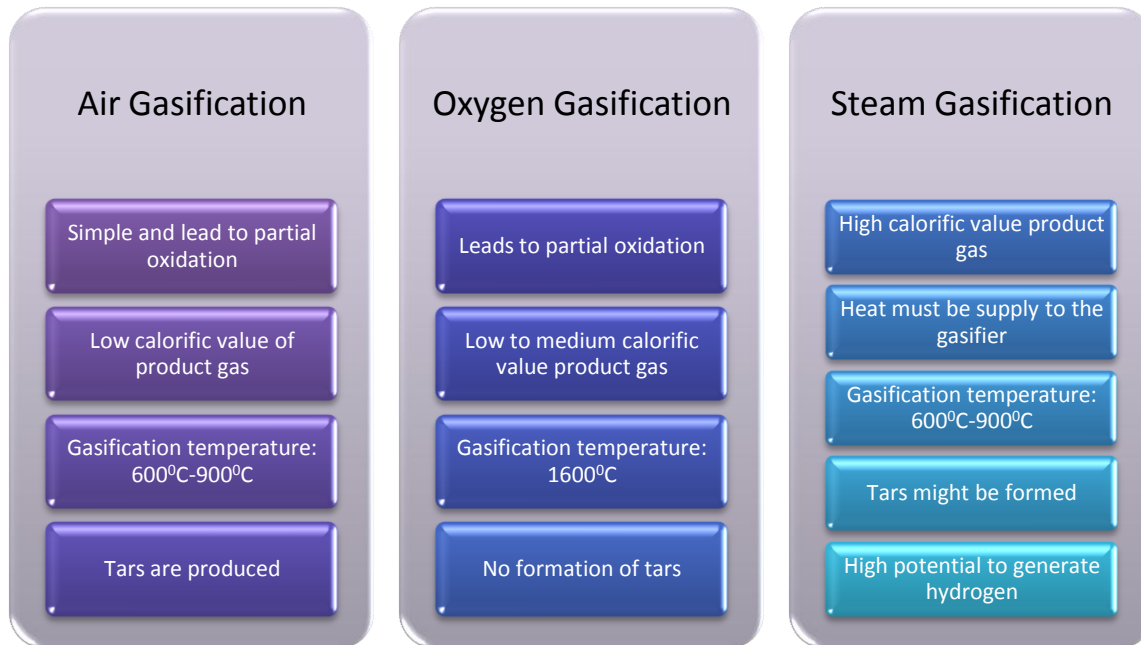


Figure 1.3: Types of gasification methods [16]

Steam gasification is also capable of producing high heating value (HHV) gas with 30-60% H₂ content [14, 17]. Steam gasification has become an area of growing interest as it produces higher H₂ product gas [13, 18]. Furthermore steam gasification is capable of maximizing the gas product with higher heating rate involved, advantageous residence time characteristic and efficient char and tar reduction. However, steam gasification are endothermic process therefore, sufficient heat needs to be provided to the system [3, 6, 14, 19].

Nowadays biomass is converted into gaseous fuel through hydrothermal gasification [19] or absorption enhanced reforming (AER) [3, 19]. AER technique uses unpressurised steam to gasify biomass with simultaneous CO₂ absorption using CaO as the sorbent in order to shift the was-gas shift reaction towards H₂ and CO₂ [3, 19]. It is reported that through AER, a H₂ rich product gas with reduced CO and CO₂ concentration will be produced [3, 19]. H₂-rich gas produced from biomass gasification can be utilized in fuel cell units for electricity production, as H₂ source for refinery hydrotreating operation, ammonia production and methanol and Fisher-Tropsch synthesis [7].

1.1.3 Fluidized Bed Gasifier

In many years, fluidized bed gasifier has been used for coal gasification. There are three types of fluidized bed reactor, which are circulating fluidized bed, bubbling bed and internally circulating bed. The details of each gasifier are as shown in Table 1.1. Fluidized beds have been applied widely in several process involving gasification, pyrolysis and combustion for wide range of particulate materials including biomass [20, 21]. The advantages of using fluidized bed reactor include good gas solid contact, excellent heat transfer characteristic, better temperature control, large heat storage capacity, good degree of turbulence, high volumetric capacity and ability to handle wide variation in particulate properties [20-22].

Fluidized bed is typically comprises of a column of solid particles, which is resting on a porous surface or grate such as shown in Figure 1.4. The gasifying agent is introduced through the bottom of the column at certain superficial velocity or flow rate that is sufficient enough to support the weight of the solid particles. The buoyant force from the gasifying agent allows the solid particle to behave similar like fluid [23].

Table 1.1: Types of fluidized bed gasifier [8]

Type	Description	Advantages	Disadvantages
Circulating	<ul style="list-style-type: none"> - Bed material is circulated between reaction vessel and cyclone separator - Ash is removed in cyclone separator and bed material and char are return to the reaction vessel 	<ul style="list-style-type: none"> - Able to cope with high capacity - Can be operated at elevated pressure 	<ul style="list-style-type: none"> - Potential for slugging of bed material
Bubbling	<ul style="list-style-type: none"> - Consist of vessel with grate at the bottom where air is introduced - Above the grate is the moving bed where biomass feed is introduced - Regulation of bed temperature by controlling air/biomass ratio 	<ul style="list-style-type: none"> - Low tar content product gas - Excellent solid-gas mixing 	<ul style="list-style-type: none"> - Potential for slugging of bed material
Internally circulating bed	<ul style="list-style-type: none"> - Consist of two interconnected chambers - Different operating condition can be set to each of the chamber. 	<ul style="list-style-type: none"> - Heat transfer between the two chambers enhances the fuel consumption - Product gas has high heating value since not been diluted with Nitrogen 	<ul style="list-style-type: none"> - Complex of construction - Potential mixing of product gas and exhaust gas

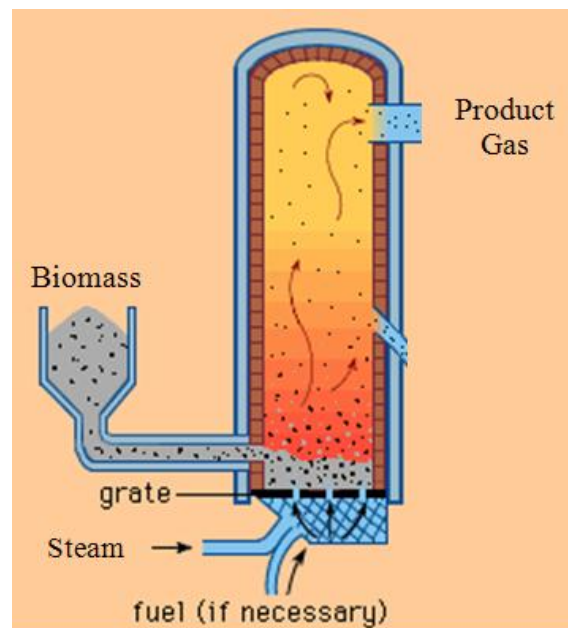


Figure 1.4: Typical Fluidized bed gasifier

In steam gasification process, gasifier usually operates at the temperature range of 800-900 °C [14]. As soon as biomass is fed into the bottom of the fluidized bed gasifier, an exquisite contact between biomass and hot bed particles such as sand, catalyst or adsorbent occurs followed by exchange of heat and mass. The overall process of biomass gasification can be divided into 4 stages. The first stage is drying where the moisture of biomass evaporates. The second stage is where the volatile compounds in biomass evaporate and this is called devolatilization. This is then followed by pyrolysis, the stage where the major part of the carbon content of biomass is converted into gaseous compounds. Carbon-rich solid residue called char is also produce during the pyrolysis process. In the last stage, the char is partly gasified with steam and also converted into gaseous products. The product gas from biomass steam gasification consists of mixture of H₂, CO, CO₂ and small amount of CH₄ and tar [14]. The main reaction involves during biomass gasification are as shown in Table 1.2.

Table 1.2: Main Biomass Gasification Reactions

Name of Reaction	References	Chemical Reaction Equation	Energy (kJ/mol)	Phase
Biomass Gasification	[14, 22, 24]	$C + H_2O \rightarrow CO + H_2$	+131.5	Solid
Boudouard	[14, 24]	$C + CO_2 \rightarrow 2CO$	+172	Solid
Water-gas Shift	[8, 14, 22, 25]	$CO + H_2O \rightarrow CO_2 + H_2$	-41	Gas
Methanation	[14]	$C + 2H_2 \rightarrow CH_4$	-74.8	Solid
Methane Reforming	[14, 25]	$CH_4 + H_2O \rightarrow CO + 3H_2$	+206	Gas
Absorption	[17]	$CaO + CO_2 \leftrightarrow CaCO_3$	-181.4	Gas-Solid

1.1.4 In-situ CO₂ adsorption

Steam gasification can provide high content of H₂. However, undesired product such as CO₂ and tars are also produced during the gasification process [26]. In order to enhance the efficiency of the steam gasification, simultaneous CO₂ capture using Calcium Oxide (CaO) has been reported can improve the yield of H₂ [17, 26-28].

CaO is a unique material that can play combine roles of catalyst and adsorbent [26, 27]. Several advantages have been reported when CaO is used as in-situ CO₂ adsorbent material in gasification process. Some of the advantages are gasification can be operated at significantly lower temperature (600°C), the increase in reactant conversion, high purity H₂ production (>95%) and the reducing downstream purification system [2].

Mainly, there are two stages of CO₂ adsorption process by CaO. The first stage is governed by surface area of CaO and the second stage is governed by the diffusivity of CO₂. Figure 1.5 shows the schematic diagram of the process of CO₂ adsorption by a CaO particle. At the first stage, the carbonation process takes place on the external and internal surfaces of the CaO adsorbent. This fast process forms a carbonate layer at the outer surface of the CaO particle. The second stage which is governs by the CO₂ diffusivity is a much slower process and highly dictates by CO₂ partial pressure in the system. The CO₂ further diffuses through the carbonate layer into the unreacted core CaO active sites. Therefore, higher reactivity and faster kinetics will be obtained if smaller particle size of CaO with higher porosity structure is used [2].

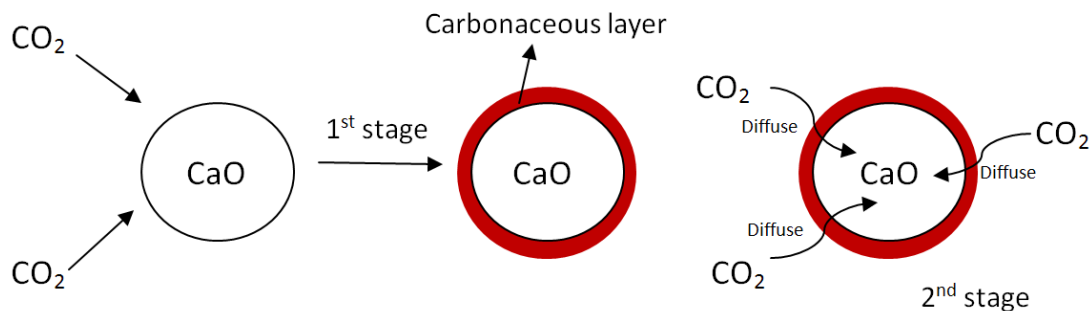


Figure 1.5: CO₂ adsorption process by CaO

1.1.5 Computational Fluid Dynamic

The recent development of mathematical modelling of particulate solids behaviour together with increasing computation power enables researcher to simulate the behaviour of fluidized biomass particle and to link fundamental particle properties directly to the particle behaviour and predict the interaction between particles and gaseous or liquid fluids [29, 30]. In this case, computational fluid dynamic (CFD) modelling provides a fundamental tool to support engineering design and research in multiphase system [30].

CFD is the science of predicting fluid flow, heat transfer, chemical reaction and other related phenomena by solving numerical set of governing mathematical equations [29, 31]. The results of CFD analysis are useful for conceptual studies of new design, detail product development, troubleshooting and redesign. Besides, CFD modelling also is cost saving, timely, safe and easy to scale-up [29]. CFD has proven to be extremely useful and accurate to predict single phase flows and multiphase flows [31]. CFD analysis complements testing and experimentation because CFD can reduce the total effort required in the experiment design and data acquisition [32]. CFD codes turn computers into a virtual laboratory and perform equivalent “numerical experiment”, which conveniently providing insight, foresight and return on investment.

With the improvement of numerical method and more advanced hardware technology, the time needed to run CFD codes is decreasing. Once the model has been validated (calculation is in good agreement with experimental data), the model can be used to make sensitivity analysis because CFD model provides the flexibility to change parameters especially for simulating fluidized bed dynamics [30, 33, 34].

CFD now is a standard tool for single phase flows and it is now at the development stage for multiphase system, such as fluidized bed [35]. CFD modelling also provides a fundamental tool to support engineering design and research in multiphase systems as it can increase process efficiency and reduce the number of scale-up steps in the design of reliable commercial plants [30].

CFD modelling for biomass gasification is still face significant challenges due the complexity of biomass feedstock. Biomass is a mixture of hemicellulos, lignin and minor amounts of other organic chemical structure. Inorganic ash is also part of the biomass composition. The complex structure makes biomass composition react or degrade at different rate by different mechanisms and this makes biomass particle feedstock has anisotropic properties in physical characterization. To deal and simplify the complex process is a key point for the CFD simulation model.

1.1.6 Biomass Gasification Modelling Approach

Numerical simulation is an effective technology to study and to optimize the performance of gasifier [36]. It is also can be considered as the best method for scale-up investigations. Mathematical model also can help in understanding the combustion and gasification processes and to predict the emission from the gasifier [33, 36, 37].

The successful design and operation of H₂ production form biomass gasification is depends on the ability to predict the behaviour of hydrodynamics, mixing of individual phases, mass transfer and multiple chemical reactions [38]. An experimental approach to directly measure all these behaviour is quite difficult and it involves high cost of operation. CFD modelling is a powerful tool and more economical in investigating the detail flow phenomena and its hydrodynamics, predicting the reaction conversion and estimating the H₂ production [38-40].

The development and application of CFD model is attracting more attention recently especially in order to model and simulate the fluidized bed gasifier. The modelling approach is focused mainly in two types of field; the first is to study the hydrodynamics of the fluidized bed gasifier and the other is to study the reacting flow and the gasification process of biomass particles.

For example, Dou et al. (2008) [38] had utilized the CFD approach in order to estimate the H₂ production from steam reforming of glycerol and predict the performance of a fluidized bed reactor base on the hydrodynamics information and reaction kinetics using Fluent[®] 6.3. Eulerian-Eulerian two-fluid approach with species transport is adopted to simulate the gas-solid flow and reactions.

In order to understand the phenomena of fluidization for the purpose of improving and optimizing the gas-solid fluidized bed reactor, Hulme et al. (2005) [41] had chosen the commercial CFD package FLUENT[®] 6.0.20 in order to model the effect of time step, differencing scheme, solid stress closure equations and frictional stress on bubble properties. Their findings had proven that the developed model showed a promising result in determining the hydrodynamics of a gas-solid fluidized bed reactor [41].

The numerous studies and researches using CFD approach shows that CFD is a growing field of study and it keeps evolving from time to time. The flexibility and reliability of CFD simulation are also one of its main advantages especially for process optimization and engineering design. For this study, CFD approach is utilized in order to model the fluidized bed gasifier using the commercial CFD package ANSYS Fluent[®] 6.3. Both the hydrodynamics and reaction models are developed in Fluent and further validated with experimental data from literature.

1.2 Problem Statement

A lot of studies have been done regarding development of biomass gasification in fluidized bed reactor. The gasification of biomass is capable of producing high quality of product gas, which is characterized by low inert, low tar concentration and high H₂ concentration. However, experimental study of biomass gasification is rather costly to build and operate the fluidized bed reactor and to supply the steam to the system. It is also dangerous for human as the biomass gasification process usually occurs as high temperature which is at 600-1000 °C and it involves highly flammable and explosive gaseous.

Simulation and modelling approach turns computer into “virtual laboratory” that performs equivalent “numerical experiment” conveniently providing all the data required to study biomass gasification provided if the model is successfully validated with actual experiment data. Therefore, simulation and modelling approach is expected to be much more cost saving, safe and easy to scale up in order to model the biomass gasification process and to find the optimum condition for biomass gasification. There are at least five potential factors i.e. temperature, steam to biomass ratio, pressure, space time and bed composition that can affect the performance of the biomass gasification process [42]. But in the gasification process with in situ CO₂ adsorption step, the adsorbent to biomass ratio can also affect the gasification performance. As the focus in this work is to investigate the operations conditions that how these influence on the gasification process.

1.3 Objectives of Research

The overall research objective for this study is to optimize the biomass gasifier reaction conditions in order to obtain the highest H₂ production from biomass gasification using CFD software, ANSYS Fluent[®] V6.3. This overall objectives leads to several main objectives which are:

1. To perform hydrodynamics study on fluidized bed gasifier with respect to different solid particle size, steam inlet velocity and bed height to diameter ratio to solid fluidization in the gasifier using CFD simulation.
2. To perform the study on the effect of reaction temperature and steam to biomass ratio to H₂ production from biomass gasification reaction using CFD simulation.
3. To study the effect of in-situ CO₂ adsorption to H₂ production from biomass gasification.

1.4 Scope of Research

Scope of study:

1. Literature review regarding biomass gasification process and study of fluid dynamic and transport equation that might involve in the simulation.
2. Developments of fluidized bed reactor mesh file using GAMBIT[®] V2.2.3 software.
3. Simulation of fluidized bed reactor using Fluent[®] V6.3 ANSYS software including heat and mass transfer and reaction.
4. Model validations and data analysis of simulation results.

CHAPTER 2

LITERATURE REVIEW

2.1 History of Biomass Gasification

Gasification has a long history with applications in town gas in the 19th and 20th century and a revival of small-scale gasification during World War II, due to an acute shortage in liquid fuels. Oil crisis in 1970s played a major role in the renewal of interest for biomass gasification. Since then, significant R&D researches in this area have been done in Europe and North America [43].

Figure 2.1 shows the five dominating application of gasification in USA from 1976-2006. Mainly the purpose of biomass gasification is to produce Fischer Tropsch liquid. However, the production of chemicals such as ammonia, methanol and H₂ is increasing steadily [43].

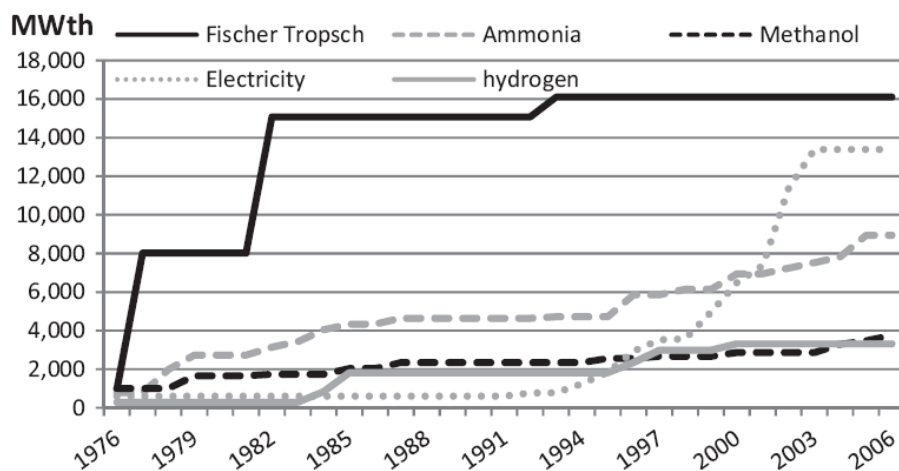


Figure 2.1: Main application of gasification [43]

According to Basu [44], the first gasification technology was developed in the early 80s by Lurgi from Germany and Ahlstrom from Finland. Lurgi used it for ore roasting while Ahlstrom became interested in the technology as a method to burn “difficult” fuel such as biomass and bark in pulp and paper industry. In 1990, the increase awareness in climate change resulted in renewed interest in biomass gasification. Many developed country such as USA, Austria and Sweden start to involve in the gasification development together with Germany and Finland.

In biomass gasification, two equally relevant periods can be distinguished, which are the first one is in the 70s until about 1987. The development is as a response to the oil crisis and mainly led by the USA. In this period Lurgi and Foster Wheeler have developed successful concepts. A second period takes off in late 1990s, focuses mainly on biomass gasification and the main drive force is the climate change. European countries have been dominating this development and followed by Japan and China after 2000 [43].

Development of both biomass and coal gasification are closely linked. Both are subjected to similar driving forces, which are availability of feedstock, prices of fossil fuel and concern regarding disruption supply and global warming [43]. In 1994, Hauserman [45] had discovered that H₂ production by catalytic coal gasification could be extended to wood, which is biomass. The technology transfer from coal to biomass was successfully done with minor substitution in feeding and solids handling component.

In 1996, Timpe et al. [46] continued the study on wood and coal gasification at the bench scale and pilot scale. From their experimental study, catalyst screening showed that potassium-rich minerals and wood ash provided the best rate enhancement. They produced H₂ as about 50 mol% at the temperature between 700-800 °C at 1 atm.

While Hauserman [45] and Timpe et al. [46] are developing biomass gasification from coal gasification technology, Cox et al. [47] presented a new approach to biomass gasification to produce H₂. The process was based on catalytic steam gasification of biomass with concurrent separation of H₂ in a membrane reactor. The process was well suited for wet biomass and conducted at the temperature as low as 300 °C at pressure range of 103.41 – 206.82 kPa. The optimal gasification conditions were found to be about 500 °C, at atmospheric pressure and steam to biomass ratio equal to 10/1. In the presence of Nickel catalyst H₂ at 65 vol% was produced under these optimal conditions.

Biomass steam gasification continues to develop since then. In the year 2002, Lin et al. [48] investigated the effect of CO₂ adsorbent which is CaO to the yield of product gas from coal steam gasification. The experiment was done at the temperature range of 600-700 °C at the pressure range of 0.1-11MPa in a fixed bed reactor. The experimental results show that high concentration of H₂ (85%) can be produced by adding the CO₂ adsorbent into the gasification system.

Based on CaO potential discovered by Lin et al., [48] Hanaoka et al. [49] continued the work by investigating the effect of CO₂ adsorbent to biomass steam gasification. Hanaoka et al. [49] discovered that CaO plays the role not only as a CO₂ adsorbent but also as a catalyst for biomass gasification. With the presence of CO₂ adsorbent, no CO₂ was detected in the product gas and H₂ gas yield increased to 800 ml (STP) g-wood⁻¹.

As the continuation from work done by Hanaoka et al. [49], Fujimoto et al. [50] gasified woody biomass in the presence of steam at high temperature (649.85 °C) and pressure (6.5 MPa) with the presence of a CO₂ adsorbent using a batch reactor with 50 cm³ capacity. The evolved CO₂ was completely adsorbed in the adsorbent and no CO₂ was found in the product gas. The gas conversion ratio is 50% at 649.85 °C.

Mahishi and Goswami [27] also discovered that H₂ yield from conventional steam gasification at atmospheric pressure could be enhanced by integrating the gasification and adsorption reactions. The method involved steam gasification of carbonaceous fuel or biomass in the presence of a CO₂ adsorbent. Experiments were conducted by gasifying pine bark in the presence of CaO. The process was performed at atmospheric pressure at temperature ranging from 500 – 700 °C. The H₂ yield increases by 48.6% in the presence of adsorbent at the temperature of 600 °C due to the reforming of tars and hydrocarbons in the raw product gas. It was also discovered that CaO played the dual role of adsorbent and catalyst in biomass steam gasification.

2.2 Biomass Gasification Study: Experimental Approach

2.2.1 Hydrodynamics Study

In the last decade, considerable progress has been made in the area of hydrodynamics of fluidized beds. Fluidized beds are widely employed in industrial operations for their excellent heat and mass transfer characteristics [30, 37, 51, 52]. These characteristics of fluidized bed can be related to the presence of bubbles and their behaviour. The presence and movement of bubbles ensure that the particles are circulated through the bed and the properties and process condition could be considered uniform [23, 30, 51, 53, 54].

The mixing and segregation behaviour of fluidized bed is largely determined by the bubble characteristics and bubble dynamics [54]. In order to describe the hydrodynamics phenomena of fluidized bed, which is related to the mixing and segregation of the bed material, several experimental studies have been done in order to study the factors that might affect the mixing and segregation of the fluidized bed. The summary of the recent studies are as shown in Table 2.1.

Table 2.1: Summary of recent experimental study on hydrodynamics

Author	System	Scope of work	Parameters	Findings
L. Shen et al. [55]	Reactor: Cold model of Bubbling Fluidized Bed Solid: 8 mm wood particles Gas: Air Temperature: Room Pressure: Atmospheric	Mixing/ segregation of particles in bed	Superficial velocities: 0.35-1.22m/s (1-4 U_{mf})	<ul style="list-style-type: none"> • Mixing of biomass solid not only caused by movement interaction and coalescence of bubbles, but also bursting bubbles at the surface • The higher the superficial velocity the faster the vertical mixing. • Biomass concentration at the bottom of the bed decreases as superficial velocity increase while at upper region increase. • Biomass more uniformly distributed at lower superficial velocities • Increase of superficial velocity influence segregation
Y. Zhang et al. [56]	Reactor: Fluidized bed Solid: Sand and cotton stalk Gas: Air Bed height: 300mm Temperature: Room Pressure: Atmospheric	Mixing/ segregation of particles in bed	Gas velocity: 1-10 U_{mf}	<ul style="list-style-type: none"> • Increase of gas velocity promotes biomass to accumulate at the top of the bed. • There exists a gas velocity producing the maximum mixing. Below this velocity mixing overtakes segregation and above this velocity segregation overcome mixing.
G.A. Bokkers et al. [54]	Reactor: pseudo-2D fluidized bed Solid: Spherical glass beads, 2.5mm diameter Gas: Air	Simulation and experimental of solid mixing and segregation	Background velocity: 1.2-1.7m/s	<ul style="list-style-type: none"> • Background velocity has hardly any effect on the bubble shape, the number of particles inside the bubbles and the initial mixing of particles. • Higher the background velocity, increase particle mixing because more particles are transported in the wake of the bubbles.
C.N. Lim et al. [23]	Reactor: Perspex-walled 2D fluidized bed Solid: Ballotini glass beads, 106-212 μ m Bed height: 690 mm Gas: Air	Identifying and interpreting the dynamics of bubbles	Superficial velocity: 10-110 mm/s	<ul style="list-style-type: none"> • Bubble void fraction relate consistently to the amount of gas supply • Measured bubble void fraction can be used as the feedback of closed-loop control implementation of the bubbling process via fixed-gain PID controller.

Y. Zhang et al. [56] has developed an experimental setup in order to study the influence of gas velocity on the mixing and segregation pattern in a fluidized bed. Their findings are concluded in Figure 2.2. When gas is introduced to the fluidized bed at certain velocity, the biomass particles float to the top of the bed. Due to the gravitational force, the biomass tends to move back downwards and improve mixing in the system. However as the gas velocity increase, moving downwards towards the bottom is becoming difficult and segregation tends to occur.

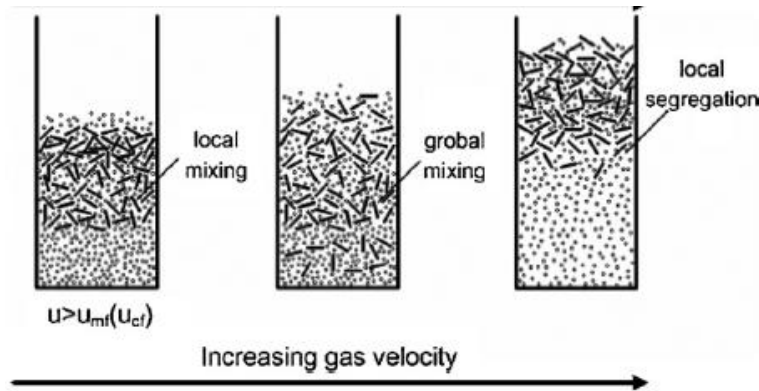


Figure 2.2: Progress of mixing and segregation with the gas velocity [56]

Figure 2.3 shows the experimental findings by C. N. Lim et al. [23]. Based on their study it is observed that bubbles population and bubble average size increase with increasing gas flow rates.

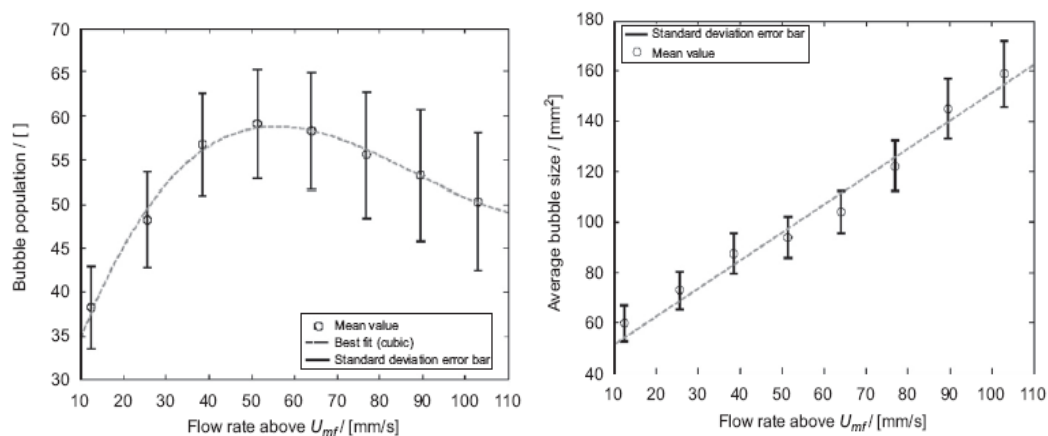


Figure 2.3: Effect of gas flow rate on bubble dynamics [23]

Overall, most of the experimental studies on hydrodynamics of fluidized bed gasifier are related to mixing and segregation of solid particles in the bed which are mainly affected by gas superficial velocity. However, K.S. Lim et al. [57] in their review work also highlighted that solids mixing might also be influenced by the height to diameter ratio (H/D), particle size, density and shape. Harrison et al. [58] also pointed out that there are several factors that might affect the fluidizing quality such as the gasifying gas velocity, solid and gas density ratio, solid particle size, operating pressure and temperature and also fluidizing gas viscosity. The main constrain in experimental study of hydrodynamics is to overcome the limitations by digital image analysis [57]. Therefore simulation approach is much more preferable in order to study the effect of other parameters such as height to diameter ratio (H/D) and particle size on solid mixing and fluidization.

2.2.2 Reaction Study

Composition of gases produced from the gasification process are highly governed by the operating condition of the gasifier such as reaction temperature, pressure, gasifying medium, as well as type of catalyst [17, 22, 26]. Reaction parameters affect various performance aspects like efficiency, product gas quality and energy efficiency. A lot of studies have been done in order to investigate the optimum parameters to obtain maximum H₂ yield from biomass gasification [12]. The summary of some recent experimental studies on biomass gasification are shown in Table 2.2.

Table 2.2: Summary of experimental study on biomass gasification reaction

Author	System	Scope of Work	Parameters	Findings
S. Rapagna et al. [7]	Reactor: Fluidized Bed Bed material: Sand Solid: Biomass Gas: Steam Catalyst: Nickel and calcined dolomite	To characterize the influence of operating parameters on the catalytic transformation of tar into CO and H ₂ in the presence of steam	Temperature : 665, 760, 830 °C Gas Hourly Space Velocity: 9000-27700 h ⁻¹	<ul style="list-style-type: none"> • Fresh nickel based catalyst are extremely active for the elimination of CH₄ and tars • H₂ content higher than 60 vol% is produced
S. Lin et al. [48]	Reactor: High pressure flow type reactor with fixed bed Solid: Coal Gas: Steam Adsorbent: CaO	To convert CO and remove CO ₂ completely during coal gasification	Temperature : 873-973K Pressure: 0.1-11 MPa CaO weight: 2.3g, 5g	<ul style="list-style-type: none"> • H₂ composition in product gas is higher compared to general coal pyrolysis when adsorbent is added into the fixed bed (84.8 vol%) • H₂ produce at 973K was nearly twice and four times higher than H₂ produce at 923 K and 873K respectively. • H₂ production increase about 1.5 times when pressure was raised from 1-6 MPa.
T. Hanaoka et al. [49]	Reactor: Autoclave Solid: Woody biomass Gas: Steam Adsorbent: CaO	To study the effect of adsorbent to carbon molar ratio, reaction pressure and temperature on biomass gasification using batch reactor	Ca/C: 0-4 Temperature : 873K, 923K, 973K Pressure: 0.3-8.4 MPa	<ul style="list-style-type: none"> • H₂ yield and carbon conversion exhibit maximum value at Ca/C of 2. • H₂ yield and carbon conversion increase with increasing reaction pressure up to 0.6 MPa and decrease at higher pressure. • H₂ yield increase with increasing reaction temperature.
P. M. Lv et al. [59]	Reactor: Small scale fluidized bed Solid: Pine sawdust Gas: Air and low temperature steam Pressure: Atmospheric	To explore the effect of some critical parameters on gasification performance	Particle size: 0.2-0.9 mm Temperature : 700-900 °C ER: 0.19-0.27 S/B: 1.35-4.04	<ul style="list-style-type: none"> • H₂ concentration increase with temperature and opposite trend is observed for CH₄. • Below 830 °C, CO content was higher than H₂. • H₂ content slightly varied as ER increase. • Higher ER causes gas quality to degrade. • H₂ content increase as S/B increase • Particle size has insignificant effect on H₂.

Author	System	Scope of Work	Parameters	Findings
S. Koppatz et al. [17]	Reactor: CHP Guessing dual fluidized bed system Solid: Biomass Gas: Steam Adsorbent: CaO	First time application of AER in industrial scale	Temperature : 650-700 °C.	<ul style="list-style-type: none"> • The higher the reaction temperature, the higher the CO₂ content in the product gas and opposite trend is observed for H₂ and CH₄. • At temperature below 690 °C, the CO₂ content in the product gas decreases significantly due to selective CO₂ removal in the gasifier using CaO. • H₂ yield and carbon conversion efficiency increase by 48.6% and 83.5% respectively at 600 °C as CO₂ adsorbent is added into the gasifier.
W. Wu et al. [4]	Reactor: Bench scale fluidized bed Solid: Waste wood Gas: Steam and oxidizing agents Catalyst: Commercial Ni	To establish a fuel processor for an advance power generation system	Temperature : 750°C, 850°C, 950°C. S/C: 0-4.44	<ul style="list-style-type: none"> • H₂ production increase as temperature increase. • Maximum H₂ production (39 vol%) is observed at 950 °C, S/C= 1.54 and ER = 0.2. • Temperature plays a dominant role in H₂ production and the addition of steam and O₂ mainly improve the thermal degradation of hydrocarbon and this leads to a slight increase in CO₂. • Steam addition has the same effect as increasing temperature on H₂ formation.
W.P. Walawender et al. [60]	Reactor: Bench scale fluidized bed Solid: Cellulose Gas: Steam	To generate datum lines for the gas composition, yield, heating value, energy recovery and carbon conversion	Temperature : 865-1060 K	<ul style="list-style-type: none"> • The most important factor that influences any gasification process is the reactor temperature. • H₂ formation increase with increasing temperature.
N. Gao et al. [61]	Reactor: Updraft gasifier with continuous biomass feeder Solid: Pine sawdust Gas: Steam and air	To investigate H ₂ -rich gas produced from biomass	Temperature : 800-950 °C ER: 0-0.3 S/B: 1.05, 2.05, 2.53, 3.47	<ul style="list-style-type: none"> • H₂ concentration increase from 39-55 vol% with temperature. • H₂ concentration decrease from 44.45-23.56 vol% as ER increase • H₂ concentration increase as S/B increase.

Author	System	Scope of Work	Parameters	Findings
B. Acharya et al. [62]	Reactor: Stainless steel fixed bed reactor Solid: Saw dust Gas: Steam Adsorbent: CaO	To study the effect of steam to biomass ratio, temperature and adsorbent to biomass ratio on the composition of product gas	Steam to biomass ratio: 0.58-1.58 Temperature : 600, 670, 710 °C Adsorbent to biomass ratio: 0-2	<ul style="list-style-type: none"> • Increasing steam to biomass ratio from 0.58 to 1.58 increases the H₂ yield. • Increasing temperature increases H₂ yield but above 670 °C, concentration of H₂ in product gas is low. • Increasing adsorbent to biomass ratio greatly increases the yield and concentration of H₂ in product gas.
P. Weerachainai et al. [26]	Reactor: Batch type bubbling fluidized bed Solid: Larch wood Gas: Steam and N ₂	To study the effect of type of bed material, temperature and gasifying agent on gasification products.	Bed material: silica sand, calcined lime stone, calcined waste concrete Temperature : 650 and 750 °C Gasifying agent: steam and N ₂	<ul style="list-style-type: none"> • High concentration of H₂ and CO₂ is obtained when calcined lime stone and calcined waste concrete is used as bed material. • Increasing temperature increases the % of Low Heating Value and decreases the tar content. • Increasing temperature decreases the ability of calcined lime stone bed to capture CO₂ and converting CO to H₂ and CO₂ via water gas shift reaction. • Steam utilization in gasification increase the amount of gas product.

A lot of studies have been done and it is proven that steam gasification has several advantages upon others, which are product gas has higher H₂ content, it can eliminate the needs for an expensive oxygen plant, it can reduce the diluting effect of Nitrogen (N₂) from air and it can increase the heating value of syngas produced [4, 61]. Other than the gasifying agent, effect of different parameters was also studied. W. Wu et al., [4] P.M. Lv et al. [59], N. Gao et al. [61] and L. Shen et al. [14] have investigated the effect of temperature, equivalence ratio (ER) and steam to biomass ratio (S/B) to the production of H₂ gas. P.M. Lv et al. [59], and M. B. Nikoo and Mahinpey [22] also study the effect of biomass particle size and N. Gao et al. [61] have performed the study on the effect of porous ceramic filter on the gas composition.

Effect of gasification temperature

Gasification temperature not only affects the product yield but also governs the process energy input. High gasification temperature particularly between 800 and 850 °C produces product gas that is rich in H₂ and CO with small amounts of CH₄ and higher hydrocarbon. As temperature increases both carbon and methane are formed and at about 726.85 °C, both are reduced to very small amount and get converted into CO and H₂. This explains the increase of H₂ production at higher temperature [12]. At temperature higher than 756.85 °C, H₂ yield starts reducing because of the water-gas-shift reaction [63].

Walawender et al. [60] has worked on the steam gasification of pure cellulose which is one of the main components in biomass in a fluidized bed reactor and has found that the most important factor that influences any gasification process is the reactor temperature. Based on the experimental results that have been conducted for temperature range of 865-1060K, Walawender et al. [60] has concluded that the gasification of cellulose composed of two distinct regime. The first regime is dominated by the cracking of volatiles up to temperature of 940K. At temperature higher than 940K the second regime, dominated by the water-gas shift reaction shows a dramatic rise in gas yield with increase in temperature [60].

Figure 2.4 shows the experimental results obtained by S. Koppatz et al. [17] from biomass steam gasification on industrial scale. From the figure, it is observed that below 690 °C, the CO₂ content in the product gas decreases significantly due to the selective removal in the gasifier [17].

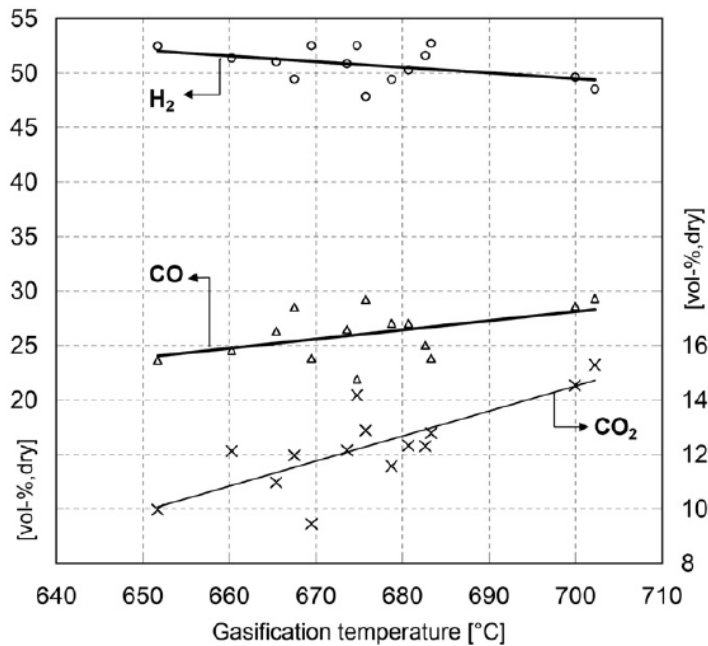


Figure 2.4: Product gas composition vs. gasification temperature for biomass steam gasification [17]

Effect of Steam to Biomass ratio (S/B)

The use of steam leads to higher H₂ yield due to additional H₂ produced from decomposition of H₂O through water-gas shift reaction [1, 4]. The effect of gasifying agent had been study previously and it is reported that maximum H₂ yield is achieved in the absence of O₂ [1].

Steam addition has the same effect as increasing temperature on H₂ production [4]. However, steam can have both a positive and negative effect on H₂ production. From Wei Wu et al. [4], the H₂ production increase from 18.7-27 vol% as the steam to carbon ratio increase from 0-1.67. However at steam to carbon ratio higher than 1.67 H₂ content apparently decrease on the addition of more steam. This is because excess steam leads to the increase of CO₂ and hydrocarbon production [4].

Similar to temperature, steam to biomass ratio has a strong influence on both product gas composition and energy input. At low steam to biomass ratio, solid carbon and methane are formed. As more steam is supplied to the system, both of these species are converted to CO and H₂ therefore, higher yield of H₂ is obtained as S/B increase [12].

N. Florin & A. Harris [1] highlighted that in order to enhance the production of H₂, operating variables such as reactor temperature and steam to biomass ratio can be manipulated [28]. The highest H₂ concentration reported in literature are in the range of 40-60 vol% at the temperature around 1000K and steam to biomass ratio between 0.8-0.9 [64-66].

Experimental results from N. Gao et al. [61] shows that H₂ concentration increase as steam to biomass ratio increase as shown in Figure 2.5. However, the opposite trend is observed for CO₂ and CH₄. On the basis of experiment, higher steam to biomass ratio produce larger amount of H₂ yield, however, high water yield was also observed from the gasification process, which requires a separation system of steam from product gas. More energy is also required in order to produce excess steam therefore, it is necessary to select optimal steam to biomass ratio. From their findings, the optimal steam to biomass ratio for their operating condition is 2.05 [61].

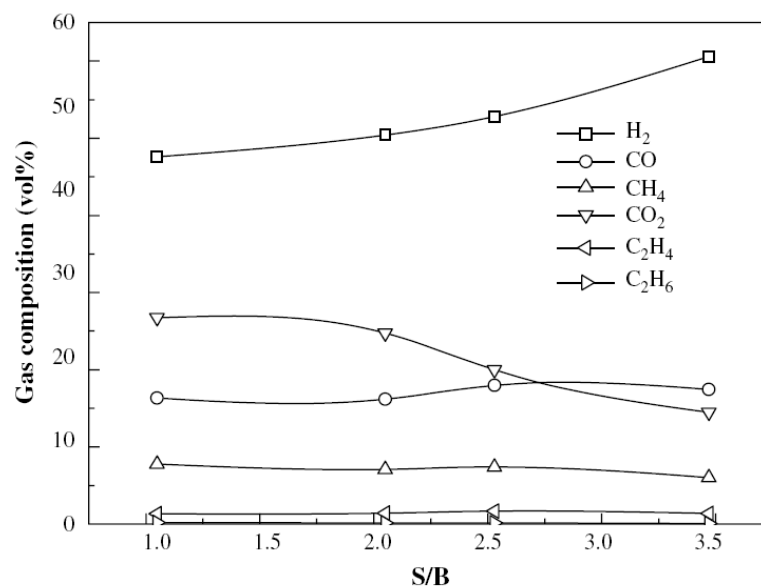


Figure 2.5: Effect of steam to biomass ratio (S/B) on gas composition [61]

Effect of CO₂ adsorbent

CO₂ removal, capture and storage have been in several research and development activities worldwide [17]. The combination of CO₂ removal with gasification process has been proposed and studied by various researchers. Balasubramanian et al. [67] had proposed the use of CO₂ sorbent for enhancing the H₂ yield of conventional steam methane reforming. The addition of CO₂ adsorbent has been proven to increase the H₂ yield even though it is only effective at certain temperature [27].

Huges et al. [68] have reported that at atmospheric pressure, the optimum temperature for carbonation of CaO should be in the range of 650-750 °C and the capability of CO₂ adsorption is dependant on the CO₂ partial pressure in the gasifier [26].

Conventional gasification process without CO₂ adsorbent usually takes place at the temperature range of 850-900 °C [17]. In order to enforce CO₂ adsorption using calcium oxide (CaO) at atmospheric pressure, a temperature range for gasification of 600-750 °C is necessary since the adsorption reaction is exothermic and high temperature is not favorable [17, 26]. In other word, incorporating CO₂ adsorbent into the gasification system actually improve the energy efficiency for the system since the gasification reaction occurs at lower temperature and at the same time CO₂ adsorbent can improve the purity of H₂ in the product gas.

Figure 2.6 shows the experimental results obtained by B. Acharya et al. [62] on the effect of adsorbent to biomass ratio to the gas composition produced from biomass steam gasification. The results show that increasing the ratio from 0 to 1 increase the volumetric composition of H₂ from 22.29 vol% to 53 vol%. The yield of H₂ increased by more than double when the adsorbent to biomass ratio increase from 0 to 1, which shows that adding CO₂ adsorbent into the system does help to improve H₂ production from the gasification process [62].

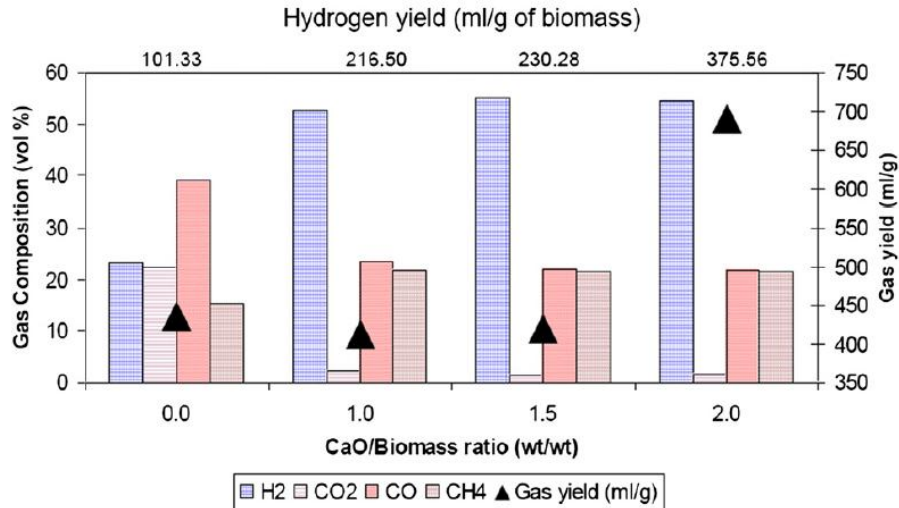


Figure 2.6: Effect of Adsorbent to Biomass ratio on product gas composition [62]

Overall, experimental studies have proven that reaction conditions do affect the composition and yield of H₂ from biomass gasification process. The similar trends or observations are expected to be obtained from the developed model and the results from literature are going to be used for validation.

2.3 Biomass Gasification Study: Modelling Approach

2.3.1 Hydrodynamics Study

In recent years, mass conservation and momentum balance for gas and solid have been applied to simulate the hydrodynamics of bubbling fluidized bed [69]. The fluidized bed gasifier for biomass gasification is a multiphase system consists of solid biomass particles and also the gas gasifying agent, which in this study is referring to steam. Phase is a class of matter with a definable boundary and a particular dynamic response to the surrounding flow. Phase are generally identified by solid, liquid or gaseous states but can also refer to other form such as material with different chemical properties but in the same state or phase for example the oil-water system. The multiphase fluid system is defined by primary and multiple secondary phases as shown in Figure 2.7. The continuous phase is considered as the primary phase while the other dispersed material or phase within the continuous phase is the secondary phase.

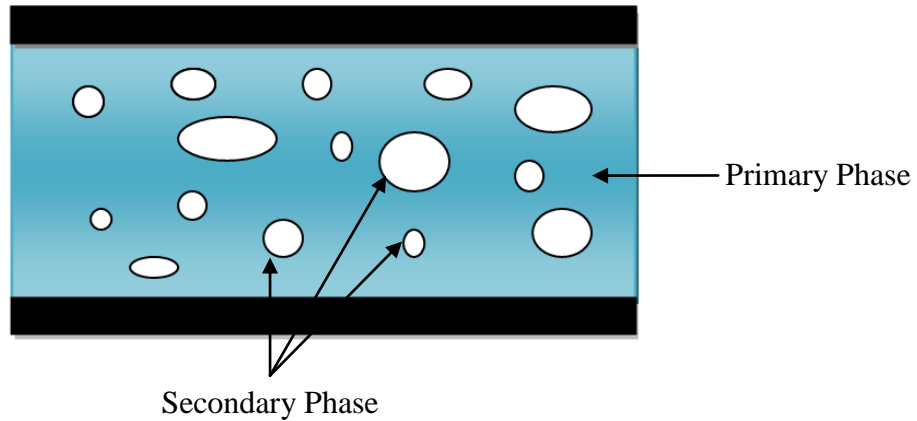


Figure 2.7: Multiphase fluid system

Two main groups of CFD multiphase models are the Eulerian-Eulerian (E-E) model (continuum models) and the Eulerian-Lagrangian (E-L) models (discrete particle models) [40, 70-72]. E-E model continuous medium model describes each phase with conservation law of mass, momentum and energy in the Eulerian coordinate. This model can compute effectively and treat boundary condition easily [72].

E-L model takes gas phase as a continuum phase while particles are seemed as dispersed phase. Motion of continuous phase is studied in Eulerian coordinate while particle motion is track in Lagrangian coordinate which is also known as Particle Trajectory Model [72]. E-L models do not require supplementary approximation for the granular solid phase since the motion of each individual particle models is calculated separately from the particle collision and external forces acting on the particles. This makes the computational effort is huge and the number of particles that can be modelled is limited (about 10^6) [35, 52, 73, 74]. However, in large scale fluidized bed the number of particles is much higher typically 10^9 - 10^{12} , therefore, the E-E model is much more appropriate for hydrodynamics modelling [52, 70, 71, 75, 76].

The E-E model is the preferred choice for simulating macroscopic hydrodynamics [30, 35, 37, 51]. The general idea in formulating the multiphase model is to treat each phase as an interpenetrating continuum and to construct integral balances of continuity, momentum and energy for both phases [40]. Since the solid phase has no equation of state and lacks variables such as viscosity and normal stress, certain averaging techniques and assumptions are required to obtain complete momentum balance for the solid phase [30]. In the recent E-E models kinetic theory of granular flow (KTGF) are incorporated which is an extension of the classical kinetic gas theory on dense particulate flows taking non-ideal particle-particle collisions and the gas-particle drag into account [70, 76]. Many researchers has tried to develop a theory of particle collision based on the kinetic theory of granular flow and numerous studies has proven that kinetic theory of granular flow (KTGF) approach is capable to model the bubbling flow fluidized beds [30, 37, 52]. Several researchers had employed CFD E-E modelling of fluidized bed together with the KTGF. The summary of recent study using E-E model and KTGF is as shown in Table 2.3.

Table 2.3: Summary of hydrodynamics modelling using E-E model and KTGF

Author	Simulation Scheme	Scope of Work	Parameters	Findings
L. Huilin et al. [77]	Software: n/a Model: E-E & E-L + KTGF Dimension: 2D Compare with Exp: Yes Particle group: A & B	To investigate gas-solid flow	Mean diameter of particles: 2-5 mm Fluidizing velocity: 2.5 m/s, 3.2 m/s	<ul style="list-style-type: none"> • Larger and heavier particles tend to settle down at the bed bottom while smaller particles tend to move to the bed top. • Better mixing are obtained by increasing fluidizing velocity
A. Boemer et al. [76]	Software: Fluent Model: E-E + KTGF Dimension: 2D Compare with Exp: Yes Particle group: B	To verify resulting flow pattern from simulation with measurements from experiment	Granular temperature model	<ul style="list-style-type: none"> • E-E + KTGF able to describe bubble formation process in fluidized bed • Granular temperature of $10^{-5} < \Theta < 0.1 \text{ m}^2/\text{s}^2$ is suitable for fluidized beds
R. Panneerselvam et al. [71]	Software: ANSYS CFX-10 Model: E-E Dimension: 2D, 3D Compare with Exp: Yes Particle group: n/a	Understanding the complex hydrodynamics of 3 phase fluidized bed for coarser particle	Interphase drag models Dimension: 2D, 3D Bubble size: 5, 13, 17 mm	<ul style="list-style-type: none"> • 3D simulation gives more accurate prediction of axial solid velocity • Tomiyama (1998) drag model are closer to experimental results. • Hold-up profiles for bubble size 13 and 17 mm are closer to experimental results
S. Gerber et al. [78]	Software: MFIX Model: E-E + KTGF Dimension: 2D Compare with Exp: Yes Particle group: D	Simulation of wood gasification in dense fluidized bed	Solid initial bed height: 30-40 cm	<ul style="list-style-type: none"> • Influence of solid initial bed height on the gaseous component in the product gas is relatively weak. • Decreasing bed height leads to increasing bed temperature.

Patil et al. [79] investigates the hydrodynamics of bubbling gas-solid fluidized beds using Eulerian-Eulerian model. A constant viscosity model and KTGF are tested and compared with each other and with experiments. Both models perform fairly similar. However, including frictional contribution on the KTGF model improved more on the results [80].

Due to high particle concentration in the gas-solid fluidized bed; Boemer et al. [75] used the E-E model approach and KTGF to simulate the process of spontaneous bubble formation in a two-dimensional fluidized bed and the model was found to be in good agreement with experiments and also the empirical model. From the comparisons it is proven that the Eulerian-Eulerian model and KTGF can be used to predict the fluid dynamics of bubbling fluidized bed [75].

For this study, Eulerian-Eulerian multiphase flow model are specifically chosen to model the fluidized bed gasifier for biomass gasification. In order to give better prediction of the fluid dynamic in the bubbling fluidized bed, the Eulerian-Eulerian multiphase model is coupled with KTGF. The hydrodynamics model developed was then used to study the effect of solid particle size, steam inlet velocity and bed height to diameter ratio to the solid fluidization in the fluidized bed gasifier.

2.3.2 Reaction Study

Although numerical simulation has been widely used to simulate the gas-solid flow, there has been little study on the simulation of gas-solid flow coupling with chemical reactions for biomass [37]. Standard CFD model with additional finite rate chemistry model is a potentially powerful tool for design and optimization of biomass gasifier [24].

Modelling of biomass steam gasification is a great challenge because of the variability (composition, structure, reactivity, physical properties, etc.) of biomass material and because of the severe conditions (temperature, residence time, heating rate, etc.) required [25]. Mainly, there are two different modelling approaches that have been used to model the thermochemical conversion of biomass which are the thermodynamic approach and kinetics approach.

In thermodynamic approach, the focus is on thermodynamic equilibrium and the solver minimized the Gibbs energy of the closed system in order to give the composition of the mixture. The kinetic approach is much more sophisticated models and has been derived at particle scale. The model solves the mass and energy balance over the particle and the boundary condition associated [25]. The summary of recent studies that had been done using both of these models is shown in Table 2.4.

Table 2.4: Summary of reaction study using modelling approach

Author	Simulation Scheme	Scope of Work	Parameters	Findings
E. Simsek et al. [81]	Software: LEAT & ANSYS-CFX Model: Kinetic (Arrhenius) Dimension: 3D Compare with Exp: Yes Process: Drying, Pyrolysis and Combustion	To simulate the motion and chemical conversion of solid fuel in packed bed moving forward acting grate.	N/A	<ul style="list-style-type: none"> Modeling shows qualitatively reasonable results for the pyrolysis and char combustion in term of temperature distribution.
M. R. Mahishi et al. [3]	Software: ASPEN PLUS Model: Thermodynamic Dimension: n/a Compare with Exp: No Process: Gasification	To enhance H ₂ yield by integrating the gasification and adsorption reaction	Temperature: 500-900 °C Pressure: 1-24 atm Steam/Ethanol: 3-8 CaO/Ethanol: 0-6	<ul style="list-style-type: none"> As temperature increase, H₂ molar flow rate increase and reach maximum at 725 °C. Above 800 °C H₂ yield starts decreasing because of reverse WGS reaction. Steam reforming of ethanol is best done at atmospheric pressure. Addition of steam increase H₂ yield H₂ production increase by separation of CO₂ using CaO Maximum H₂ production with the presence of CaO is observed at 650 °C
D.F. Fletcher et al. [24]	Software: CFX4 Model: Kinetic (Arrhenius) Dimension: n/a Compare with Exp: No Process: Air combustion and gasification	To simulate the flow and reaction in an entrained flow biomass gasifier	Particle diameter: 0.3-1.0 mm	<ul style="list-style-type: none"> The model shows a hot zone at the base of the gasifier where combustion occur. The composition of exit gas are 11% CO, 15% CO₂, 23% H₂, 0.06% CH₄, 9% H₂O and 40% N₂ by volume. Simulation results we found to be insensitive to the particle diameter.

Author	Simulation Scheme	Scope of Work	Parameters	Findings
M.B Nikoo and N. Mahinpey [22]	Software: ASPEN PLUS and FORTRAN Model: Kinetics and thermodynamics Dimension: n/a Compare with Exp: Yes Process: Air-steam biomass gasification	To develop simulation capable of predicting steady state performance of an atmospheric fluidized bed gasifier	Temperature: 700-900 °C ER: 0.19-0.27 S/B: 0-4 Particle size: 0.25-0.75 mm	<ul style="list-style-type: none"> • Better prediction of H₂ production at temperature higher than 800 °C. • H₂ production increase with increase of temperature • Increase amount of air increase gasification however more CO₂ is produced. • Higher steam flow rate of steam decrease CO and increase CO₂. • Based on hydrodynamics model, larger biomass particle results in a higher volume fraction of solid that improves carbon conversion efficiency. • Increase of particle size does not improve H₂ production
L. Shen et al. [14]	Software: ASPEN PLUS Model: Thermodynamics Dimension: n/a Compare with Exp: No Process: Steam gasification and combustion	To proposed a novel process for H ₂ production from biomass gasification in interconnected fluidized bed	Temperature: 650-900 °C S/B: 0.4-0.9	<ul style="list-style-type: none"> • H₂ content was maintained around 40-60 mol% at temperature range 650-900 °C. • Maximum H₂ content of 60.5 mol% was obtained at 800 °C. • Favorable temperature for gasifier is between 750-800 °C. • S/B has weak effect on gas composition • H₂ yield reached maximum at S/B of 0.7 at 800-850 °C.
B. Duo et al. [38]	Software: Fluent Model: Kinetics Dimension: 2D Compare with Exp: No Process: Steam reforming of glycerol	To investigate the steam reforming of glycerol using a three-step reaction scheme	Reaction time: 0-4 s	<ul style="list-style-type: none"> • Glycerol conversion increase from 22% to 45% from 1-4 s reaction times. • Most of the product gas is formed during the initial 2 s.
P. Ji et al. [36]	Software: Fortran Model: Kinetics Dimension: 2D Compare with Exp: Yes Process: Biomass air-	To analyzed the proposed integrated process for production of ultrapure H ₂ in term of pure H ₂ yield and	Equivalence Ratio: 0.25-0.4 Temperature: 973-1173K	<ul style="list-style-type: none"> • Increasing equivalence ratio increases combustible gases and tar, which leads to the increase of CO₂ in the product gas. • Higher bed temperature favors the conversion of

Author	Simulation Scheme	Scope of Work	Parameters	Findings
	steam gasification	overall thermodynamic efficiency		tar and CH ₄ and this increases the production of H ₂ and CO.
N. Florin and A. Haris [28]	Software: FACTSage 5.2 Model: Thermodynamic Dimension: - Compare with Exp: No Process: Biomass steam gasification with CaO as CO ₂ adsorbent.	To investigate the thermochemical gasification of biomass using steam and to enhance H ₂ yield	Temperature: 500-1300K Presence of CaO.	<ul style="list-style-type: none"> • H₂ production from the proposed process is 40-50 vol%. • The addition of CaO is a viable method for boosting H₂ yield. • Increasing temperature increases H₂ concentration from 500-900K.

Mahishi and Goswami [82] used a thermodynamic equilibrium model to predict the chemical composition of the product gas from biomass gasification. The effect of reaction temperature on the equilibrium H₂ yield was studied using Stanjan (v 3.93L) software. From the findings, the highest H₂ production of 54% was obtained at the optimum gasification temperature of 726.85 °C.

P. Ji et al. [36] proposed an integrated process for the production of ultra pure H₂ production from biomass gasification with air. A non-isothermal model has been developed to simulate the fluidized bed gasifier and the model was used to study the effect of gasification parameters, which are equivalent ratio (ER) and operating temperature. The results from their findings are shown in Figure 2.8. From Figure 2.8, it is observed that the production of CO and H₂ increases as temperature increases and the opposite trend is observed for CO₂ and CH₄.

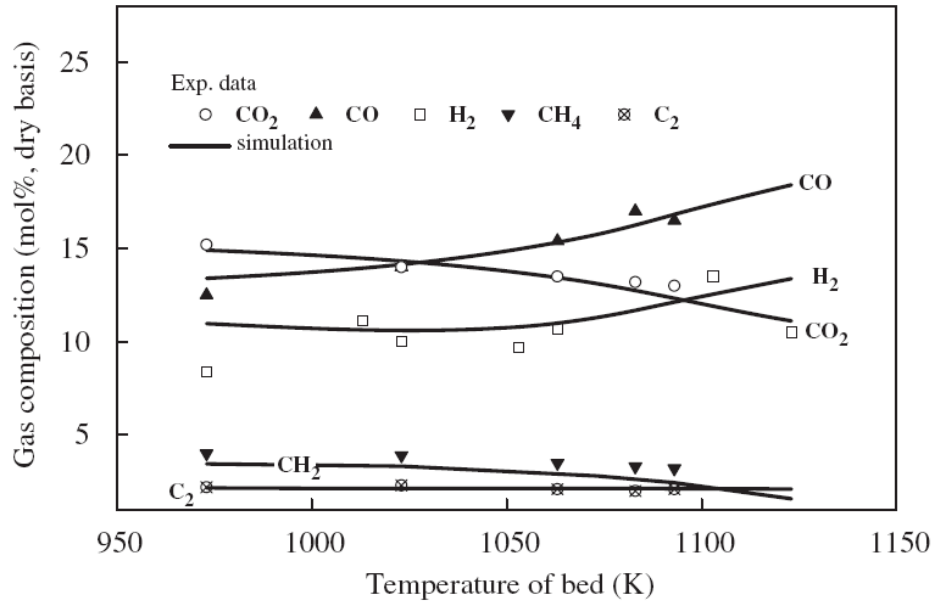


Figure 2.8: Effect of operating temperature on product gas composition from simulation of biomass air-gasification [36]

L. Shen et al. [14] proposed a novel process of H₂ production from biomass gasification in interconnected fluidized beds. The proposed process separates the combustion process and gasification process. The circulating fluidized bed is designed for combustion fed with air and the bubbling fluidized bed for biomass gasification fed with steam. ASPEN PLUS software was used to demonstrate the possible available efficiencies of the interconnected fluidized beds. The results from their simulation are as shown in Figure 2.9.

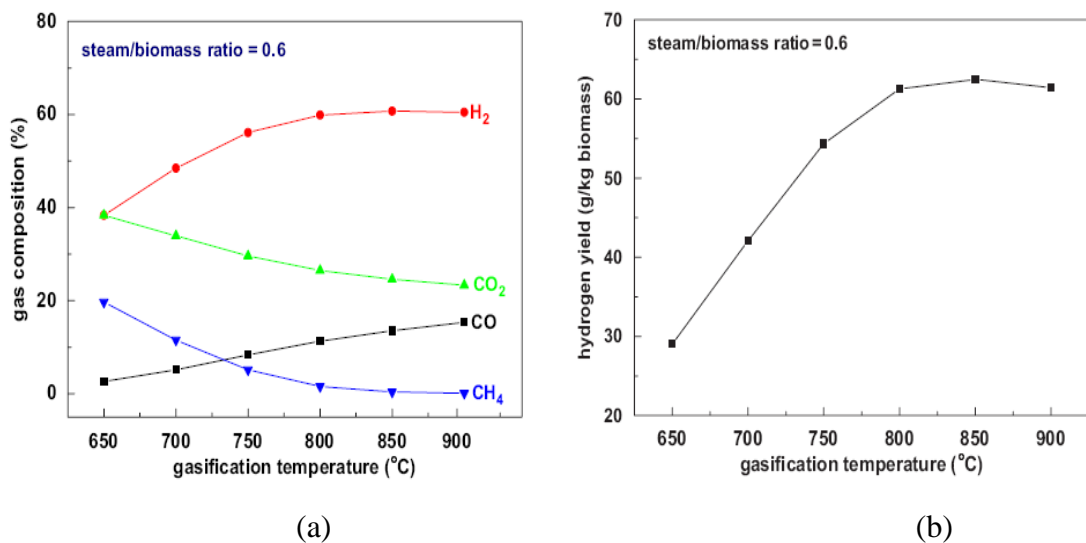


Figure 2.9: Effect of gasifier temperature on (a) product gas composition (b) H₂ yield from biomass steam gasification [14]

Based on equilibrium model, N. Florin & A. Harris [28] predicted the H₂ concentration for steam gasification of carbon with and without the addition of CaO as CO₂ adsorbent. In the absence of CaO, the H₂ concentration increases with the increase in temperature from 500-900K and the maximum H₂ concentration produced is 50 vol%. When CaO is added into the system, the maximum predicted H₂ concentration increases to 77 vol% at 900K [28].

Figure 2.10 shows the contour of concentration distribution of glycerol, steam, H₂ and CO₂ from steam reforming of glycerol from simulation results produced by B. Dou et al [38]. B. Dou et al. [38] used the computational fluid dynamic approach in order to simulate the gas-solid flow and reaction in the fluidized bed reactor.

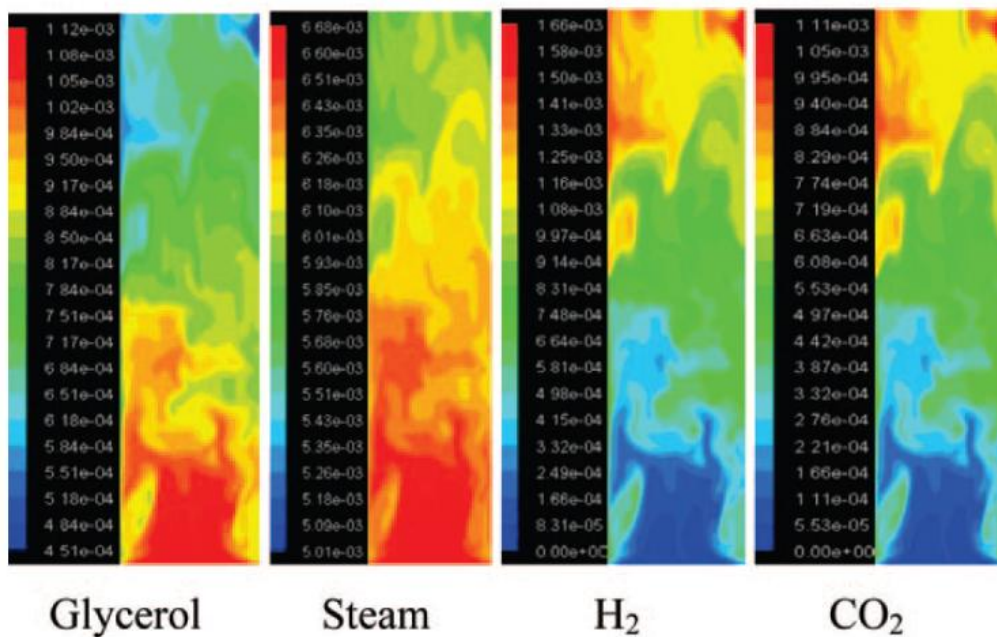


Figure 2.10 : Contour of concentration distribution of species in fluidized bed reactor [38]

The development of reaction model using CFD approach is still facing significant challenge especially in incorporating multiphase system with the reacting flow. In addition to that, on going research using CFD shows that it has high potential to be utilized especially for optimization of biomass gasification process. In this study, CFD approach is utilized in order to predict the production of H₂ and other species from biomass steam gasification in fluidized bed gasifier and also to study the effect of reaction condition to the quality of product gas produced.

CHAPTER 3

SIMULATION APPROACH AND METHOD

3.1 Computational Domain for Fluidized Bed Gasifier

One of the most important parts of CFD modelling is the construction of flow domain and grid topology. The advantages of CFD approach are it is time and cost saving, easy for scale up and safe to human being as compared to actual experimental set-up of fluidized bed gasifier. The magnificent of CFD is that it can predict the physical and chemical behaviour of a system by solving the numerical Navier-Stokes equations on certain 2D or 3D domain. Of course the 3D domain is much a representative of the actual case however, running a 3D simulation is rather time consuming and requires high human and computer capabilities. Based on previous work, a lot of studies have been done in order to solve the complex 3D system and making in into a much simpler 2D simulation and still providing prediction of results as good as the 3D simulation. The essential key in 2D simulation is to select the correct axissymmetry plane of a 3D domain based on certain assumptions.

The example of 3D domain of biomass gasifier is as shown in Figure 3.1. Figure 3.2 shows how the 2D axissymmetry plane was selected from the 3D domain. In order to select a good 2D axissymmetry plane of this 3D domain, first the bottom part of the 3D domain as indicated by line A need to be removed. This is because this bottom part creates a lot of mixing problem as both the biomass and steam enters here.

Based on the assumption of steam and biomass has a perfect mixing as it enters the gasifying zone, this bottom part of the gasifier can be removed. Once the bottom part is removed, the 3D domain left is just a simple cylinder. From the cylinder the cross-section was selected as the 2D axissymmetry plane. The domain grid was then generated in GAMBIT[®] software.

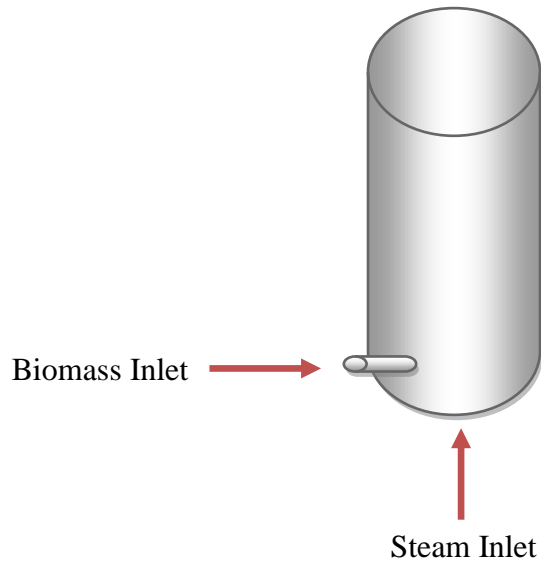


Figure 3.1: 3D domain of a fluidized bed gasifier

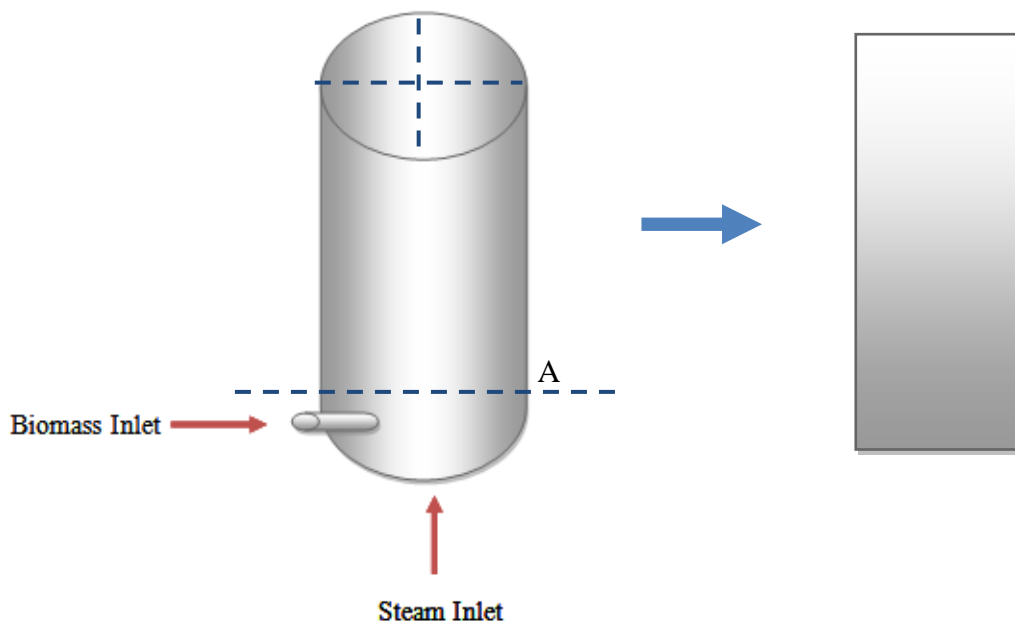


Figure 3.2: 2D Axissymmetry plane from the 3D domain

3.2 Grid Generation Study

In CFD, numerical sets of Navier-Stokes equations used for the simulation require an arrangement of discrete set of grids or cells in the flow field [83]. This is essential for accurate numerical simulation of fluid flow and heat transfer as more accurate approximation of the boundary shape and condition can be done. Consequently, the goal of grid or mesh generation is to transform the complex physical domain to a simple rectangular or triangle domain on which the crucial boundary conditions may be more accurately approximated [84].

The generation of computational grid or mesh should be done in such a way as to attain the following objectives:

- Minimize numerical error- Grid resolution and orientation with respect to flow direction may impact sources of numerical error such as round-off and truncation error.
- Provide numerical stability- The stability is depends on the size of the discretization element.
- Provide computational economy- More computation is required as the number of grid nodes increase, therefore optimum number of grids are important.
- Provide ease in handling boundary condition- In some cases, boundary condition may involve normal derivatives.

It is reported that grid or mesh spacing will affects the amount of numerical error and stability in the simulation [83, 84]. Therefore, in this grid generation study, five different grid sizes has been considered, which are 1.5mm, 1mm, 0.5mm, 0.3mm and 0.25mm. All these grids have been generated using the GAMBIT[®] V2.2.3 software. Figure 3.3 shows the grid generated in Gambit[®] V2.2.3 and Table 3.1 shows the number of cells generated for each of the grid size tested.

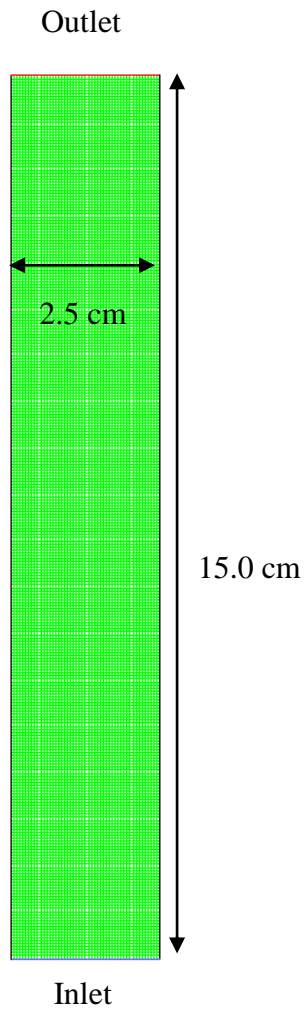


Figure 3.3: 2D grid of fluidized bed gasifier

Table 3.1: Number of cells for each grid size

Grid Size	No. of Cells
0.25 mm	60000
0.30 mm	41500
0.50 mm	15000
1.00 mm	3750
1.50 mm	1700

3.3 Hydrodynamics Model Development and Validation

The flow in the fluidized bed gasifier is a mixture of phases which are classified as solid, liquid or gas. The biomass particles exist in solid form while the gasifying agent is in the form of gas phase. This two phase flow of fluidized bed gasifier especially the bubbling phenomenon has been studied widely for the last three and a half decades especially on parameters that may affect the hydrodynamics, mass and heat transfer between the different phases at different flow regime [57]. The two phase flow of fluidized bed incorporates the phenomena of jetting, bubbling, slugging and dynamic mass and energy balances [20]. Figure 3.4 shows the discretization of fluidized bed gasifier into 3 different regions.

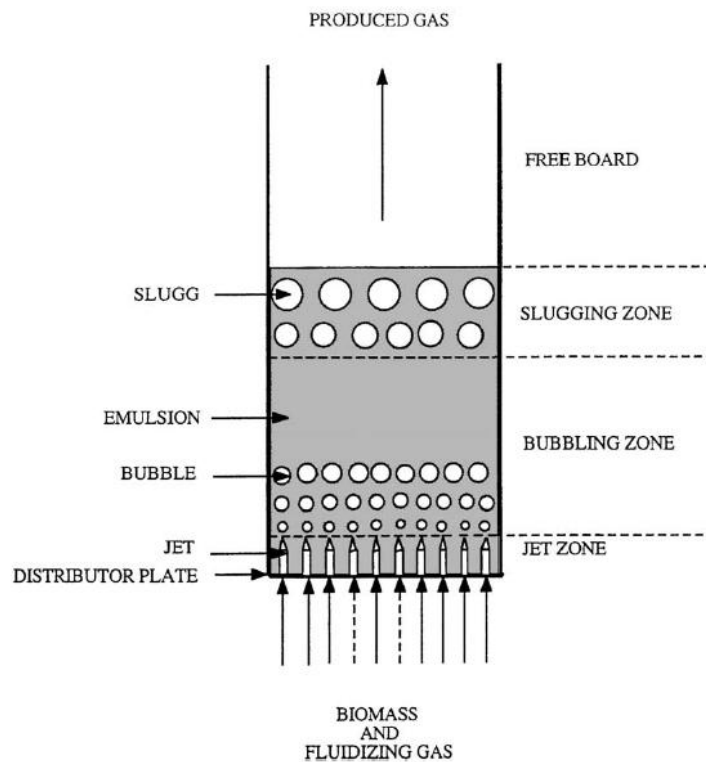


Figure 3.4: Flow regions in fluidized bed [20]

The fluidizing gas enters the bed through nozzles in a jet form and these jets degenerate into bubbles, which rise through the bed and grow by coalescence with other bubbles to form slugs. Slug is a bubble whose diameter becomes larger than one third of the reactor diameter. The formation of slug usually occurs in improper fluidization [20].

3.3.1 Minimum fluidization velocity

Fluidization occurs when a gas is forced to flow vertically through the bed of particles at such velocity that the buoyed weight of the particles is completely supported by the drag force imposed by the gas. The particles then able to move relatively to one another and have the fluid like behaviour [21]. The minimum velocity to fluidize the solid particles is called the minimum fluidization velocity (U_{mf}). The U_{mf} is a function of particle shape, size, density and fluidizing gas transport properties. In order to calculate the U_{mf} for the system, several assumptions have been made, which are:

- 1) The particle size are uniform size
- 2) The particle is sphere in shape
- 3) Particle density and viscosity are taken at reference temperature of 25 °C at atmospheric pressure
- 4) Fluidizing gas density and viscosity are taken at reference temperature of 25 °C at atmospheric pressure

The equation used to calculate the U_{mf} is as shown in Table 3.2.

Table 3.2: Equation for U_{mf} calculation

No.	Description	Equation	References
1	Minimum Fluidization Velocity	$U_{mf} = \left(\frac{\mu_g}{d_p \rho_g} \right) \left((27.2^2 + 0.0408Ar)^{1/2} - 27.2 \right)$	[85]
2	Archimedes number (Ar)	$Ar = \frac{d_p^3 \rho_g (\rho_s - \rho_g) g}{\mu_g^2}$	[20]

3.3.2 Modelling multiphase flow

Base on previous studies, Eulerian-Eulerian approach is the most suitable approach in order to model the hydrodynamics of fluidized bed gasifier that involves multiphase system and large number of solid particles. There are several multiphase flow models available under Eulerian-Eulerian approach, which is shown in Table 3.3. Based on the suitability of each model, Eulerian multiphase model is the preferred choice for simulating fluidized bed gasifier. The general idea in formulating multiphase model is to treat each phase as an interpenetrating continuum and therefore to construct integral balances of continuity, momentum and energy for both phases.

Table 3.3: Multiphase model for Eulerian-Eulerian approach [32]

No.	Multiphase model	Description
1	Volume of Fluid (VOF)	Surface tracking technique applied on fixed Eulerian mesh
2	Mixture	Simplified Eulerian approach based on small stokes numbers. Design for two or more phases. Each phases is treated as penetrating continua
3	Eulerian	The most complex multiphase model that solve conservation equation for each phase. Suitable for granular flow (fluid-solid)

Appropriate assumptions need to be made in order to obtain a complete momentum balance. The assumptions for the model are:

- 1) A single pressure is shared by all phases
- 2) Solid fluctuating energy (granular temperature) is solve using partial differential equation
- 3) Solid phase shear and bulk viscosities are obtain by KTGF
- 4) Frictional viscosity is neglected
- 5) The flow in the system is Laminar flow

Simulations of the bubbling behaviour of the fluidized bed were performed by solving equations of motion of a multiphase system. KTGF also needs to be applied in order to solve the conservation of the solid's fluctuation energy. For the present case of two-phase flow, the model has to solve several equations related to scalar continuity equation, mass and momentum balance equations.

Volume Fraction

For Eulerian-Eulerian model, the volume fractions are assumed to be continuous functions of space and time, and their sum is equal to one since the volume of one phase can never be occupied by the other phase as shown below [32]:

$$\varepsilon_g + \varepsilon_s = 1 \quad (3.1)$$

Continuity Equation

The continuity equation for gas and solid phases are given by [32]:

$$\frac{\partial}{\partial t} (\varepsilon_g \rho_g) + \nabla \cdot (\varepsilon_g \rho_g \vec{v}_g) = 0 \quad (3.2)$$

$$\frac{\partial}{\partial t} (\varepsilon_s \rho_s) + \nabla \cdot (\varepsilon_s \rho_s \vec{v}_s) = 0 \quad (3.3)$$

Momentum Equation

The momentum balance equations for each phase are derived based on the assumption of there are no mass transfer between the two phases and no lift force, external body force and virtual mass force acting on the secondary phase of the system. The momentum balance equations for each phase are as follows [32]:

$$\frac{\partial}{\partial t} (\varepsilon_g \rho_g \vec{v}_g) + \nabla \cdot (\varepsilon_g \rho_g \vec{v}_g \vec{v}_g) = \nabla \cdot \overline{\overline{S}}_g + \varepsilon_g \rho_g \vec{g} - \vec{I}_g \quad (3.4)$$

$$\frac{\partial}{\partial t} (\varepsilon_s \rho_s \vec{v}_s) + \nabla \cdot (\varepsilon_s \rho_s \vec{v}_s \vec{v}_s) = \nabla \cdot \overline{\overline{S}}_s + \varepsilon_s \rho_s \vec{g} - \vec{I}_g \quad (3.5)$$

The interphase momentum change is further defined by the granular kinetic theory in order to estimate the rheological properties for the solid phase. Standard drag models are also employed to estimate the momentum exchange between phases at the particle boundaries.

$$\vec{I}_g = -\varepsilon_s \nabla P_g - F_g (\vec{v}_s - \vec{v}_g) \quad (3.6)$$

The fluid-solid momentum exchange coefficient in the interphase momentum change equation for dense fluidized bed can be further described by Gidaspow drag function as follows [86]:

For $\varepsilon_g > 0.8$:

$$F_g = \frac{3}{4} \frac{\varepsilon_s \varepsilon_g \rho_g}{d_p} C_{ds} |\vec{v}_s - \vec{v}_g| \varepsilon_s^{-2.65} \quad (3.7)$$

For $\varepsilon_g \leq 0.8$:

$$F_g = 150 \frac{\varepsilon_s (1 - \varepsilon_g) \mu_g}{\varepsilon_g d_p^2} + 1.75 \frac{\rho_g \varepsilon_s |\vec{v}_s - \vec{v}_g|}{d_p} \quad (3.8)$$

Where:

$$C_{ds} = \frac{24}{\varepsilon_g Re_s} \left[1 + 0.15 (\varepsilon_g Re_s)^{0.687} \right] \quad (3.9)$$

$$Re_s = \frac{\rho_g d_p |\vec{v}_s - \vec{v}_g|}{\mu_g} \quad (3.10)$$

For granular flows in the compressible regime where the solid volume fraction is less than its maximum allowed value, a solid pressure is calculated independently and used for the pressure gradient term in the granular-phase momentum equation. Because a Maxwellian velocity distribution is used for the particles, a granular temperature is introduced into the model and appears in the expression for the solid pressure and viscosities [87]. The solid pressure is composed of a kinetic term and particle collisions term:

$$P_s = \varepsilon_s \rho_s \theta_s (1 + 2g_0 \varepsilon_s (1 + e_s)) \quad (3.11)$$

Radial distribution function is a correction factor that modifies the probability of collisions between grains when solid granular phase becomes dense. For one solid phase, the equation for radial distribution function is as follows [32]:

$$g_0 = \left[1 - \left(\frac{\varepsilon_s}{\varepsilon_s^{max}} \right)^{1/3} \right]^{-1} \quad (3.12)$$

Solid stress tensor contains shear and bulk viscosities arising from particle momentum exchange due to translation and collision. In this simulation, frictional component of viscosity is assumed negligible. The solid shear stress equation with collisional and Gidaspow [86] kinetic viscosity is as follows:

$$\mu_s = \frac{4}{5} \varepsilon_s \rho_s d_p g_0 (1 + e_s) \left(\frac{\theta_s}{\pi} \right)^{0.5} + \frac{10 \rho_s d_p \sqrt{\theta_s \pi}}{96(1+e_s) \varepsilon_s g_0} \left[1 + \frac{4}{5} g_0 \varepsilon_s (1 + e_s) \right]^2 \quad (3.13)$$

Solid bulk viscosity accounts for the resistance of the granular particles to compression and expansion. In Fluent, the solid bulk viscosity has the following form from Lun et al. [87]:

$$\lambda_s = \frac{4}{3} \varepsilon_s \rho_s d_p g_0 (1 + e_s) \left(\frac{\theta_s}{\pi} \right)^{0.5} \quad (3.14)$$

Kinetic Theory of Granular Flow (KTGF)

The transport equation derived from kinetic theory takes the form as follows [32]:

$$\frac{3}{2} \left[\frac{\partial}{\partial t} (\rho_s \varepsilon_s \theta_s) + \nabla \cdot (\rho_s \varepsilon_s \vec{v}_s \theta_s) \right] = (-P_s \bar{I} + \bar{\tau}_s) : \nabla \vec{v}_s + \nabla \cdot (k_{\theta_s} \nabla \theta_s) - \gamma_{\theta_s} + \phi_{gs} \quad (3.15)$$

The diffusion coefficient is further described by Gidaspow [86] as follow:

$$k_{\theta_s} = \frac{150 \rho_s d_p \sqrt{\theta_s \pi}}{384 (1+e_s) g_0} \left[1 + \frac{6}{5} \varepsilon_s g_0 (1 + e_s) \right]^2 + 2 \rho_s \varepsilon_s^2 d_p g_0 (1 + e_s) \sqrt{\frac{\theta_s}{\pi}} \quad (3.16)$$

The collisional dissipation energy represent the rate of energy dissipate within the solid phase due to collisions between particles. This term is represented by the equation derived by Lun et al. [87]:

$$\gamma_{\theta_s} = \frac{12 (1-e_s^2) \rho_s g_0}{d_p \sqrt{\pi}} \varepsilon_s^2 \theta_s^{3/2} \quad (3.17)$$

3.3.3 Hydrodynamics Model Validation

The model was validated using the results obtained by Busiglio et al. [30]. The domain dimension and simulation parameters used in the validation model are the same as used by Busiglio et al. [30], which are shown in Figure 3.5 and Table 3.4, respectively.

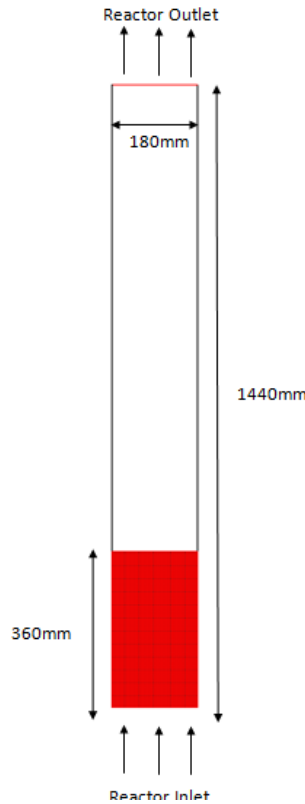


Figure 3.5: Domain dimension for model validation

Table 3.4: Simulation Parameters for model validation

Property	Value	Remarks
Solid density, ρ_s	2500 kg/m ³	Glass Ballotini
Solid particle diameter, d_p	231 μ m	Fixed
Solid viscosity, μ_s	1.72 x 10 ⁻⁵ kg/m.s	Constant
Air density, ρ_g	1.225 kg/m ³	Air
Air viscosity, μ_g	1.7894 x 10 ⁻⁵ kg/m.s	Constant
Superficial gas velocity	0.0891 m/s	Constant
Restitution coefficient	0.9	Busiglio et al., 2009
Initial solid packing	0.65	Busiglio et al., 2009
Maximum solid packing	0.8	Fixed
Static bed height	360 mm	Constant
Bed width	180 mm	Constant
Gravitational force	9.81 m/s ²	Constant

3.3.4 Hydrodynamics model variables and simulation parameters

The fluidization quality of a bed is highly dependent on the distribution of bubbles and bubble dynamics [54]. Ideally, good quality of fluidization must have high population of bubbles, bed should be large but bubbles should be small in size, homogeneously occupy the bed and have low rise velocities. This shows that studies on bubbles are important for investigating fluidized bed fluid dynamic [30, 57].

The main objective of this simulation is to study the solid fluidization in the fluidized bed gasifier with respect to the change in inlet velocity of steam, bed height to diameter ratio (H/D) and particle size. The summary of case studies table and the simulation parameters used in the model are shown in Table 3.5 and Table 3.6, respectively.

Table 3.5: Hydrodynamics model case studies

No. Case	Steam Inlet Velocity (m/s)	Bed Height to Diameter Ratio (H/D)	Solid Particle Size (μm)
1	0.1443 (3Umf)	2 (5.0cm)	250
2	0.1684 (3.5Umf)	2 (5.0cm)	250
3	0.1924 (4Umf)	2 (5.0cm)	250
4	0.2405 (5Umf)	2 (5.0cm)	250
5	0.1684 (3.5Umf)	3 (7.5cm)	250
6	0.1684 (3.5Umf)	4 (10cm)	250
7	0.1684 (3.5Umf)	5 (12.5cm)	250
8	0.1684 (3.5Umf)	2 (5.0cm)	100
9	0.1684 (3.5Umf)	2 (5.0cm)	300
10	0.1684 (3.5Umf)	2 (5.0cm)	400

Table 3.6 : Simulation Parameters for Biomass Gasifier

Property	Value	Remarks
Biomass density, ρ_s	2000kg/m ³	Carbon (s)
Biomass particle diameter, d_p	250 μ m	Fixed
Biomass viscosity, μ_s	1.72 x 10 ⁻⁵ kg/m.s	Constant
Min fluidization velocity, u_{mf}	0.028m/s	Constant
Water vapor density, ρ_g	0.5kg/m ³	Water-Vapor
Water vapor viscosity, μ_g	1.9 x 10 ⁻⁵ kg/m.s	Constant
Restitution coefficient	0.9	Busiglio et al., 2009
Initial solid packing	0.65	Busiglio et al., 2009
Maximum solid packing	0.95	Fixed
Bed width	25mm	Design required
Gravitational force	9.81m/s ²	Constant

In order to study solid mixing in the fluidized bed, solid concentration from five different locations has been measured from Fluent[®]. The five different locations are shown in Figure 3.6.

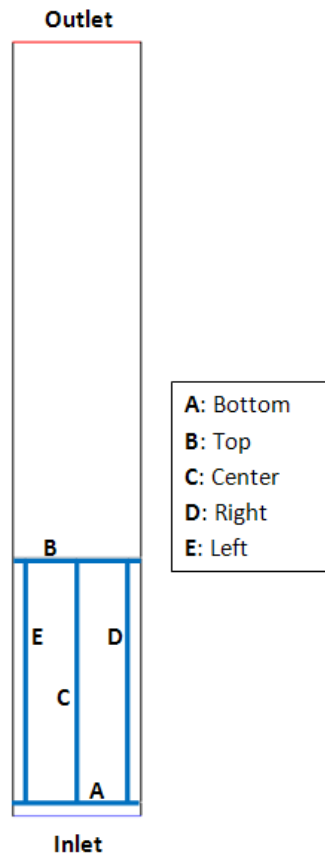


Figure 3.6: Location of solid concentration analysis

3.4 Reaction Model Development and Validation

Biomass gasification has been identified as a potential method for producing H₂ [3, 5]. Gasification is the conversion of biomass into gaseous fuel by heating in a gasification medium such as air, oxygen or steam [8]. Biomass gasification process involves multiple simultaneous reactions. These reactions need to be solved by the reaction model in Fluent.

3.4.1 Modelling reacting flow

CFD approach can be used in order to model the mixing and transport of chemical species by solving conservation equations of convection, diffusion and reaction source for each component species in the system. Multiple simultaneous chemical reactions occurring in bulk phase (volumetric reaction), on wall or particle surfaces and in the porous region can be modelled. Fluent provides several models for chemical species transport and chemical reaction. Chemical reactions that can be modelled by Fluent[®] are shown in Table 3.7.

The volumetric reaction model or also known as generalized finite rate model is suitable for wide range of application including laminar and turbulence reaction system, and combustion system with premixed, non-premixed or partially-premixed flames. In the volumetric model, Fluent[®] predict the local mass fraction of each species by solving the convection-diffusion equation for each of the species involved in the species. The general conservation equation is in the following form [88]:

$$\frac{\partial}{\partial t}(\rho Y_i) + \nabla \cdot (\rho \vec{v} Y_i) = -\nabla \cdot \vec{J}_i + R_i + S_i \quad (3.18)$$

This equation will be solved for $N-1$ species where N is the total number of species in the system. Since the summation of mass fraction is equal to 1, the N th mass fraction is determined as 1 minus the sum of the $N-1$ solved mass fraction. The reaction rate term (R_i) are computed in Fluent[®] by one of the three model as stated in Table 3.8.

Table 3.7: Chemical Reactions

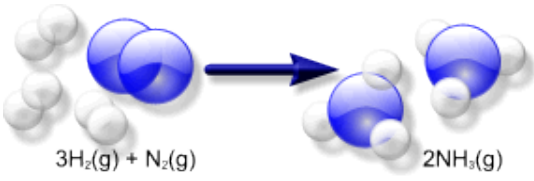
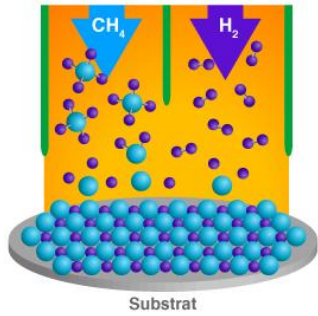
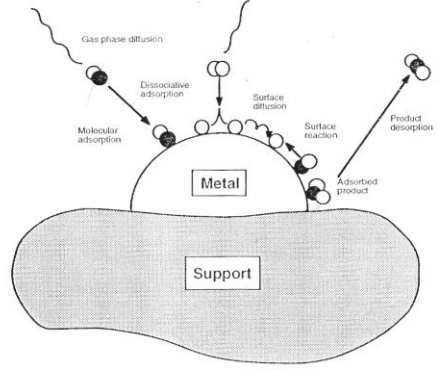
Chemical Reaction	Description	Example
Volumetric reaction	Homogeneous chemical reaction in single phase	<p>Haber reaction [89]</p>  <p>$3\text{H}_2(\text{g}) + \text{N}_2(\text{g}) \rightarrow 2\text{NH}_3(\text{g})$</p>
Surface reaction	Reaction that occurs at solid wall boundary	<p>Chemical vapor deposition reaction [90]</p>  <p>Substrat</p>
Particle surface reaction	Reaction that occurs at the surface of discrete-phase particle	<p>Catalytic reaction [91]</p> 

Table 3.8 : Generalized finite-rate model

No.	Generalized Finite Rate Model	Description
1.	Laminar finite-rate model	The effect of turbulent fluctuations are ignored, and reaction rates are determined by Arrhenius expression
2.	Eddy-dissipation model	Reaction rates are assumed to be controlled by the turbulence, therefore Arrhenius chemical kinetic calculations can be avoided.
3.	Eddy-dissipation-concept (EDC) model	Detailed Arrhenius chemical kinetics can be incorporated in turbulent flames.

In surface reaction model, the gas phase reaction is defined on a volumetric basis and the rate of creation and destruction of chemical species becomes the source term in the species conservation equation. The rate of deposition is governed by both the chemical kinetics and the diffusion rate from the fluid to the surface. The surface reaction thus create source and sinks of chemical species in the bulk phase and determine the rate of deposition of the surface species. Surface reaction can be limited so that they can only occur at some of the wall boundary in the system. The reaction rate in surface reaction model is defined and computed per unit surface area in contrast to the volumetric reaction model which are based on unit volume.

Particle surface reaction model is mainly used for fundamental study of reaction process especially for combustion. Multiple simultaneous equations that occur on discrete-phase particle can be modelled. Figure 3.7 shows the example of one particle undergoing a reaction in the gas phase. Table 3.9 shows the type of reaction that can be modelled using the particle surface reaction model. In general, for particle surface reaction model, the rate of reaction is given as the following equation:

$$R_{j,r} = R_{kin,r} \left(p_n - \frac{R_{j,r}}{D_{0,r}} \right)^{N_r} \quad (3.19)$$

And the kinetic rate of reaction is further defined as Arrhenius equation:

$$R_{kin,r} = A_r T^\beta e^{-(E_r/RT)} \quad (3.20)$$

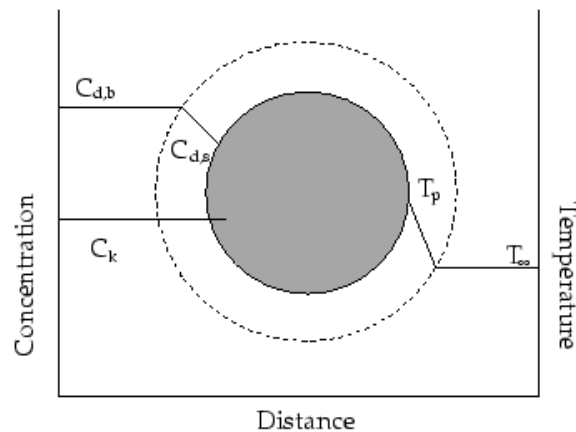


Figure 3.7 : Reacting particle in particle surface reaction model

Table 3.9 : Particle surface reaction model

No.	Types of reaction	Description	Remarks
1.	Gas-Solid	$particle\ species\ j(s)$ + $gas\ phase\ species\ (n)$ → $products$	Can be both endothermic and exothermic
2.	Solid-solid	$particle\ species\ 1(s)$ + $particle\ species\ 2(s)$ → $products$	Particle surface reactants and product exist on the same particle
3.	Solid decomposition	$particle\ species\ 1(s)$ + $particle\ species\ n_{max}(s)$ → $gas\ species\ (j) + products$	Diffusion limited species is the gaseous product of the reaction
4.	Solid deposition	$gas\ species\ 1$ + $gas\ species\ n_{max}(s)$ → $solid\ species\ j(s) + products$	For the particle surface species to be deposited on a particle, a finite mass of the species must already exist in the particle
5.	Gas-solid catalyzed reaction	The solid particle species does not involve in the reaction	The solid species acting as catalyst is defined in the reaction model however there is no solid species in the reaction stoichiometry

Biomass gasification in fluidized bed gasifier is a two-phase system consists of solid and gas. Since biomass gasification reaction is an endothermic reaction, the temperature inside the gasifier tends to decrease as the reaction occurs inside the gasifier. For this reason, heat input is necessary in the system in order to keep the temperature inside the gasifier constant. Steam at 250 °C is introduced into the system as the heat supply to heat up the gasifier. The fundamental problem encountered in modelling heat transfer mechanism of gas-solid fluidized bed is the phase interface and interactions between the variables are understood only for a limited range of condition. In order to improve the performance of the model, several assumptions have to be made in order to simplify the complex gas-solid system.

One of the assumptions made is that, as soon as the solid biomass enters the bottom of the gasifier, an exquisite contact occurs between the solid biomass and the hot steam followed by intense exchange of heat and mass. This makes the major part of the carbon content of biomass is instantaneously converted into gaseous compounds. Therefore, all of the major biomass gasification reactions will occurs in homogeneous gas phase. Based on this assumption, volumetric reaction model is the most suitable model for biomass gasification.

The flow inside the gasifier also is a laminar flow since the calculated Reynolds number is less than 2000, therefore, Laminar finite-rate model is used in order to calculate the reaction rate using the Arrhenius expression. According to literature [14, 49, 61], the carbon content in biomass is normally in the range of 36-60%. Therefore, in this study, the carbon content in the biomass is assumed to be 50% based on weight. There are also several other assumptions considered in modelling the gasification process:

- The process is in steady-state.
- All the gases are uniformly distributed in the gasifier.
- Reaction does not dependant on pressure.
- The gasifying agent is pure steam.
- Fluid in the system is incompressible.

3.4.2 Modelling Species Transport and Finite-Rate Chemistry

Fluent[®] can model the missing and transport of chemical species by solving several conservation equations related to convection, diffusion and reaction sources for each component species. In the volumetric reaction model, the model was used to solve several equations related to continuity balance equation, mass and momentum balance equation and also to predict the H₂ production from the gasifier.

Continuity Equation

The continuity equation which was derived from the concept of conservation of mass can be written as follows [32]:

$$\frac{\partial \rho}{\partial t} + \nabla \cdot (\rho \vec{v}) = S_m \quad (3.21)$$

Momentum Conservation Equation

Conservation of momentum equation that is used in Fluent is as shown below [32]:

$$\frac{\partial}{\partial t} (\rho \vec{v}) + \nabla \cdot (\rho \vec{v} \vec{v}) = -\nabla p + \nabla \cdot (\bar{\tau}) + \rho \vec{g} + \vec{F} \quad (3.22)$$

And stress tensor is given by [32]:

$$\bar{\tau} = \mu \left[(\nabla \vec{v} + \nabla \vec{v}^T) - \frac{2}{3} \nabla \cdot \vec{v} I \right] \quad (3.23)$$

Energy balance equation

Fluent solve the energy equation in the following form [32]:

$$\frac{\partial(\rho E)}{\partial t} + \nabla \cdot (\vec{v}(\rho E + p)) = \nabla \cdot (k_{eff} \Delta T - \sum_j h_j \vec{J}_j + (\vec{\tau}_{eff} \cdot \vec{v})) + S_h \quad (3.24)$$

This energy equation includes pressure work and kinetic energy terms. However, for incompressible flow, these two terms are often negligible. Therefore, in this model pressure-based solver was used because in the pressure-based solver by default does not include the pressure work or kinetic energy for incompressible flow [32].

From (3.24):

$$E = h - \frac{p}{\rho} + \frac{v^2}{2} \quad (3.25)$$

Where h is further define as [32]:

$$h = \sum_j Y_j h_j \quad (3.26)$$

And

$$h_j = \int_{T_{ref}}^T c_{p,j} dt \quad (3.27)$$

The source term, S_h , in the energy equation include the source of energy due to chemical reaction which can be written as [32]:

$$S_{h,rxn} = -\sum_j \frac{h_j^0}{M_j} R_j \quad (3.28)$$

The source term also includes the energy source from radiation heat transfer. In this model, Rosseland radiation model from Fluent has been used to simulate the heating of incompressible fluid in the gasifier. The general radiative transfer equation used in Fluent is as follows [32]:

$$\frac{dI(\vec{r}, \vec{s})}{ds} + (a + \sigma_s)I(\vec{r}, \vec{s}) = an^2 \frac{\sigma T^4}{\pi} + \frac{\sigma_s}{4\pi} \int_0^{4\pi} I(\vec{r}, \vec{s}') \Phi(\vec{s}, \vec{s}') d\Omega' \quad (3.29)$$

For Rosseland radiation model, radiative heat flux vector can be approximated by the following equation [32]:

$$q_r = -\Gamma \nabla G \quad (3.30)$$

And:

$$\Gamma = \frac{1}{(3(a+\sigma_s)) - c\sigma_s} \quad (3.31)$$

The incident radiation from (3-30) can be calculated from the equation [32]:

$$G = 4\sigma n^2 T^4 \quad (3.32)$$

Replacing G into (3.30) yield:

$$q_r = -16\sigma\Gamma n^2 T^3 \nabla T \quad (3.33)$$

Since (3.33) has the same form as the Fourier conduction law, it is possible to write it as equation (3.34). This equation is use in the energy equation to compute the temperature field [32].

$$q = q_c + q_r = -(k + k_r) \nabla T \quad (3.34)$$

And

$$k_r = 16\sigma\Gamma n^2 T^3 \quad (3.35)$$

Fluent models anisotropic scattering by means of a linear-anisotropic scattering phase function [32]:

$$\Phi(\vec{s}' \cdot \vec{s}) = 1 + C\vec{s}' \cdot \vec{s} \quad (3.36)$$

Species transport equation

In order to solve the conservation equation for chemical species, Fluent predicts the local mass fraction of species, Y_i , through the solution of a convection-diffusion equation for the i th species. The conservation equation takes the following general form [32]:

$$\frac{\partial}{\partial t}(\rho Y_i) + \nabla \cdot (\rho \vec{v} Y_i) = -\nabla \cdot \vec{J}_i + R_i + S_i \quad (3.37)$$

This equation will be solve for N - I species where N is the total number of fluid phase chemical species present in the system. Since the mass fraction of the species must sum to unity, the N^{th} species should be selected as the species with the overall largest mass fraction. The term \vec{J}_i in the above equation is the diffusion flux of species i , which arises due to concentration gradients. By using the dilute approximation, the diffusion flux can be written as [32]:

$$\vec{J}_i = -\rho D_{i,m} \nabla Y_i \quad (3.38)$$

Finite-rate formulation for reaction modeling

The reaction rate source term, R_i , in the species transport equation is computed by laminar finite-rate model in Fluent. This model neglect the effect of turbulent fluctuations and reaction rates are determined by Arrhenius expressions. The net source of chemical species i due to reaction is computed as the sum of the Arrhenius reaction source over the N_R reactions that the species participate in [32]:

$$R_i = M_{w,i} \sum_{r=1}^{N_R} \hat{R}_{i,r} \quad (3.39)$$

Consider the r^{th} reaction is written in general form as follows:

$$\sum_{i=1}^N v'_{i,r} M_i \vec{k}_{b,r/f,r} \sum_{i=1}^N v''_{i,r} M_i \quad (3.40)$$

For non-reversible reaction, the backward rate constant is simply omitted. The summations in the above equation are for all chemical species in the system, but only species that appears as reactants or products will have non-zero stoichiometric coefficient. Hence, species that are not involved will drop out of the equation.

For non-reversible reaction, the molar rate of creation/destruction of species i in the reaction $r, \hat{R}_{i,r}$, is given by [32]:

$$\hat{R}_{i,r} = \Gamma (v''_{i,r} - v'_{i,r}) \left(k_{f,r} \prod_{j=1}^N [C_{j,r}]^{(n'_{j,r} + n''_{j,r})} \right) \quad (3.41)$$

The term Γ in (9.38) represents the net effect of third bodies on the reaction rate. This term is given by [32]:

$$\Gamma = \sum_j^N Y_{j,r} C_j \quad (3.42)$$

For this study, the third body effect is not included in the reaction rate calculation.

The forward rate constant for reaction $r, k_{f,r}$, is computed using the Arrhenius expression [32]:

$$k_{f,r} = A_r T^{\beta_r} e^{-E_r/RT} \quad (3.43)$$

3.4.3 Defining mixture components and its physical properties

Biomass gasification reaction involves multiple species that involves during the reaction process as reactant and also products. All these species are defined as component of mixture template in the reaction model. For this model, the mixture components are consists of chemical species as listed below:

- 1) Biomass, C
- 2) Steam, H₂O
- 3) Hydrogen, H₂
- 4) Carbon Monoxide, CO
- 5) Carbon Dioxide, CO₂
- 6) Methane, CH₄
- 7) Calcium Oxide, CaO
- 8) Calcium Carbonate, CaCO₃
- 9) Nitrogen, N₂

The physical properties for the mixture material must be defined in Fluent[®]. The physical properties required are density, viscosity, thermal conductivity, specific heat capacity and mass diffusion coefficients. For density, the incompressible ideal gas law is used to solve the density of the mixture using the equation below:

$$\rho = \frac{P_{op}}{\frac{R}{M_w}T} \quad (3.44)$$

There are two different options that can be used to calculate the viscosity of the mixture material. One is using the mass weighted mixing law or the ideal gas mixing law. Since the density of the mixture material is assumed to be behaving similar like the ideal gas, the viscosity also is assumed to have similar behaviour. In ideal gas law, the viscosity of mixture material is calculated based on kinetic theory as follows:

$$\mu = \sum_i \frac{X_i \mu_i}{\sum_j X_j \phi_{ij}} \quad (3.45)$$

Where [69]

$$\phi_{ij} = \frac{\left[1 + \left(\frac{\mu_j}{\mu_i}\right)^{1/2} \left(\frac{M_{w,j}}{M_{w,i}}\right)^{1/4}\right]^2}{\left[8 \left(1 + \frac{M_{w,i}}{M_{w,j}}\right)\right]^{1/2}} \quad (3.46)$$

The composition dependent thermal conductivity is also calculated using the ideal gas law. The mixture thermal conductivity is calculated based on kinetic theory as follows [69]:

$$k = \sum_i \frac{X_i k_i}{\sum_j X_j \phi_{ij}} \quad (3.47)$$

The specific heat capacity is defined as a mass fraction average of the pure species heat capacities as shown in the equation below:

$$c_p = \sum_i Y_i c_{p,i} \quad (3.48)$$

Mass diffusion coefficient is required in order to solve the transport equation for multicomponent flows. The mass diffusion coefficient is used to calculate the mass diffusion flux of chemical species using the Fick's law:

$$J_i = -\rho D_{i,m} \nabla Y_i \quad (3.49)$$

Where the diffusion coefficient of the mixture $D_{i,m}$ is calculated from the binary mass diffusion coefficient $D_{i,j}$ as follows [69]:

$$D_{i,m} = \frac{1-X_i}{\sum_{j \neq i} \frac{X_j}{D_{i,j}}} \quad (3.50)$$

3.4.4 Defining Reactions

As part of the reaction model, the complicated process of biomass gasification reactions were simulated as the source term of species transport equations when the reactants were consumed and the products were created. In this work there are six main reactions, which are assumed to occur in the fluidized bed gasifier including the CO₂ adsorption reaction. The six main reactions are as shown in Table 3.10.

Table 3.10: Main Biomass Gasification Reactions

Label	Name of Reaction	Chemical Reaction Equation
R1	Biomass Gasification	$C + H_2O \rightarrow CO + H_2$
R2	Boudouard	$C + CO_2 \rightarrow 2CO$
R3	Water-gas Shift	$CO + H_2O \rightarrow CO_2 + H_2$
R4	Methanation	$C + 2H_2 \rightarrow CH_4$
R5	Methane Reforming	$CH_4 + H_2O \rightarrow CO + 3H_2$
R6	Absorption	$CaO + CO_2 \leftrightarrow CaCO_3$

All of the reactions are solved using the laminar finite-rate reaction model in Fluent[®]. In laminar finite-rate reaction model, the kinetic parameters such as the Pre-exponential factor and activation energy are the required parameters in order to calculate the Arrhenius rate. Therefore, the kinetic parameters from literature that have been developed from experimental of coal, cellulose and various types of biomass have been utilized for the reaction model. The kinetic parameters used in this work are shown in Table 3.11.

Table 3.11: Kinetic data for reaction model

Reaction	Pre-exponential Factor	Activation Energy (kJ/mol)	References
R1	2.0×10^5	6000	[92-94]
R2	1.0×10^6	6370	[92, 95]
R3	4.4	1.62×10^8	[95, 96]
R4	0.12	17921	[95, 97]
R5	3.0×10^5	15000	[24, 92, 98]
R6	10.2	44.5	[99, 100]

The Stiff Laminar Chemistry System solution is also used for the laminar finite-rate reaction model. This is to provide better solution stability and to allow larger Courant (CFL) number specification.

3.4.5 Reaction model validation

The reaction model developed in Fluent[®] was validated with experimental and simulation data from literature. Since Busciglio et al. [30] does not perform experimental or simulation on biomass gasification reaction, other literature data are used for model validation. The simulated H₂ production from the model is validated with results obtained by Mehrdokht et al. [22], P.M. Lv et al. [59] and N. Gao et al. [61]. Mehrdokht et al. [22] had developed a comprehensive process model for biomass gasification in ASPEN PLUS software. P.M. Lv et al. [59] have investigated biomass air gasification in a small scale fluidized bed and N. Gao et al. [61] had run experiments on biomass air-steam gasification. The details of simulation parameters for model validation are as shown in Table 3.12.

Table 3.12 : Simulation parameters for model validation

Parameters	Value
Biomass mass flow rate (kg/s)	1.25×10^{-3}
Steam mass flow rate (kg/s)	2.5×10^{-3}
Gasifier Temperature (°C)	800
Gasifier Pressure (kPa)	101.325
Steam Temperature (°C)	250

3.4.6 Reaction model variables

Based on previous studies, it shows that H₂ production is highly affected by the reaction condition in the gasifier. Therefore, obtaining the optimum condition in which the highest H₂ production could be obtained is essential. The main objective of this simulation is to study the effect of reaction temperature and steam to biomass ratio (S/B) to the H₂ production from biomass gasifier using the model developed in Fluent. The pressure of the gasifier was kept constant at 1 atm in this study. The summary of case studies for reaction model is as shown in Table 3.13.

Table 3.13 : Case studies for reaction model

No. Case	Gasifier Temperature (°C)	Steam to Biomass Ratio (S/B)
11	700	2
12	750	2
13	800	2
14	850	2
15	900	2
16	850	1
17	850	2.5
18	850	3

The addition of CO₂ adsorbent was proven previously by researchers can improve the H₂ production from the gasifier as the reversible water-gas shift reaction can be pushed forward when the CO₂ is removed from the system. The removal of CO₂ from the system also may increase the purity of H₂ coming out from the gasifier. The effect of CO₂ adsorbent to the H₂ production can be observed by adding the CO₂ adsorption reaction into the reaction model. The CO₂ adsorption reaction is as follows:



This CO₂ adsorption reaction is an exothermic reaction which much favourable at lower temperature. However, the conventional gasification reaction usually occurs at high temperature (700-900°C). In order to observe the effect of CO₂ adsorbent to H₂ production from the gasifier, the gasifier temperature has to be reduced to 600-750 °C. The gasification condition in the gasifier needs to be further optimized with respect to reaction temperature and adsorbent to biomass ratio (A/B) with in-situ CO₂ adsorbent in the system. The summary of case studies for gasification with in-situ CO₂ adsorbent is as shown in Table 3.14.

Table 3.14 : Variable values for in-situ CO₂ adsorption

No. Case	Gasifier Temperature (°C)	Adsorbent to Biomass Ratio (A/B)
19	550	1
20	600	1
21	650	1
22	700	1
23	750	1
24	650	2
25	650	3
26	650	4

CHAPTER 4

RESULTS AND DISCUSSIONS

4.1 Grid generation study

Figure 4.1 shows the flow velocity and flow shape for five different mesh sizes obtained from the grid generation study. From the figure, it is observed that different mesh sizes do affect the results of numerical simulation. From the graph, it is observed that the flow velocity become stabilized and the solution converged as the mesh size decrease. This is because the velocity differences between 0.5mm, 0.3mm and 0.25mm mesh size are insignificant and the flow shapes also show the same trend. This shows that, at mesh size 0.5mm and below, the numerical results become independent to the mesh size, which means further decrease of mesh size will not change the numerical results obtain from the simulation.

Therefore, within the mesh size studied, it is conclude that, the most suitable mesh size is from 0.5mm-0.25mm. However, smaller mesh size require more computation time and processor capability. This makes mesh size that is too small is no longer economic. Thus, in this case, 0.5mm mesh size is taken as the most optimum mesh size for the reaction model. This is because at 0.5mm mesh size, the result of numerical simulation is no longer dependant on the mesh size which minimizes numerical error, provides numerical stability, provides ease in handling boundary condition and at the same time it is still computationally economic.

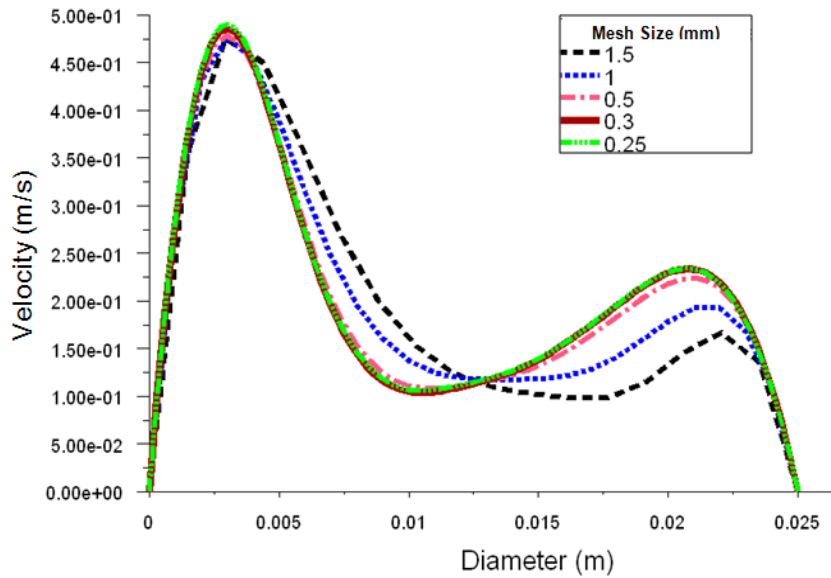


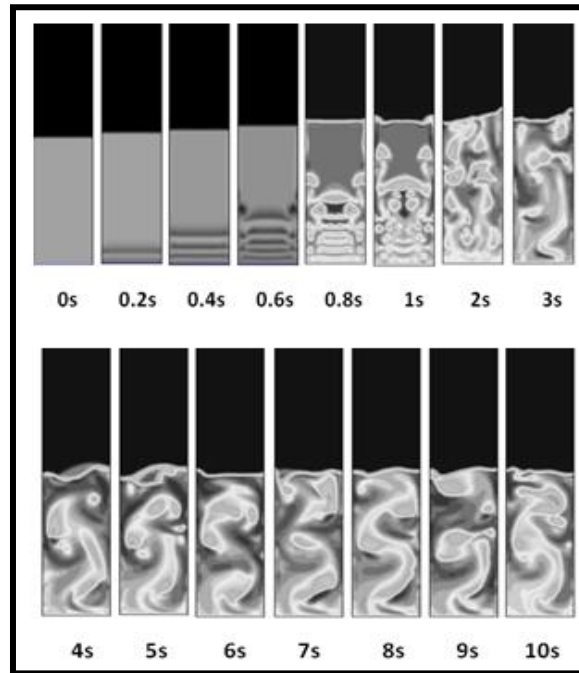
Figure 4.1: Flow velocity magnitude for different mesh sizes

4.2 Hydrodynamics model

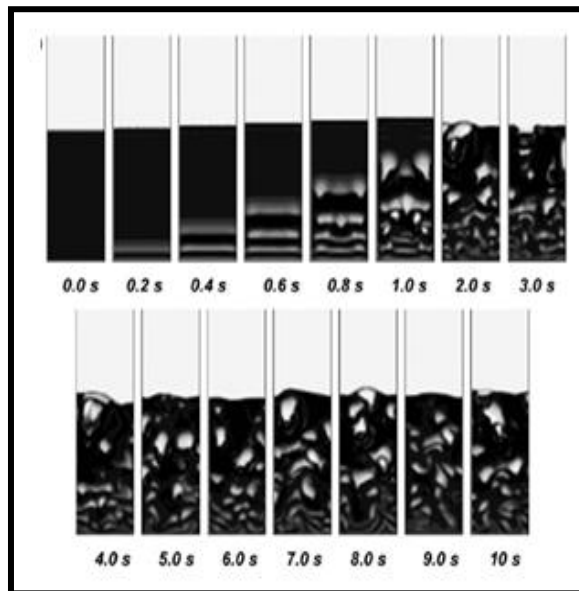
4.2.1 Model validation

The hydrodynamics model developed in Fluent is validated with experimental and simulation results obtained by Busciglio et al. [30]. Figure 4.2 shows the comparison of the contours for volume fraction of solids inside the fluidized bed gasifier before and after the solid particles being fluidized by air, which is the gasifying agent. By comparing Figure 4.2 (a) and Figure 4.2 (b), it is observed that the bubble diameter simulated by Fluent is much bigger compared to the bubbles computed by CFX, which was used in Busciglio et al. [30]. This is because fluctuation energy of solids particles or the granular temperature of solid is calculated by neglecting the loss of energy due to convection and diffusion. As the particles have higher energy than in actual case, it moves more rapidly when gasified by the air. This rapid movement cause the smaller bubbles to coalesce more rapidly and forming larger bubbles. Compared to CFX, the granular temperature of solid is calculated from the assumption of local equilibrium in the transport equation [30].

Even though the bubbles produced is much bigger, the bubble distribution inside the fluidized bed gasifier does not differ much with Busciglio et al. [30]. Figure 4.2(a) shows that uniform bubbles formation was reached after 2s of fluidization. This observation is the same as Busciglio et al. [30]. From the comparison of Figure 4.2 (a) and (b), it appears that the model used in this work is able to correctly simulate the bubble formation inside the fluidized bed reactor. However, the bubbles simulated in this model are slightly bigger than the literature study [30], which might affect the average bed height of the system. It is predicted that the bed height simulated by the code should be slightly higher due to the bigger bubble eruption on the surface of the expended bed.



(a)



(b)

Figure 4.2 : Contours for solid volume fraction at $U=1.7U_{mf}$; (a) Result obtained from simulation; (b) Result from Busciglio et al., 2009 [30]

Figure 4.3 shows the comparison of average bed height computed by this model with the experimental and simulated data obtained from Busciglio et al. [30]. From the graph in Figure 4.3, it is observed that the difference between average bed heights computed by Fluent are insignificant compared to the data obtained from CFX and experimental data. As expected, the average bed height computed by Fluent is slightly higher compared to the experimental and CFX data. The overall difference is less than 5%.

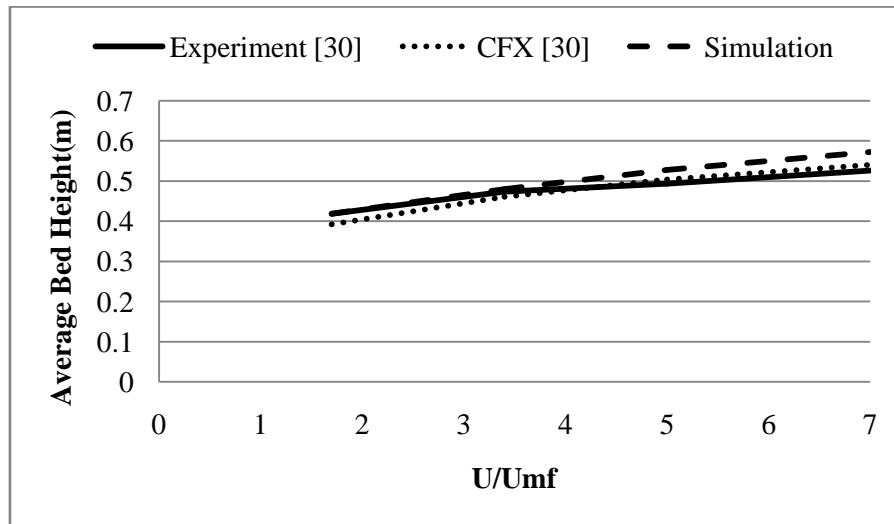


Figure 4.3 : Comparison of simulation result from Fluent with experimental data and CFX model from Busciglio et al. [30]

Figure 4.4 shows the instantaneous bed height computed by Fluent compared with instantaneous bed height from Busciglio et al. [30] for air velocity, U , equals to $3.4U_{mf}$. From the comparison, it is observed that the instantaneous bed height computed by Fluent is slightly higher compared to literature data. It is expected that the bubbles formation in Fluent is larger than bubbles formed in experimental set up and computational in CFX. Thus, bigger bubble eruption at the surface of extended bed causes the bed height to increase. Overall, the average difference between the computed instantaneous bed height in Fluent and the data from literature is less than 10% and it shows that the model can be used further to study the effect of other parameters to the solid fluidization in the fluidized bed gasifier.

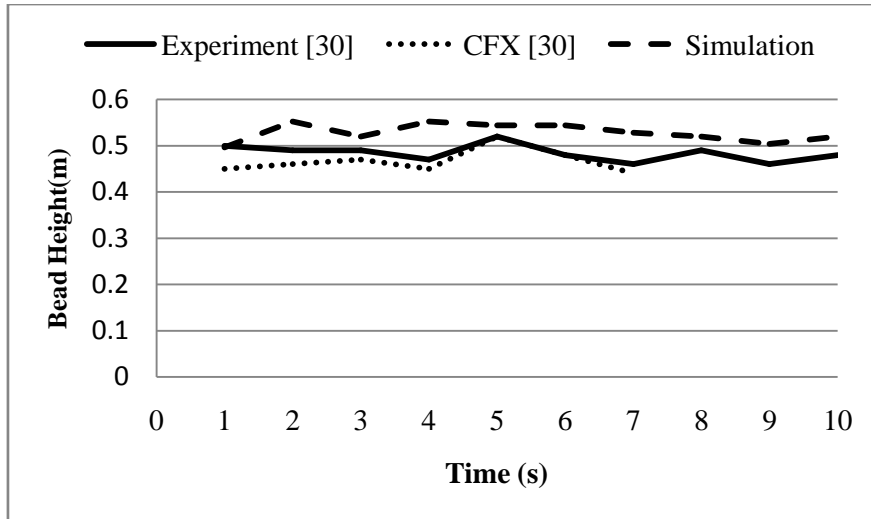


Figure 4.4: Comparison of instantaneous bed height of 3.4Umf obtained from simulation with other result from literature [30]

4.2.2 Effect of steam inlet velocity

Mixing and segregation of fluidized bed gasifier are highly determined by the bubble characteristic and bubble dynamics that form through the bed. One of the parameters that might affect the properties of bubbles form in the bed is the gasifying agent inlet velocity. In this study, the gasifying agent for the system is steam while the bed material is biomass. Figure 4.5 to Figure 4.8 show the contour of solid volume fraction that has been gasified by steam at four different superficial velocities ranging from 3-5 U_{mf} (Refer to Case 1-4). It is observed that small bubbles form at the bottom of the gasifier and their size increase as they propagate to the top of the bed and rupture. The formation, movement and rupture of these bubbles stimulate solid mixing through the bed as can be seen by different solid concentration from the contour. From physical observation, it is observed that as the steam superficial velocity increases, the size of bubbles form in the bed increases. This observation is similar to the observation obtained from experimental study by C. N. Lim et al. [23] As the bubble size in the bed increases, the flow in the bed become more vigorous and the extended bed height increases. At high steam inlet velocity (Figure 4.7 & Figure 4.8), the formation of slugs tends to occur through the bed and this formation of slugs shows poor solid mixing and fluidization in the gasifier.

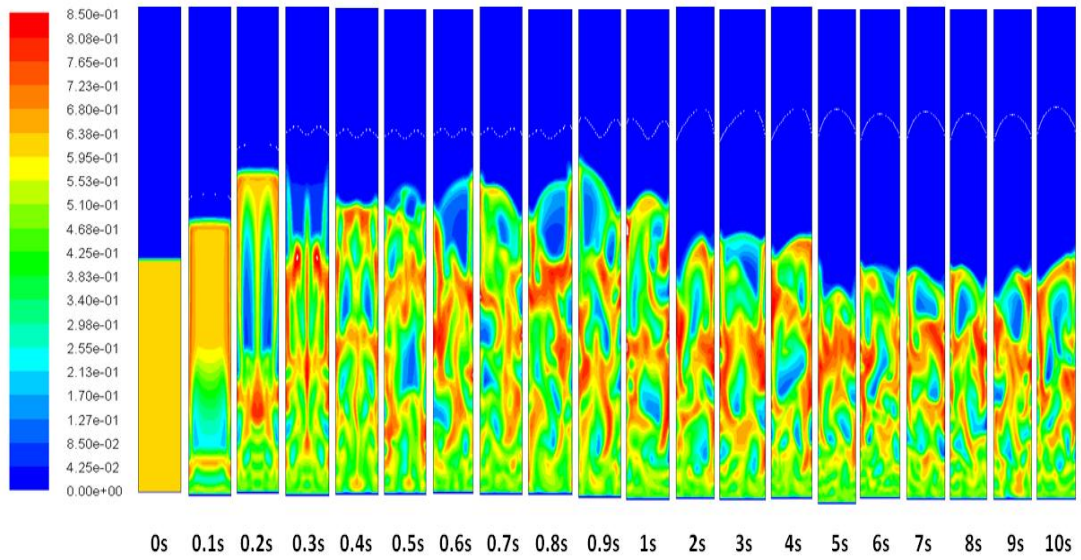


Figure 4.5: Contour of solid volume fraction at 3Umf (Case 1)

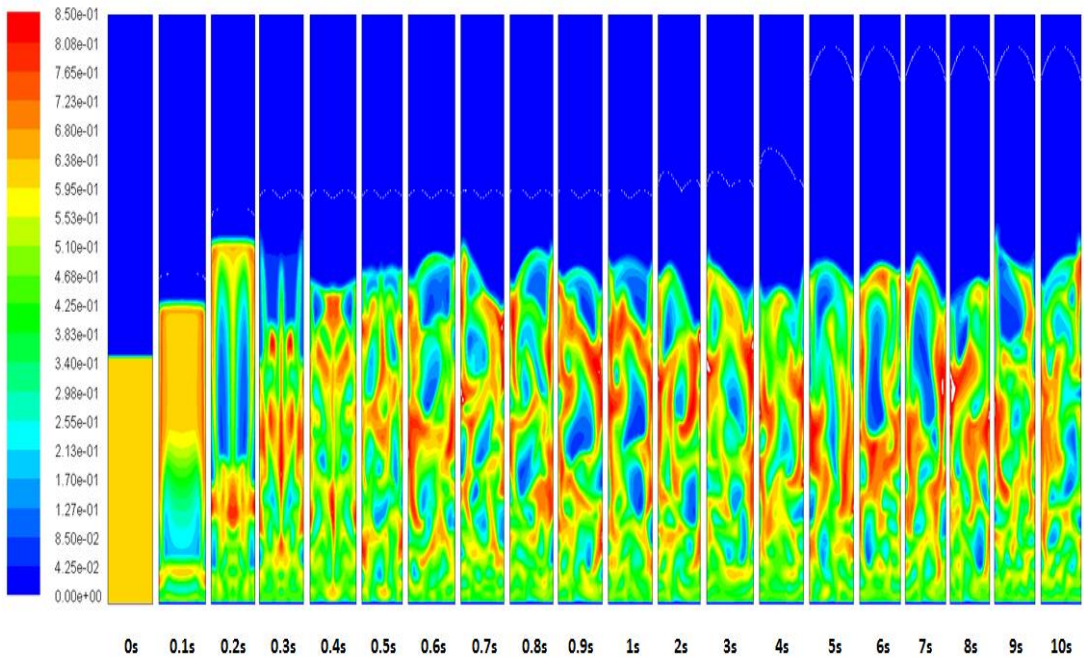


Figure 4.6: Contour of solid volume fraction at 3.5Umf (Case 2)

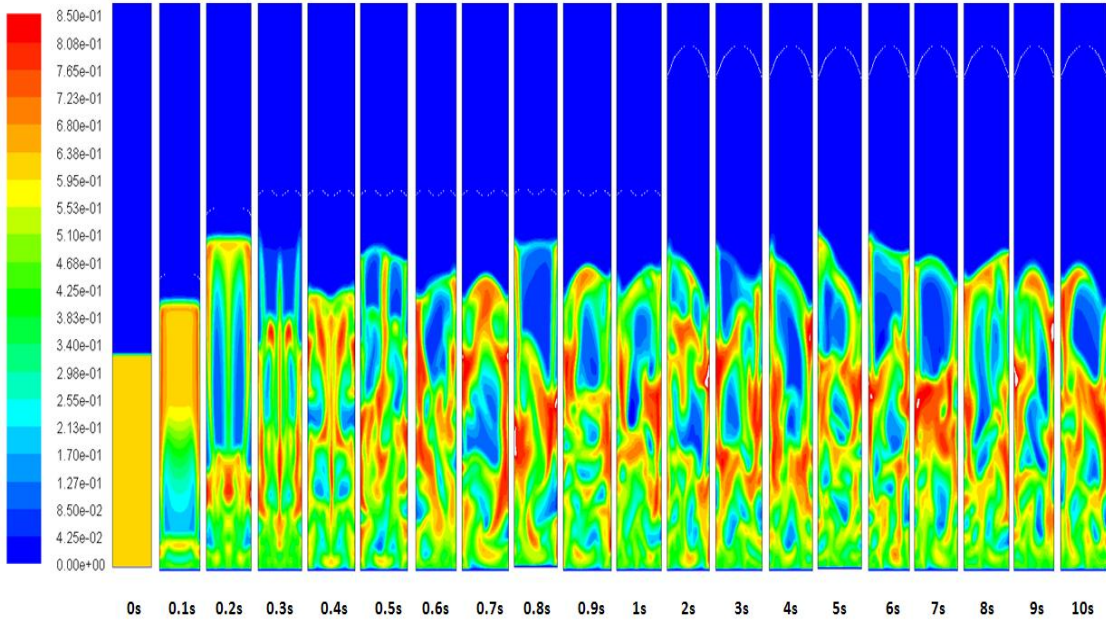


Figure 4.7: Contour of solid volume fraction at 4Umf (Case 3)

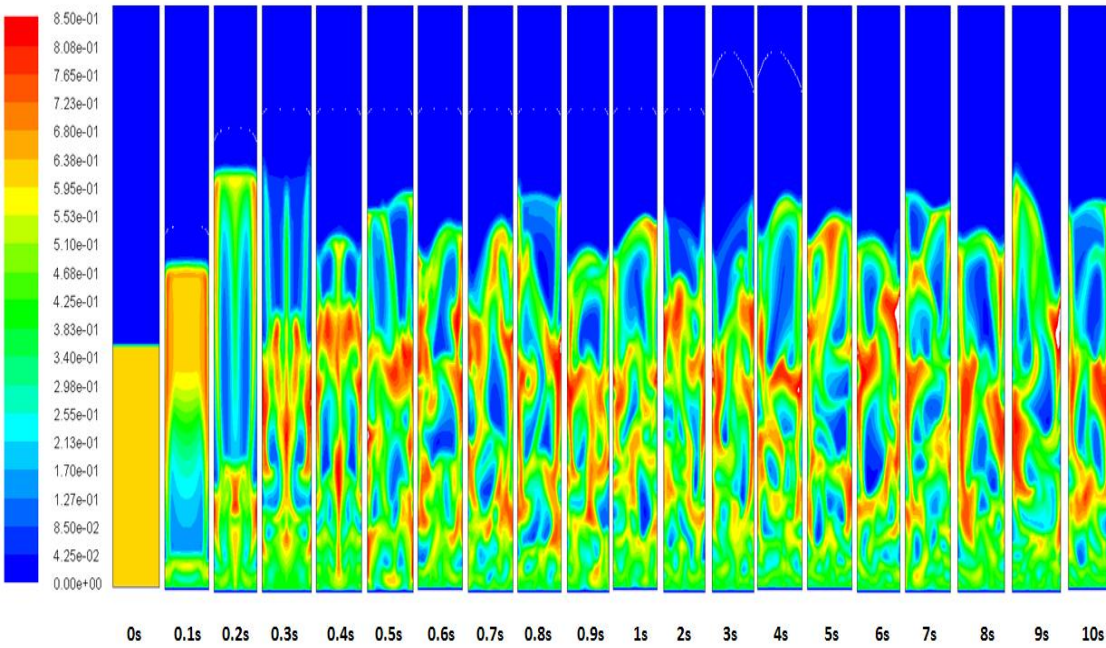


Figure 4.8: Contour of solid volume fraction at 5Umf (Case 4)

Figure 4.9 shows the time-weighted average of solid concentration at five different places in the bed for four different steam inlet velocities. From the graph, it is observed that solid concentration at the top of the bed reduced at high steam inlet velocity. This is because at higher steam velocity, bigger bubbles tend to form trough the bed and it rupture at the surface of the bed making the solid concentration surface decrease.

Solid concentration at the bottom and centre of the bed also decrease as the steam velocity increase. This is also related to the formation of bigger bubbles as the bubbles have higher velocity and coalesce much faster. Solid concentration is the highest at the right and left of the bed. This shows that solid mixing in lateral direction is faster compared to the one in axial direction. Most of the solid is “pushed” to the wall as the steam flows in the gasifier.

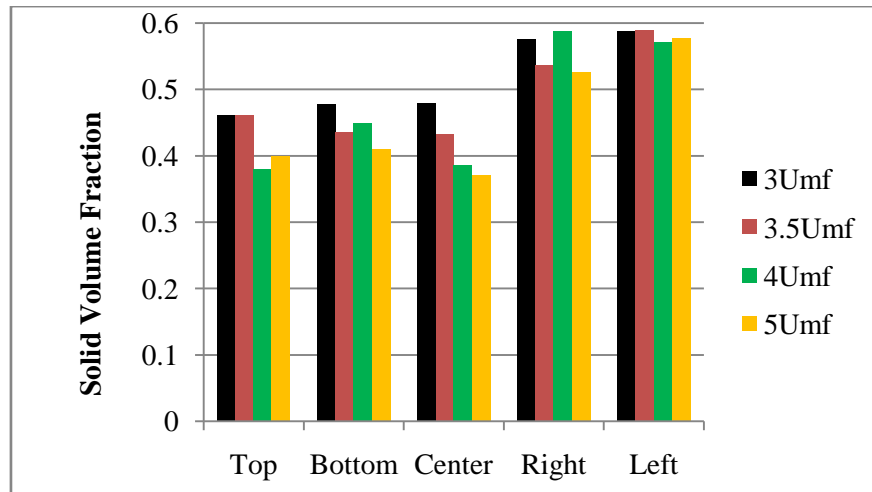


Figure 4.9: Time-weighted average of solid concentration at different steam inlet velocity

Figure 4.10 shows the concentration profile of the fluidized bed gasifier at different steam inlet velocity. From the graphs, it is observed that as the steam inlet velocity increases, the bed concentration becomes less uniform. This is probably due to the formation of slugs through the bed as the steam velocity increases. Good quality fluidization should produce almost uniform solid concentration through out the bed for best performance of biomass gasification. At high steam inlet velocity, ($4U_{mf}$ and $5U_{mf}$), it is observed that the difference in solid concentration between the five different locations become significant. Steam inlet velocity of $3U_{mf}$ and $3.5U_{mf}$ produce almost uniform solid concentration through out the bed therefore, the optimum steam inlet velocity for this system is from $3-3.5U_{mf}$.

■ Top ■ Bottom ■ Center ■ Right ■ Left

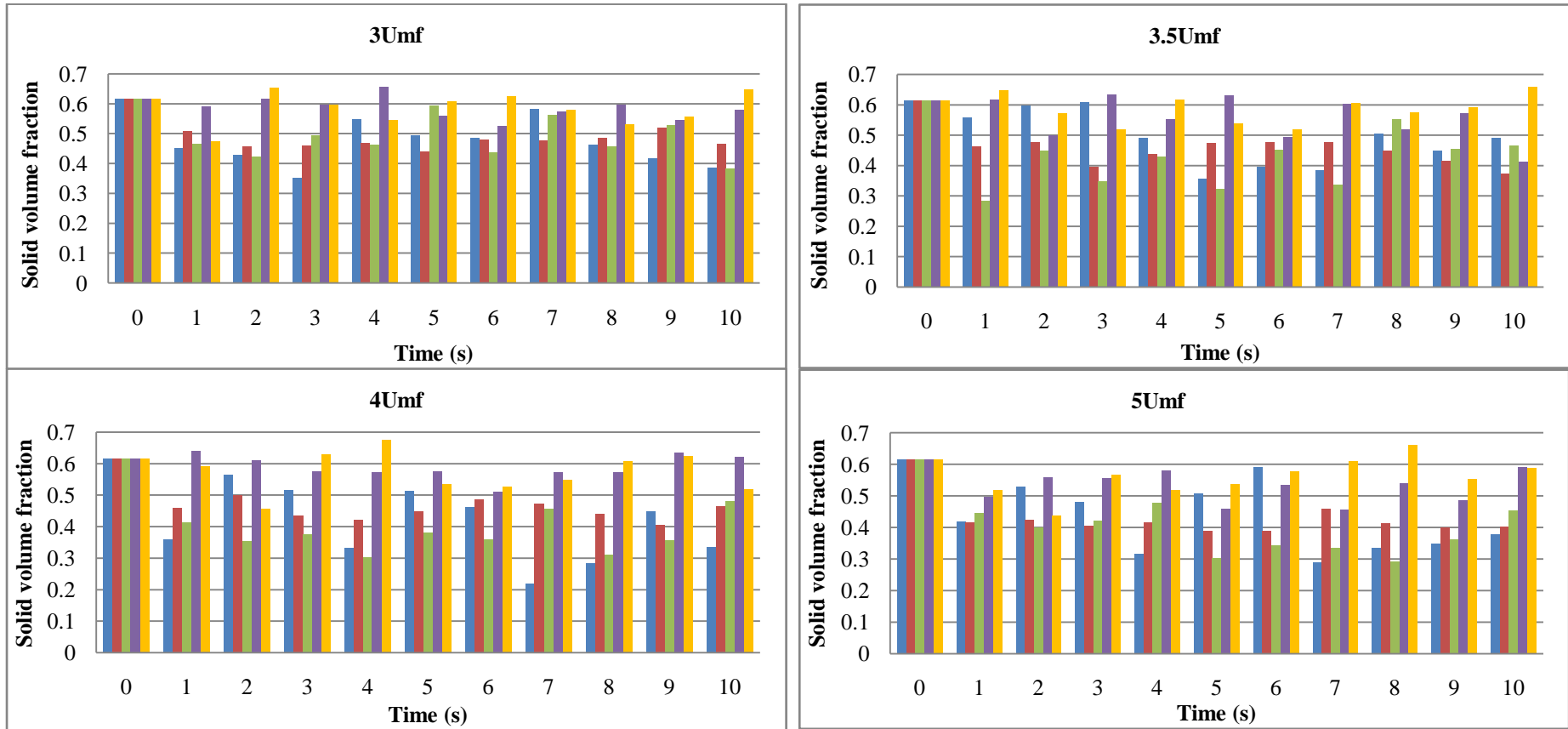


Figure 4.10 : Solid concentration profile for different steam inlet velocity

4.2.3 Effect of particle size

K.S. Lim et al. in his work also highlighted that solid mixing might also be influenced by solid particle size. In this work, the effects of solid particle size ranging from 100-400 μm to the solid fluidization in the fluidized bed gasifier are studied. Figure 4.11 to Figure 4.14 show the contour of solid volume fraction of four different particle sizes (Refer to Case 2, 8, 9 and 10). From the contour, it is observed that the smallest particle which is 100 μm is the easiest to be fluidized by the steam (Figure 4.11). It also shows that the voidage between the solid particles is too big and the solid particles are highly dispersed throughout the bed because the particles are too small and light. This kind of mixing is not really good for gasification reaction as the contact between the solid particles is almost none. As the particle size increases, it is more difficult for the steam to fluidize it as it is observed that the bed become denser as the particle size increases.

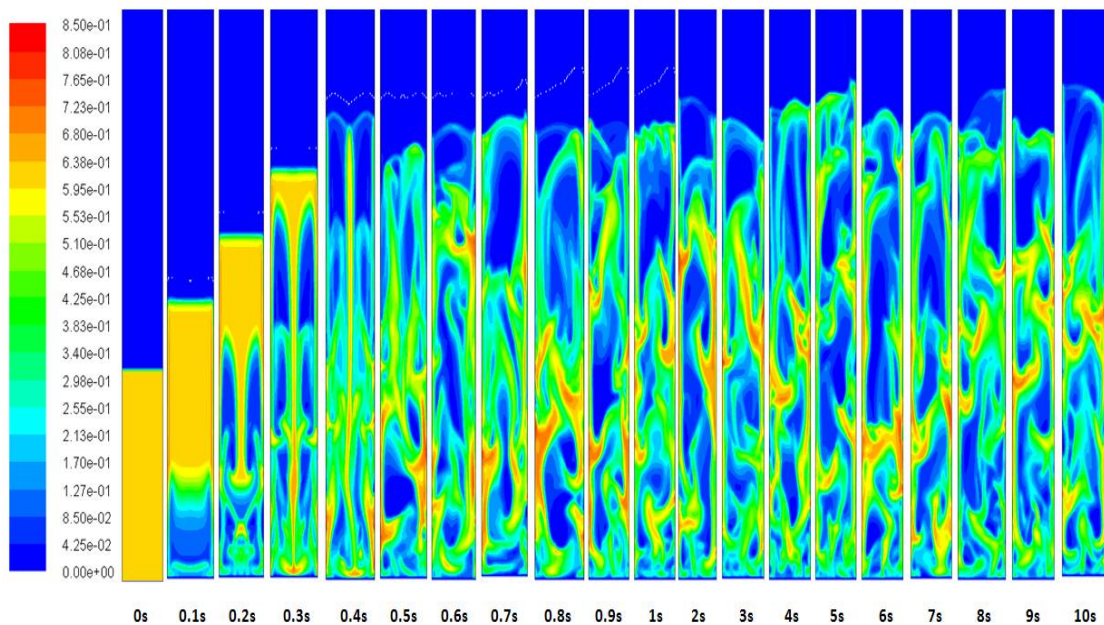


Figure 4.11: Contour of solid volume fraction for particle size of 100 μm (Case 8)

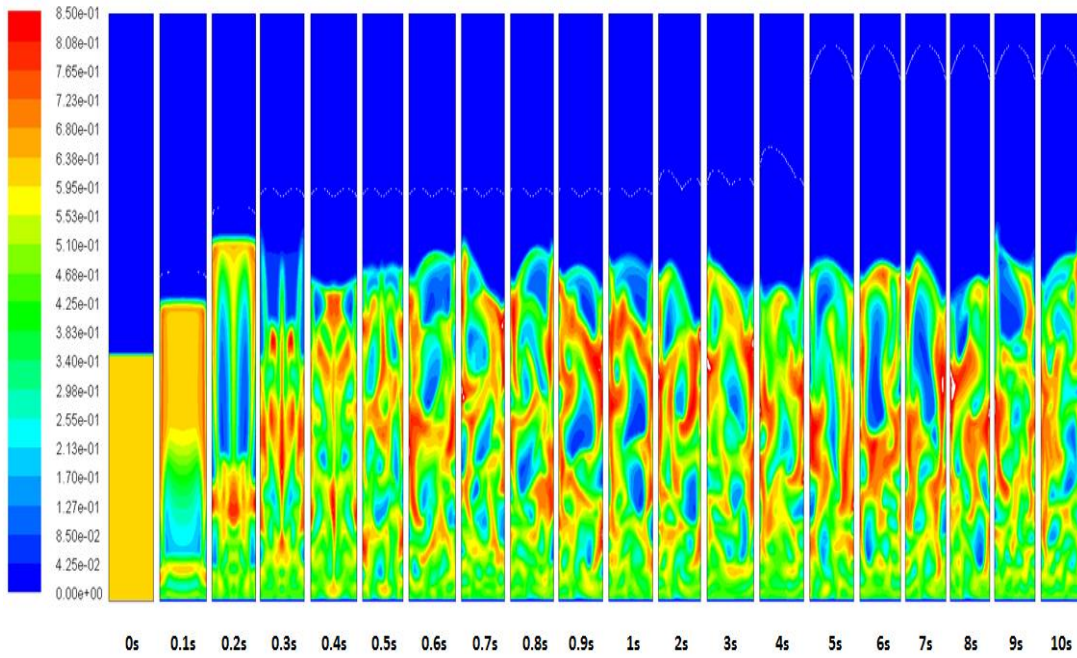


Figure 4.12 : Contour of solid volume fraction for particle size of 250 μ m (Case 2)

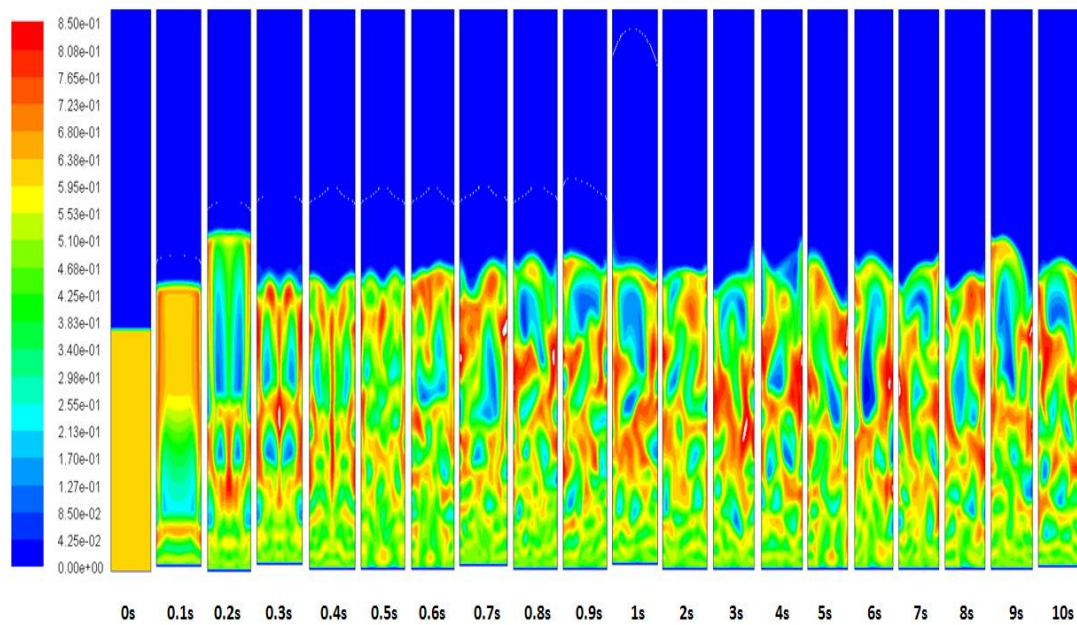


Figure 4.13 : Contour of solid volume fraction for particle size of 300 μ m (Case 9)

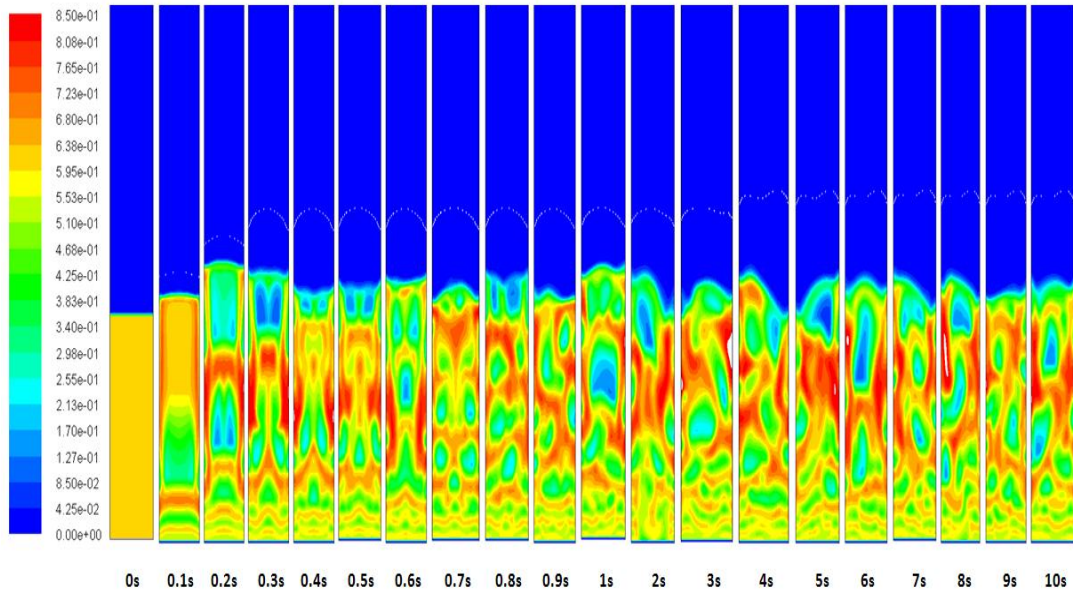


Figure 4.14 : Contour of solid volume fraction for particle size of 400µm (Case 10)

Figure 4.15 shows the time-weighted average of solid concentration for four different particle size through out the bed. From the graph, it is clearly observed that the bed become much denser as the particle size increases. This proves that, a bigger particle size is much more difficult to be fluidized by the steam at the velocity of 3.5Umf. Solid concentration is much higher on the right and left of the bed compared to at the top and bottom which shows that lateral mixing is much faster in the bed compared to in axial direction.

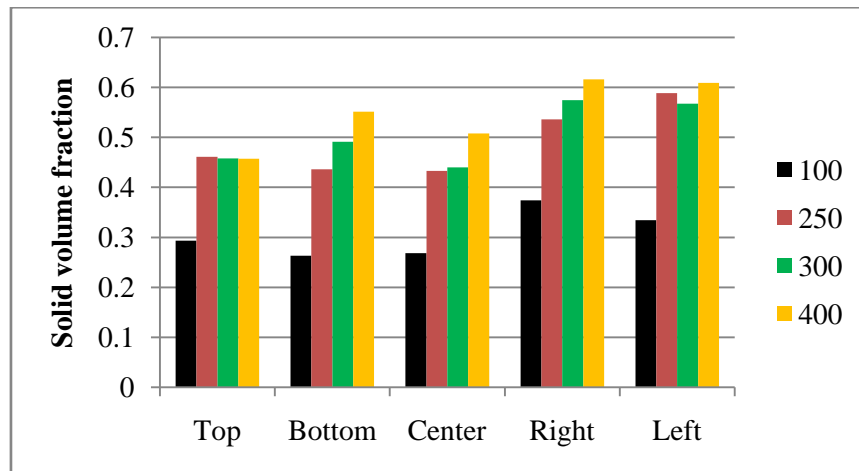


Figure 4.15: Time-weighted average of solid concentration for different particle sizes

Figure 4.16 shows solid concentration profile in the fluidized bed gasifier of four different particle sizes. From the graph, it is observed that the solid concentration for 100 μm particle is the lowest compared to others. This shows that the voidage between solid and gas phase is the highest when small particle is used. This voidage decrease as bigger particle is used as the bed material because bigger particle is much more difficult to be fluidized by the steam as it is heavier and more lift force is required to support its weight. Bigger particle also exert higher particle-particle friction making it difficult to be moved and this makes the bed become dense as shown in the graph when solid particle size of 300 μm and 400 μm is used. Therefore, for best performance of solid mixing and fluidization in the fluidized bed gasifier, particle size of 250 μm is the optimum size for the bed material.

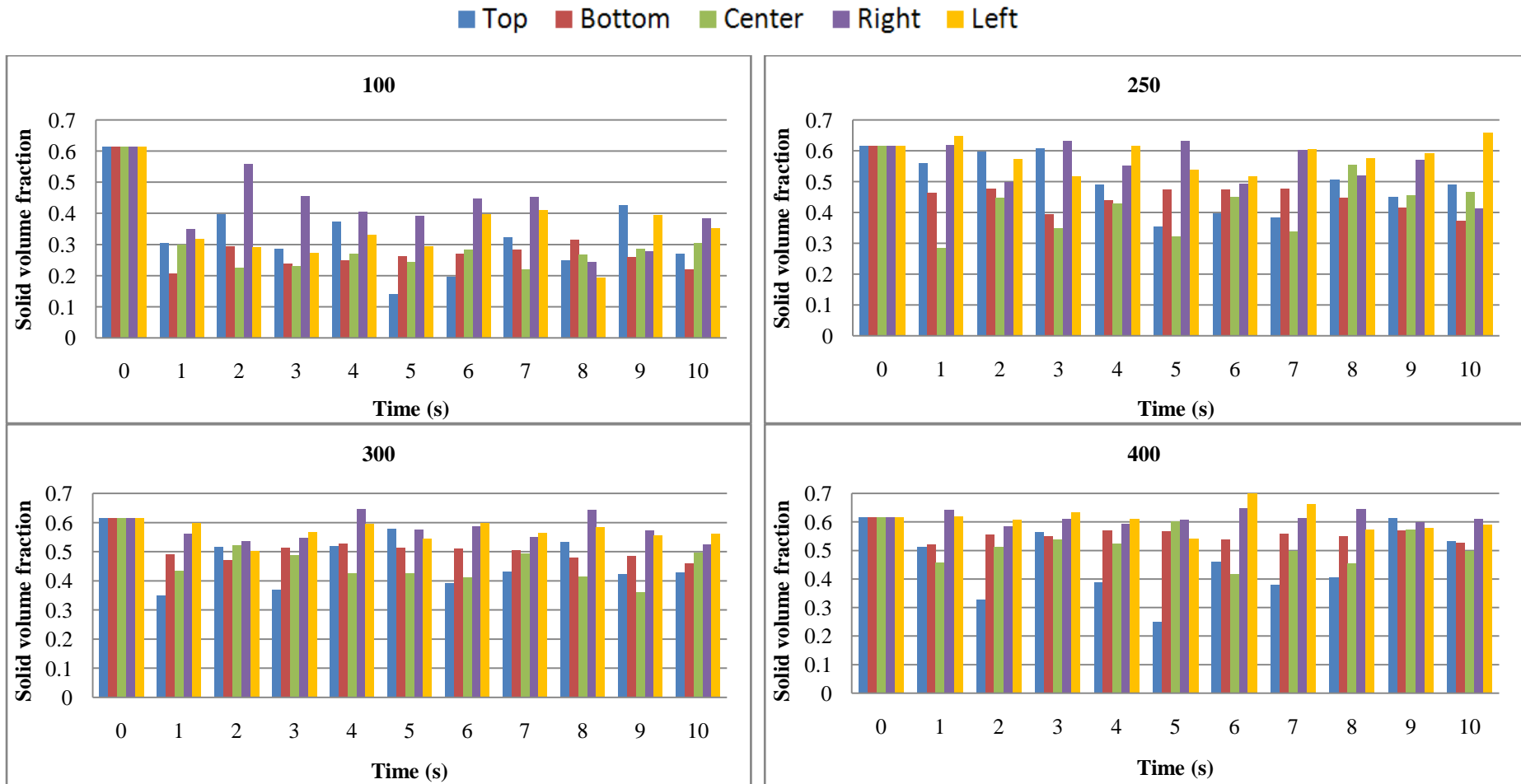


Figure 4.16: Concentration profile for different particle sizes

4.2.4 Effect of height to diameter ratio (H/D)

In this work, the effect of H/D on solid fluidization is also studied. Figure 4.17 to Figure 4.20 show the contour of solid volume fraction at different H/D (Refer to Case 2, 5, 6 and 7). From the figures, it is observed that the higher the H/D, the more difficult for the steam to fluidized the solid particles since higher H/D means more load in the bed and more energy is required in order to stimulate mixing in the bed. Higher H/D also increases the tendency of slug formation in the bed. This is because the bubbles formed in the bed have more time to coalesce with each other and form bigger bubbles that eventually turn into slug as it move upward to the surface of the bed. Formation of slug is very obvious at high H/D (3 and 4) as can be seen in Figure 4.19 and Figure 4.20. This shows very poor mixing in the bed and not suitable for biomass fluidized bed gasifier.

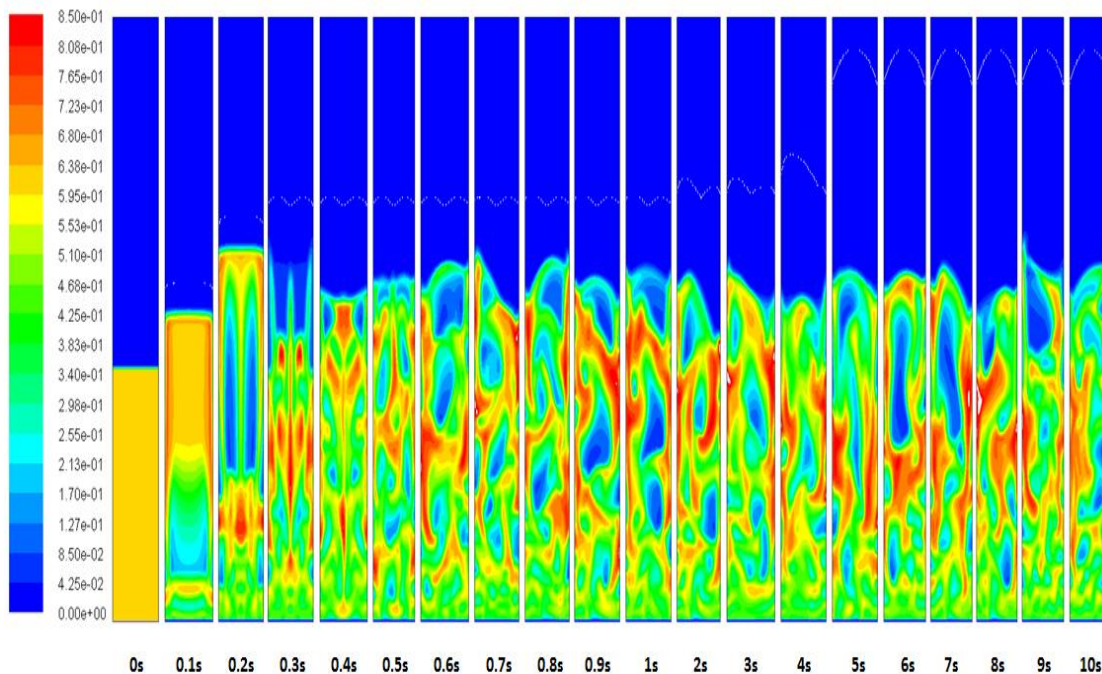


Figure 4.17: Contour of solid volume fraction for H/D of 2 (Case 2)

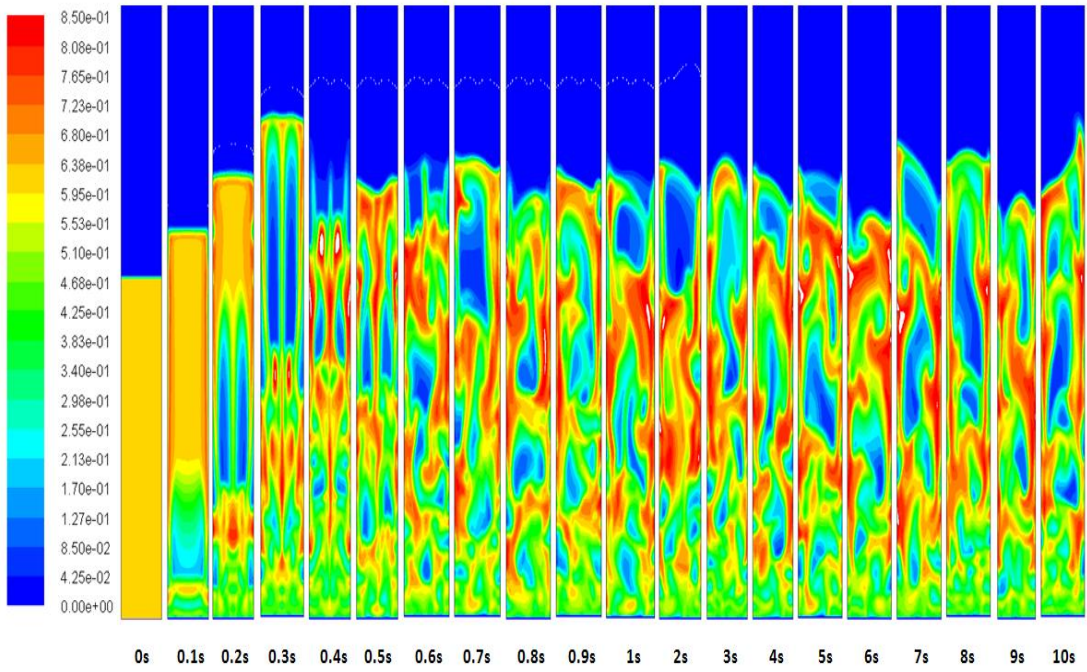


Figure 4.18: Contour of solid volume fraction for H/D of 3 (Case 5)

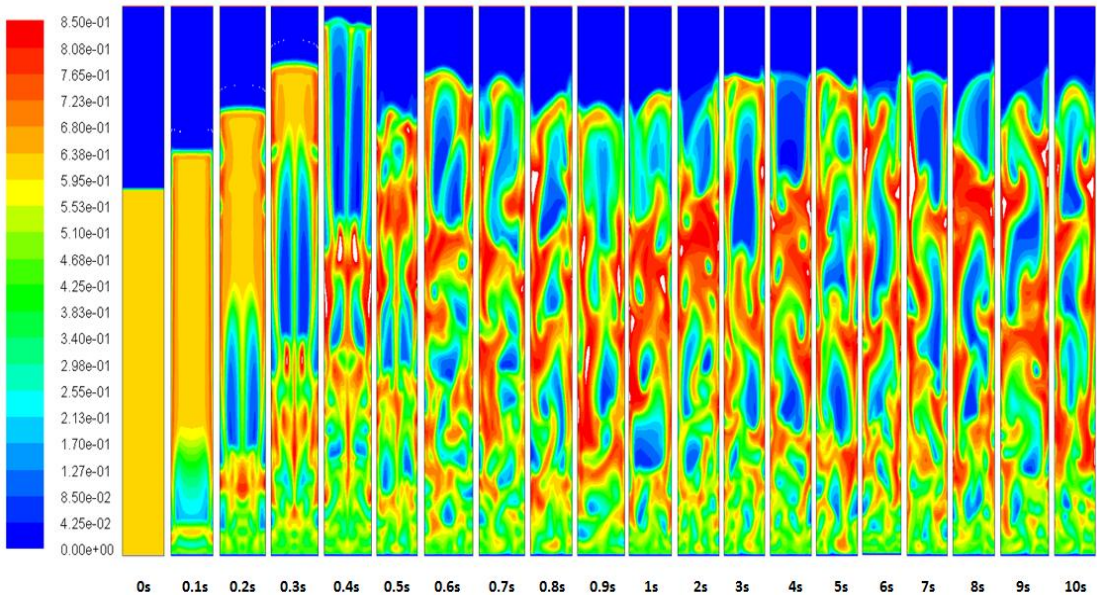


Figure 4.19: Contour of solid volume fraction for H/D of 4 (Case 6)

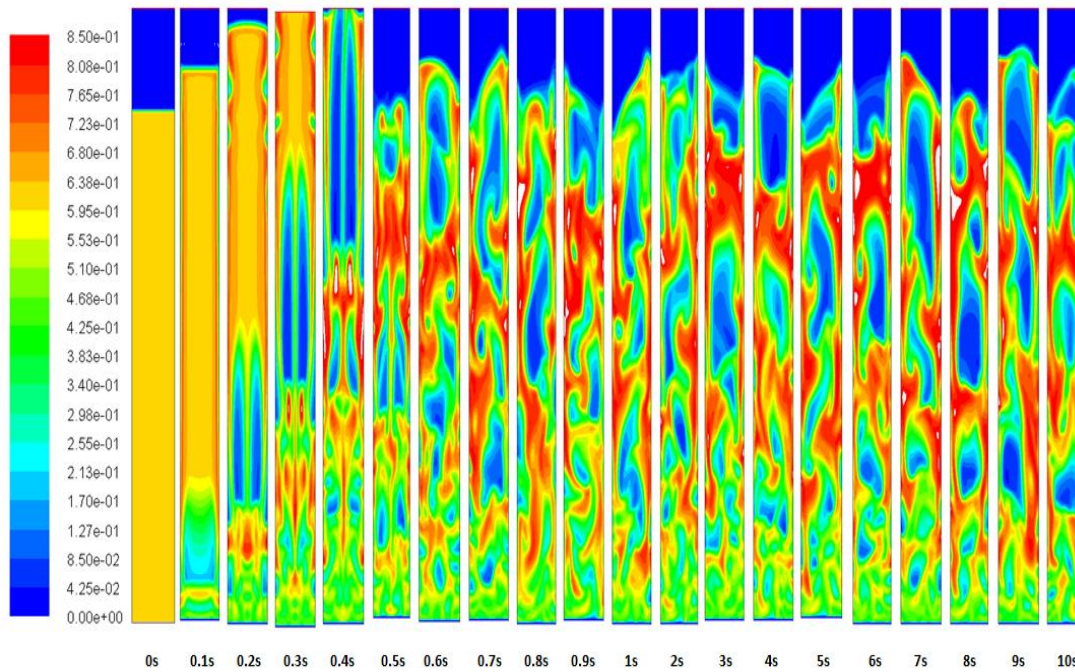


Figure 4.20: Contour of solid volume fraction for H/D of 5 (Case 7)

Figure 4.21 shows the time-weighted average of solid concentration in the fluidized bed gasifier at different H/D. Due to the formation of slug as H/D increases, the solid concentration at the centre of the bed decreases. Lateral mixing is observed to occur much faster compared to axial mixing as solid concentration is much higher at the right and left wall of the bed compared to other places.

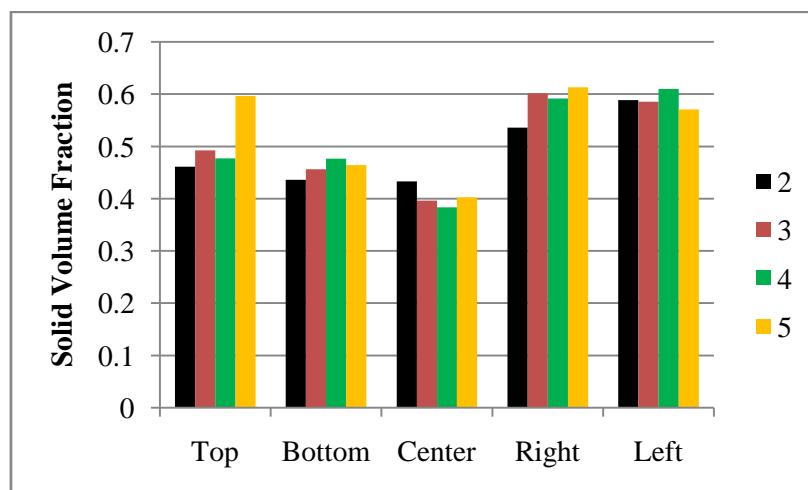


Figure 4.21: Time-weighted average of solid concentration for different H/D

Figure 4.22 shows the concentration profile of solid at different H/D. From the graph, it is observed that solid concentration in the fluidized bed gasifier increases as H/D increases. Due to the formation of slug in the bed, there is a huge different in solid concentration between the different places throughout the bed. In order to keep the condition in the bed as uniform as possible, it is best to keep the H/D at minimum which is at 3 and below. This is because higher H/D does not improve solid mixing in the bed and causing more slugs to form in the bed.

■ Top ■ Bottom ■ Center ■ Right ■ Left

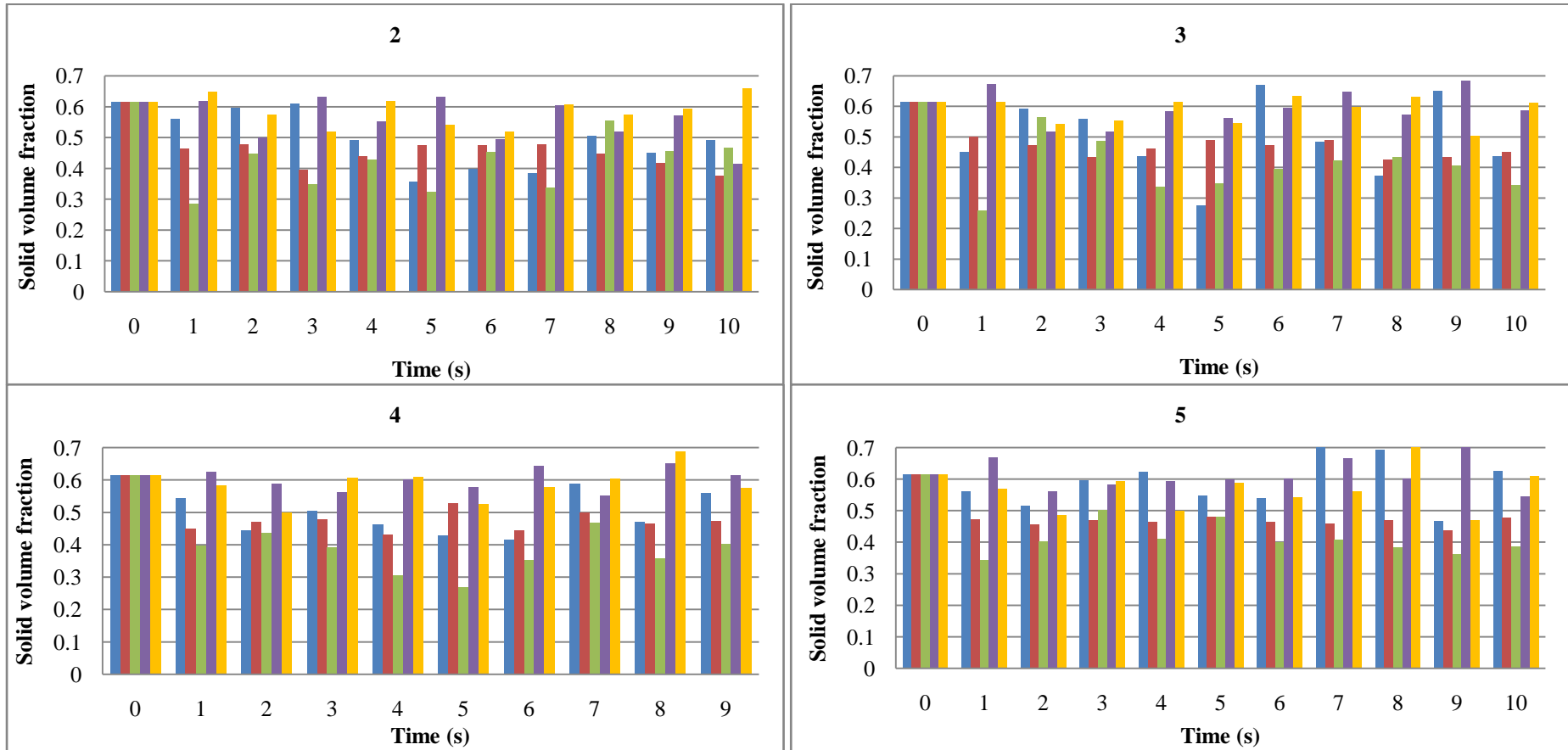


Figure 4.22: Concentration profile for different (H/D)

4.3 Reaction Model

4.3.1 Model validation

Figure 4.23 shows the comparison of estimated H₂ production from the reaction model with literature data. The H₂ concentration in term of mol% is the facet average value taken at the “Outlet” line surface of the 2D domain of the gasifier. From the graph, it is observed that the reaction model can accurately predict the H₂ production from biomass gasification at 800 °C and steam to biomass ratio of 2. The prediction of H₂ from the model is really close with the predicted H₂ production from ASPEN PLUS process simulation software by Mehrdokht et al. [22] and also from the steam gasification experimental study by N. Gao et al. [61] H₂ production from P.M. Lv et al. [59] experimental result is lower compared to predicted production from reaction model because they are utilizing air as the gasifying agent and the low H₂ concentration is due to dilution effect from N₂ exist in air. Based on this comparison, it is concluded that simulated H₂ production by the reaction model is in good agreement with literature data and the model can be further used in order to predict the effect of other reaction parameters on H₂ production from biomass gasification process.

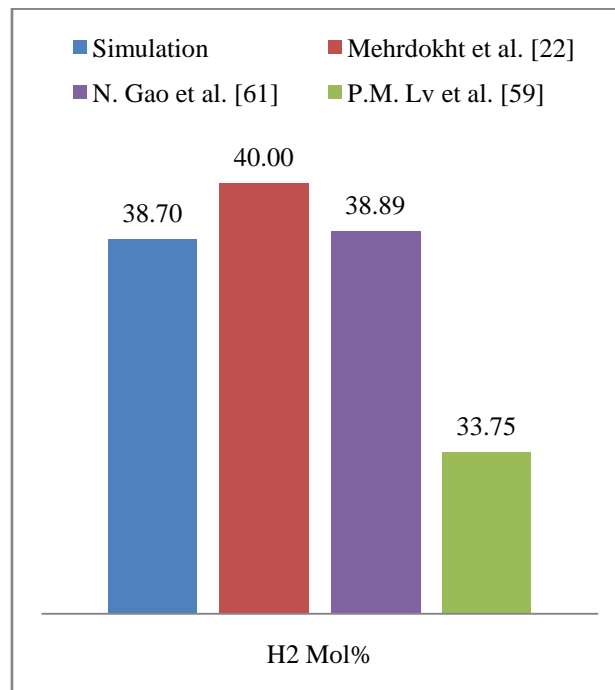


Figure 4.23: Comparison of H₂ mol% predicted by model with literature data at 800°C

4.3.2 Effect of reaction temperature

The fluidized bed gasifier temperature is one of the most important operating variables for biomass gasification. In this work, reactions were simulated at gasifier temperature ranging from 700-900 °C in 50°C increments (Refer to Case 11-15). Figure 4.24 shows the effect of fluidized bed reaction temperature on H₂ production from biomass gasification process at steam to biomass ratio of 2. From the figure, it is observed that H₂ production increases as temperature increases. This finding is similar to the experimental data obtained by P.M. Lv et al. [59] and W. Wu et al. [4]. This is because biomass gasification is an endothermic reaction; therefore, high temperature is more favourable for the reaction to occur. Estimated H₂ production from the reaction model is also compared with the data from the literature. Based on the comparison, it is observed that the model is able to accurately predict H₂ production from biomass gasification as the concentration of H₂ and trend of H₂ production is in good agreement with the literature data. The highest H₂ production is observed at a temperature of 850°C which is about 48 mol%.

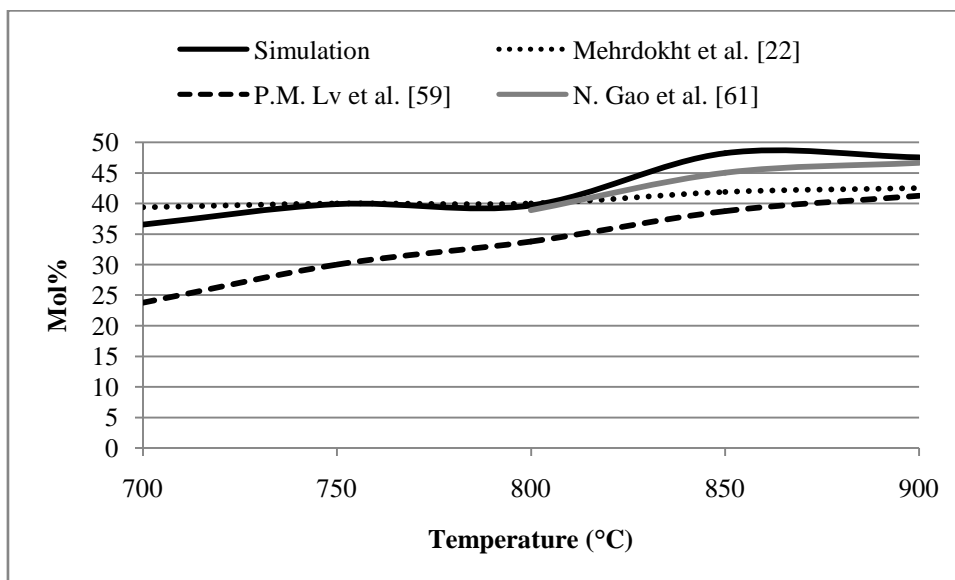


Figure 4.24: Effect of reaction temperature on H₂ production from biomass gasification*

* Data taken based on facet average at the "Outlet" line surface of the 2D domain of the gasifier

Figure 4.25 shows the effect of gasification temperature on product gas composition. From the graph, it is observed that as the temperature increases, the concentration of CO also increases and the concentration of CO₂ decreases. This is because at the temperature higher than 800 °C, CO₂ is further crack to CO making CO concentration to increase. Y. Kalinci et al. [12] also claimed that at high gasification temperature (800 – 850 °C) product gas that is rich in H₂ and CO is produced. The concentration of CH₄ remains low in the product gas since CH₄ is continuously produced and consumed at the same time during the gasification process. H₂ profile from the graph shows that gasification is effectively occur at temperature higher than 800 °C since there is a significant jump in the H₂ concentration from 800 °C onwards. Therefore, for the best performance of biomass gasification without the presence of CO₂ adsorbent, the gasifier should be operated at the temperature range of 800-900 °C for maximum concentration of H₂.

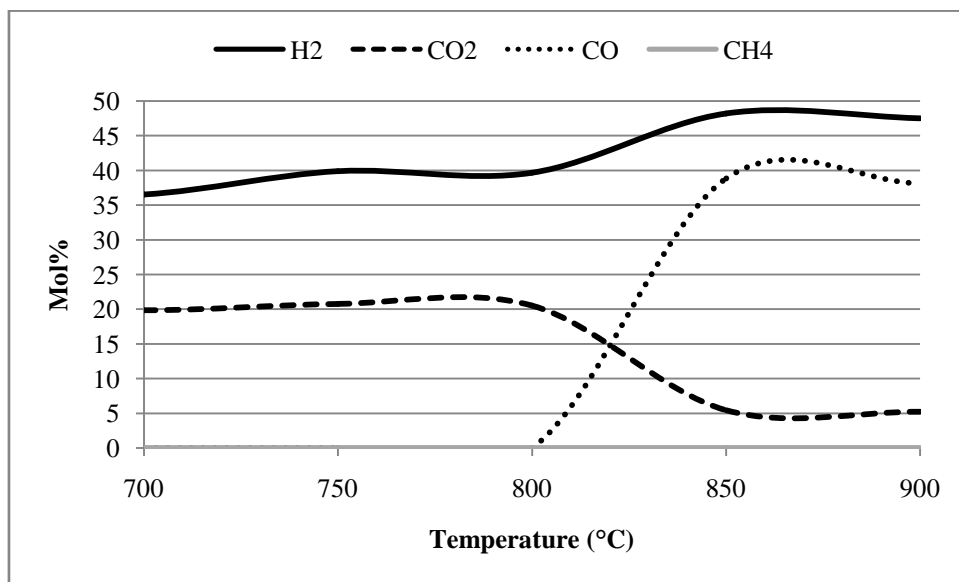


Figure 4.25: Effect of gasification temperature on product gas composition *

* Data taken based on facet average at the “Outlet” line surface of the 2D domain of the gasifier

The reaction model is also used to predict the H₂ yield from the biomass gasification reaction. The yield of H₂ was calculated using the formula [14]:

$$H_2 \text{ Yield} = \frac{H_2 \text{ produced from the gasifier (g)}}{\text{Biomass fed into the system (kg)}} \quad (4.1)$$

Figure 4.26 shows the effect of gasification temperature on H₂ yield from biomass gasification process. From the graph, it is observed that H₂ yield shows an increasing trend as gasification temperature increase. The highest H₂ yield which is 189.5 g H₂/kg biomass is obtained at the gasification temperature of 850 °C. This indicates that the optimum fluidized bed gasifier for biomass gasification process is at 850 °C where at this temperature the highest H₂ concentration and also yield is obtained.

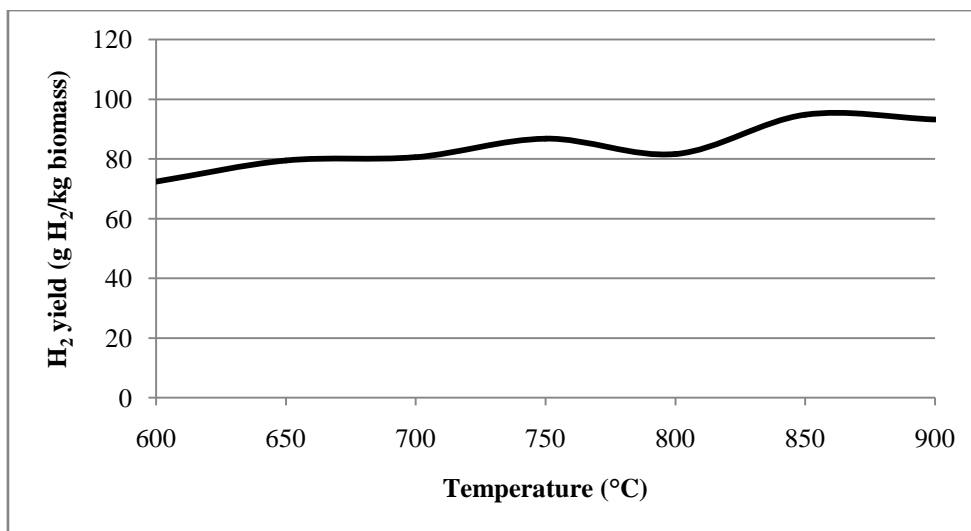


Figure 4.26: Effect of gasification temperature on H₂ yield*

The H₂ yield predicted from the reaction model is also compared with experimental data from literature such as show in Table 4.1. From the comparison, it is observed that the predicted H₂ yield from the reaction model is similar with the experimental data obtained by N. Gao et al. [61] at 850 °C. This shows that the assumptions made on biomass carbon content is valid in order to predict H₂ production from biomass gasification process using the reaction model. The predicted H₂ yield from the simulation is higher compared to experimental data obtain by L. Shen et al. [14] because the biomass used by them has lower carbon content and their gasification is operating at much lower steam to biomass ratio.

* Data taken based on facet average at the "Outlet" line surface of the 2D domain of the gasifier

Table 4.1: Comparison of simulated H₂ yield with literature data at 850 °C

	Simulation	L. Shen, 2008 [14]	N. Gao, 2008 [61]
Carbon content in biomass	50%	36.57%	44.75%
Temperature (°C)	850	850	850
Gasifying agent	Steam	Steam	Air-Steam
Steam to Biomass Ratio	2	0.6	1.4
Adsorbent	No	No	No
H ₂ yield (g H ₂ /kg biomass)	94.75	62	99.55

4.3.3 Effect of steam to biomass ratio (S/B)

It is reported that the increase of steam in the fluidized bed gasifier has the same effect as increasing gasifier temperature. For this work, the effect of increasing steam to biomass ratio on product gas composition from biomass gasification is studied. Steam to biomass ratio in the range on 1-4 is simulated using the reaction model developed in Fluent[®] (Refer to Case 14, 16, 17 and 18). Figure 4.27 shows the effect of steam to biomass ratio on product gas composition from the gasifier. From the graph, it is observed that H₂ concentration decreases as steam to biomass ratio increases. This is due to the dilution effect from the access steam that does not completely react with the biomass. The access steam further reacts with CO to produce CO₂. This explains the increase of CO₂ and decrease of CO as steam to biomass ratio increase. The same observation is obtained by W. Wu et al. [4] in their experimental study.

The increase of steam to biomass ratio also shows the increase of H₂O production from the gasifier. The increase of H₂O production means there is a need of additional downstream system in order to increase the purity of H₂ in the product gas. The highest H₂ concentration produced is observed at steam to biomass ratio at the range of 1.5-2. Therefore, in order to achieve high purity of H₂ from the gasifier, it is best to operate the gasifier at steam to biomass ratio in the range of 1.5-2.

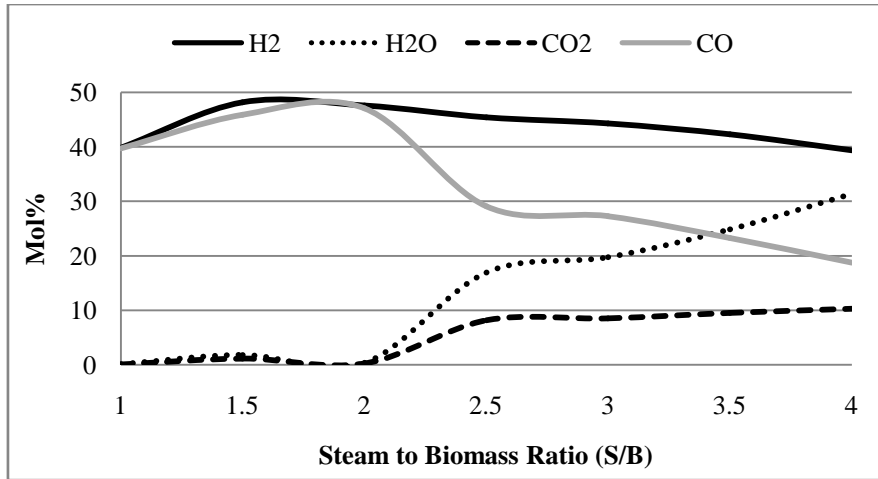


Figure 4.27: Effect of S/B on product gas composition*

Figure 4.28 shows the effect of steam to biomass ratio on biomass carbon conversion during the gasification process. The carbon conversion is calculated based on the equation below [14]:

$$\text{Carbon Conversion} = \frac{\text{gasified carbon in gasifier (kg)}}{\text{carbon of biomass fed into the system (kg)}} \times 100 \quad (4.2)$$

From the graph, it is observed that biomass carbon conversion increase as steam to biomass ratio increase from 1-4. A drastic increase in carbon conversion is observed as steam to biomass ratio increases from 1 to 1.5 and it becomes almost constant at steam to biomass ratio equals to 2 and reaches almost 100%. This shows that high carbon conversion could be achieved as more steam is added into the system because the excess steam further pushed the gasification reaction forward and making the biomass as the limiting reactant.

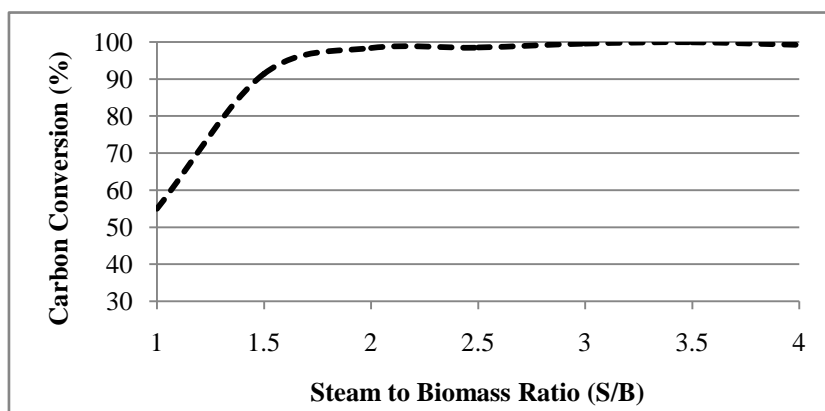


Figure 4.28: Effect of steam to biomass ratio on carbon conversion*

* Data taken based on facet average at the "Outlet" line surface of the 2D domain of the gasifier

Figure 4.29 shows the predicted H₂ yield from the simulation. From the graph, it is observed that H₂ yield increase as steam to biomass ratio increase. This shows that increasing steam into the system has the same effect as increasing the gasification temperature. Based on the Le Chatelier's principle, in order to achieve equilibrium as more steam (reactant) is added into the system, the gasification reactions is further pushed forward towards producing more H₂. That is why H₂ yield further increase as more steam is added into the system. The same concept applies as gasification temperature increase. As gasification reactions overall is an endothermic reaction, increasing temperature also further pushed the reactions forward and more H₂ could be produced from the system. That explains why increasing steam has the same effect as increasing gasification temperature.

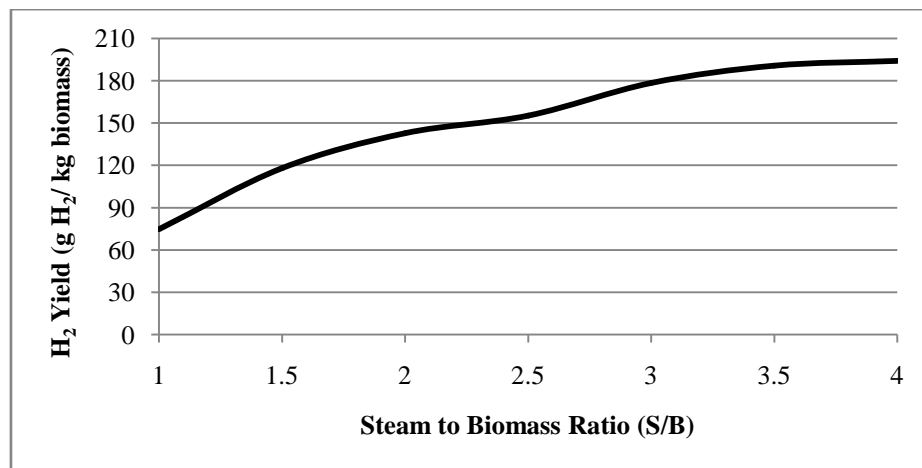


Figure 4.29: Effect of steam to biomass ratio on H₂ yield*

Based on simulation results, the optimum steam to biomass ratio for biomass steam gasification system is 2. This is because at steam to biomass ratio of 2, high concentration of H₂ could be obtained from the system and at the same time high carbon conversion could be achieve. Even though higher H₂ yield could be obtained at higher steam to biomass ratio, adding more steam into the system will not be economical since more energy is required in order to generate more steam. Therefore, in order to have economical process and at the same time still maintaining high performance of the gasifier, it is best to keep the steam to biomass ratio of 2 in the system.

* Data taken based on facet average at the "Outlet" line surface of the 2D domain of the gasifier

4.3.4 Effect of CO₂ adsorbent

Based on the previous studies, the addition of CO₂ adsorbent can increase the production of H₂ from biomass gasification process. This is because the adsorption of CO₂ further pushed the reversible water-gas shift reaction forward to produce more H₂. In this study, the effect of CO₂ adsorbent on H₂ production was studied. The simulation was done in order to observe the effect of adsorbent to biomass ratio (A/B) and adsorbent temperature on H₂ production from biomass gasification process.

Figure 4.29 shows the effect of adsorbent to biomass ratio to the composition of product gas from biomass gasification. The simulation was done at a gasification temperature of 650 °C. From the graph, it is observed that initially H₂ concentration increases as adsorbent to biomass ratio increases from 0 to 1 and decreases gradually as adsorbent to biomass ratio further increase. Similar observation is also obtained by B. Acharya et al. [62].

The concentration of CO₂ also extremely decreases as adsorbent to biomass ratio increases from 0 to 1, however, the concentration become almost constant as adsorbent to biomass ratio is further increases. The increases in adsorbent ratio higher than 1 does not further decrease the CO₂ production because CO₂ partial pressure has reached its minimum adsorption pressure. Therefore, no more CO₂ could be further adsorbed by the adsorbent which is CaO. From the graph, it is observed that the optimum adsorbent to biomass ratio is 1 as at this ratio the highest H₂ concentration is obtain from biomass gasifier and this ratio is sufficient to reduce the CO₂ production from the gasifier.

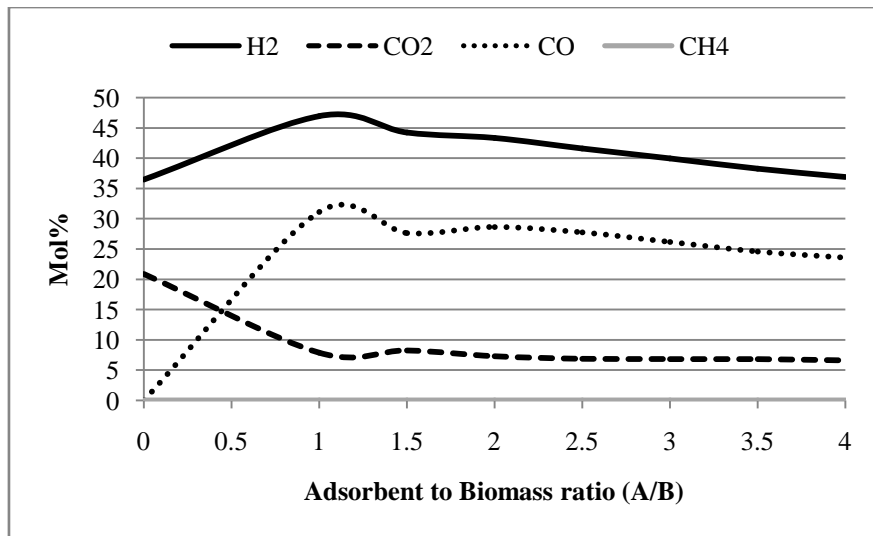


Figure 4.30: Effect of adsorbent to biomass ratio (A/B) on product gas composition *

Figure 4.30 shows the comparison of H₂ concentration in the product gas at different reaction temperature with and without CO₂ adsorbent. From the graph, it is observed that at lower temperature, the concentration of H₂ produced from biomass gasification with the existence of CO₂ adsorbent is higher than gasification without adsorbent. However, the opposite trend is observed at temperature 850 °C and higher. This is because at higher temperature, the exothermic adsorption reaction is reverse to calcinations reaction and H₂ now become the reactant to produce CaO thus reduces concentration.

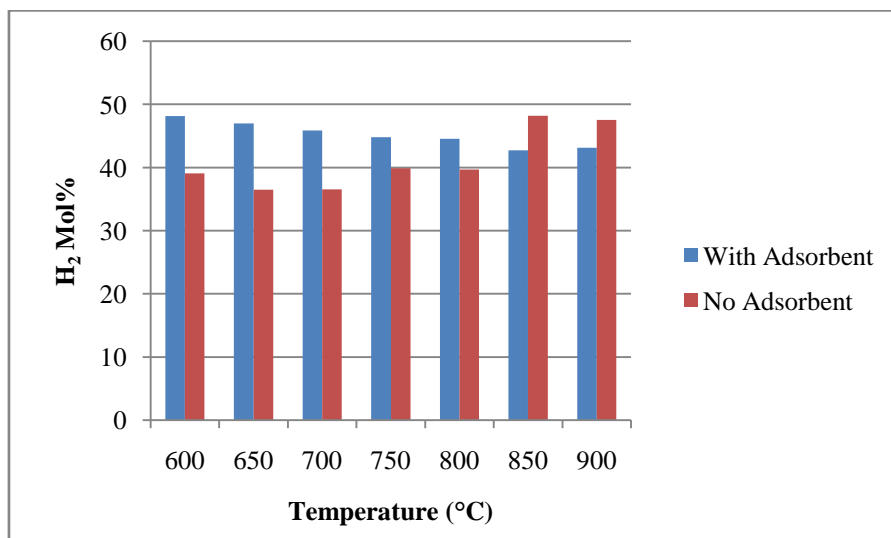


Figure 4.31: H₂ concentration from biomass gasification with and without CO₂ adsorbent

*Data taken based on facet average at the "Outlet" line surface of the 2D domain of the gasifier.

Figure 4.31 shows the comparison of H₂ yield from biomass gasification with and without adsorbent in the system. From the comparison, it is observed that the H₂ yield from the gasification system with in-situ CO₂ adsorbent is much higher compared to the gasification system without the adsorbent. The H₂ yield increases higher than 2 folds especially at the lower temperature ranging from 600-750 °C. This is because the exothermic adsorption reaction is much more favourable at lower temperature. The highest H₂ yield is observed at 600 °C which is 195.3 g H₂/kg biomass. For the best performance of biomass gasification with in-situ CO₂ adsorbent, the gasifier should be operated at a temperature range of 600-750 °C.

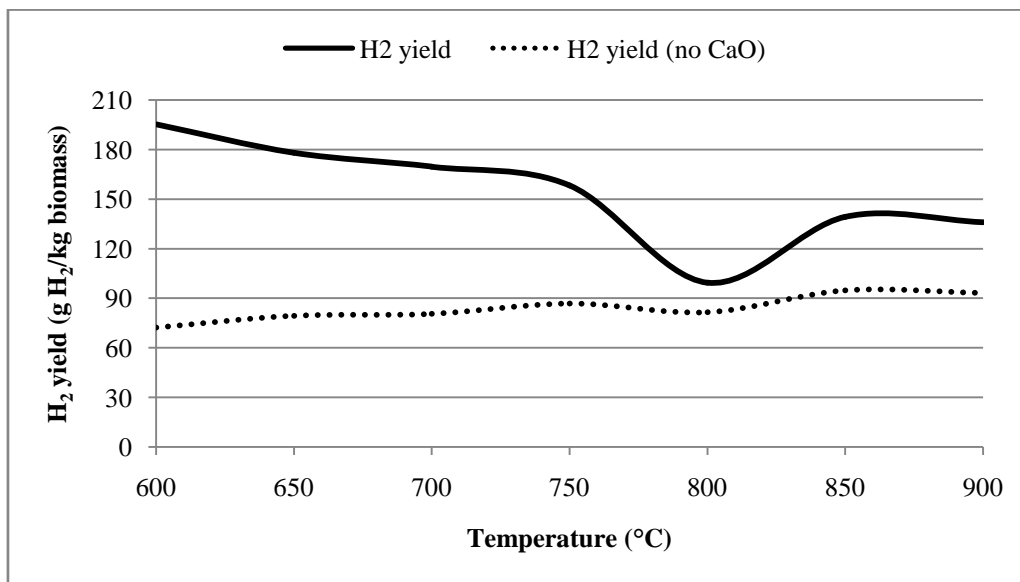


Figure 4.32: Effect of CO₂ adsorbent on H₂ yield*

* Data taken based on facet average at the “Outlet” line surface of the 2D domain of the gasifier.

CHAPTER 5

CONCLUSIONS AND RECOMMENDATIONS

5.1 Conclusion

The optimization of biomass fluidized bed gasifier with respect to different hydrodynamics and reaction parameters has been investigated in this work numerically using Fluent[®] software. Two models have been developed in Fluent[®] which are hydrodynamics and reaction model. The hydrodynamics model has been used to study the effect of steam inlet velocity, solid particle size and also height to diameter ratio (H/D) on solid fluidization in the fluidized bed gasifier. The aim of the study is to find the optimum condition that can give the best solid mixing in the gasifier. The reaction model has been used to study the effect of gasification temperature, steam to biomass ratio, and CO₂ adsorbent to the gas production from biomass gasification reaction. The aim of the study is to find the optimum reaction condition that can give the highest H₂ production from biomass gasification.

Based on the hydrodynamics model that has been developed and validated, it is observed that the difference in steam inlet velocity, solid particle size, and bed height to diameter ratio shows significant changes to the solid fluidization in the fluidized bed gasifier. As the steam inlet velocity increases, the size of bubbles forms in the bed also increases. At high steam inlet velocity, the formation of slugs tends to occur through the bed and this leads to poor solid mixing and fluidization in the gasifier. For the best performance of solid mixing in the fluidized bed gasifier, the most suitable steam inlet velocity for the system is ranging from 3-3.5 U_{mf} .

The study on the effect of solid particle size to the solid fluidization in the fluidized bed gasifier shows that as the solid particle size increases, it is more difficult for the steam to fluidize the bed a consequence, the bed becomes denser as the particle size increases. The best operating particle size for the system is 250 μm as this particle size gives the most uniform mixing through out the bed.

Height to diameter ratio of the solid bed also may affect the hydrodynamics inside the fluidized bed gasifier. The increase of height to diameter ratio does not give significant improvement to the solid fluidization in the bed. Therefore, keeping the bed height to diameter ratio minimum is much more favourable. From the simulation, it is observed that height to diameter ratio of 3 and below gives the best solid fluidization in the gasifier.

The reaction model that has been developed in Fluent[®] is used to predict H_2 production from biomass gasification reactions. The results obtained from simulation were then compared with the literature data and was found to be in good agreement. From the results obtained, it is observed that H_2 production increases as gasification temperature increases. This is because the endothermic gasification reaction is much favourable at higher temperature. The highest H_2 concentration and yield is obtained at a temperature of 850 $^\circ\text{C}$ which are 48 mol% and 94.75 g H_2/kg biomass.

The increase of steam to biomass ratio in the system improves H_2 yield and also carbon conversion of the fluidized bed gasifier. However, the increase of steam to biomass ratio higher than 2 will cause the increase in H_2O production from the gasifier, which will require additional separation system in order to improve product gas purity. The optimum steam to biomass ratio for biomass gasification system is observed to be at 2 because at this ratio, high concentration of H_2 and carbon conversion is obtained from the system.

CO₂ adsorbent helps to improve H₂ production from the gasifier. It is observed that H₂ concentration increases as adsorbent to biomass ratio increases from 0 to 1. The CO₂ production also decreases as adsorbent to biomass ratio increases. However, further increase of adsorbent to biomass ratio higher than ratio of 1 does not further reduce the CO₂ production because the minimum adsorption pressure has been reached in the gasifier. From the results obtained, it is observed that the optimum adsorbent to biomass ratio is 1. This is because at this ratio the highest H₂ concentration is obtained from biomass gasifier and this ratio is sufficient to reduce the CO₂ production from the gasifier.

CO₂ adsorption reaction is an exothermic reaction; therefore it is much favourable at lower temperature. Biomass gasification with in-situ CO₂ adsorption is normally operated at much lower temperature compared to the conventional biomass gasification process. From the simulation results, it is observed that biomass gasification with in-situ CO₂ adsorption is best to be operated at a temperature ranging from 600-750 °C. This is because at this range of temperature, high H₂ concentration and yield could be obtained. Overall, both H₂ concentration and yield increase as CO₂ adsorbent is added into the system.

5.2 Recommendation and future work

In this work, the kinetic data for biomass gasification reaction has been taken from the literature which produced the kinetic data from coal and other biomass combustion and gasification reaction. In order to improve the quality of product gas prediction from the gasifier it is recommended to use the kinetic data that is specifically developed from local biomass gasification reaction. For example kinetic data from actual gasification experimental data using TGA, micro-reactor or bench scale gasifier would be much more reliable than kinetic data from literature. Results of H₂ production from experimental data also could be used as model validation.

For the effect of in-situ CO₂ adsorption using CaO in the gasifier, further study could be done in order to improve findings and understanding more on the mechanism of CO₂ adsorption process. Detail particle surface reaction on CaO surface could be done in order to understand more the diffusion process of CO₂ into CaO pores and the limiting reactant that hinders the process.

Biomass is represented as pure carbon (C) in this current work. In order to resemble the actual biomass, it is best to use the empirical chemical formula for biomass which consists of C, H and O according to the actual biomass proximate and ultimate analysis.

Two different models have been successfully developed in these current works which are the hydrodynamics model and reaction model. For future work, the combination of these two models would give more significant representation of the actual biomass gasification process that occurs in the fluidized bed gasifier.

REFERENCES

- [1] N. H. Florin and A. T. Harris, "Enhanced hydrogen production from biomass with in situ carbon dioxide capture using calcium oxide sorbents," *Chemical Engineering Science*, vol. 63, pp. 287-316, 2008.
- [2] M. J. Hampen-Smith, P. Atanassova, J. Shen, P. Napolitano and J. Brewster, "Fuel reformer catalyst and absorbent materials", US Patent 7578986, August 25, 2009.
- [3] M. R. Mahishi, M. S. Sadrameli, S. Vijayaraghavan and Y. D. Goswami, "A novel approach to enhance the hydrogen yield of biomass gasification using CO₂ sorbent," *Journal of Engineering for Gas Turbines and Power*, vol. 130, pp. 1-8, 2008.
- [4] W. Wu, K. Kawamoto and H. Kuramochi, "Hydrogen-rich synthesis gas production from waste wood via gasification and reforming technology for fuel cell application," *Journal of Mater Cycles Waste Management*, vol. 8, pp. 70-77, 2006.
- [5] P. U. Foscolo, A. Germana, N. Jand and S. Rapagna, "Design and cold model testing of a biomass gasifier consisting of two interconnected fluidized bed," *Powder Technology*, vol. 173, pp. 179-188, 2007.
- [6] C. Pfeifer and H. Hofbauer, "Development of catalytic tar decomposition downstream from a dual fluidized bed biomass steam gasifier," *Powder Technology*, vol. 180, pp. 9-16, 2008.
- [7] S. Rapagna, N. Jand and P. U. Foscolo, "Catalytic gasification of biomass to produce hydrogen rich gas," *International Journal of Hydrogen Energy*, vol. 22, pp. 551-557, 1997.

- [8] P. McKendry, "Energy production from biomass (part 3): gasification technologies," *Bioresource Technology*, vol. 83, pp. 55-63, 2002.
- [9] A. Faaij, "Modern biomass conversion technologies," *Mitigation and Adaptation Strategies for Global Change*, vol. 11, pp. 343-375, 2006.
- [10] S. Kaneko, S. Sato, Y. Kobayashi, T. Kabata, K. Kobayashi, Y. Takeuchi, K. Takuda, A. Hashimoto, K. Shinoda, K. Takeno, S. Matsumoto, H. Ohta, T. Yamamoto, M. Sakai, T. Takegawa and Y. Seike, "Biomass gasification furnace and system for methanol synthesis using gas produced by gasifying biomass", US Patent 6991769 B2 ,January 31,2006.
- [11] R. J. Bender, J. P. Tomassi and F. Asplund, "Variable moisture biomass gasification heating system and method", US Patent 6485296 ,November 26,2002.
- [12] Y. Kalinci, A. Hepbasli and I. Dincer, "Biomass-based hydrogen production: A review and analysis," *International Journal of Hydrogen Energy*, vol. 34, pp. 8799-8817, 2009.
- [13] F. Miccio, K. Svoboda, J. Schosger and D. Baxter, "Biomass gasification in internal circulating fluidized beds: a thermodynamic predictive tool," *Korean Journal of Chemical Engineering*, vol. 25, pp. 721-726, 2008.
- [14] L. Shen, Y. Gao and J. Xiao, "Simulation of hydrogen production from biomass gasification in interconnected fluidized beds," *Biomass and Bioenergy*, vol. 32, pp. 120-127, 2008.
- [15] H. Inoue and M. Hario, "Method of biomass gasification", US 2004/0180971 A1 ,September 16,2004.
- [16] T. Steer,"Method for obtaining combustion gases of high calorific value", US Patent 7507266 ,March 24,2009.

- [17] S. Koppatz, C. Pfeifer, R. Rauch, H. Hofbauer, T. Marquard-Moellenstedt and M. Specht, "H₂ rich product gas by steam gasification of biomass with in situ CO₂ adsorption in a dual fluidized bed system of 8 MW fuel input," *Fuel Processing Technology*, vol. 90, pp. 914-921, 2009.
- [18] A. Ajilkumar, T. Sundararajan and U. S. P. Shet, "Numerical modeling of a steam-assisted tubular coal gasifier," *International Journal of Thermal Sciences*, vol. 48, pp. 308-321, 2009.
- [19] T. Marquard-Mollenstedt, P. Sichler, M. Specht, M. Michel, R. Berger, K. R. G. Hein, E. Hoftberger, R. Rauch and H. Hofbauer, "New approach for biomass gasification to hydrogen," in *2nd World Conference on Biomass for Energy, Industry & Climate Protection*, Rome, Italy, 2004.
- [20] S. S. Sadaka, A. E. Ghaly and M. A. Sabbah, "Two phase biomass air-steam gasification model for fluidized bed reactors: Part I-model development," *Biomass and Bioenergy*, vol. 22, pp. 439-462, 2002.
- [21] D. A. Nemtsov and A. Zabaniotou, "Mathematical modelling and simulation approaches of agricultural residue air gasification in a bubbling fluidized bed reactor," *Chemical Engineering Journal*, vol. 143, pp. 10-31, 2008.
- [22] M. B. Nikoo and N. Mahinpey, "Simulation of biomass gasification in fluidized bed reactor using ASPEN PLUS," *Biomass and Bioenergy*, vol. 32, pp. 1245-1254, 2008.
- [23] C. N. Lim, M. A. Gilbertson and A. J. L. Harrison, "Characterisation and control of bubbling behavior in gas-solid fluidised beds," *Control Engineering Practice*, vol. 17, pp. 67-79, 2009.
- [24] D. F. Fletcher, B. S. Haynes, F. C. Christo and S. D. Joseph, "A CFD based combustion model of an entrained flow biomass gasifier," *Applied Mathematical Modelling*, vol. 24, pp. 165-182, 2000.

- [25] C. Dupont, G. Boissonnet, J. Seiler, P. Gauthier and D. Schweich, "Study about the kinetic processes of biomass steam gasification," *Fuel*, vol. 86, pp. 32-40, 2007.
- [26] P. Weerachancai, M. Horio and C. Tangsathitkulchai, "Effects of gasifying conditions and bed materials on fluidized bed steam gasification of wood biomass," *Bioresource Technology*, vol. 100, pp. 1419-1427, 2009.
- [27] M. R. Mahishi and Y. D. Goswami, "An Experimental study of hydrogen production by gasification of biomass in the presence of a CO₂ sorbent," *International Journal of Hydrogen Energy*, vol. 32, pp. 2803-2808, 2007.
- [28] N. Florin and A. Harris, "Hydrogen production from biomass," *Environmentalist*, vol. 27, pp. 207-215, 2007.
- [29] Y. Wang and L. Yan, "CFD simulation on biomass thermochemical conversion," *International Journal of Molecular Sciences*, vol. 9, pp. 1108-1130, 2008.
- [30] A. Busciglio, G. Vella, G. Micale and L. Rizzuti, "Analysis of the bubbling behavior of 2D gas solid fluidized beds Part II. Comparison between experiments and numerical simulations via Digital Image Analysis Technique," *Chemical Engineering Journal*, vol. 148, pp. 145-163, 2009.
- [31] J. R. Grace and F. Taghipour, "Verification and validation of CFD models and dynamic similarity for fluidized beds," *Powder Technology*, vol. 139, pp. 99-110, 2004.
- [32] Anonymous "User's Guide, Fluent 6.3 Documentation", 2006.
- [33] Z. Deng, R. Xiao, B. Jin, H. Huang, L. Shen, Q. Song and Q. Ji, "Computational Fluid Dynamics Modeling of Coal Gasification in a Pressurized Spout-Fluid Bed," *Energy & Fuels*, vol. 22, pp. 1560-1569, 2008.

- [34] N. Reuge, L. Cadoret, C. Coufort-Saudejaud, S. Pannala, M. Syamlal and B. Caussat, "Multifluid Eulerian modeling of dense gas-solid fluidized bed hydrodynamics: Influence of the dissipation parameters," *Chemical Engineering Science*, vol. 63, pp. 5540-5551, 2008.
- [35] M. Muthu Kumar and E. Natarajan. , "CFD simulation for two-phase mixing in 2D fluidized bed", *International Journal of Advance Manufacturing Technology*, Special Issue, 2009, DOI: 10.1007/s00170-008-1875-9.
- [36] P. Ji, W. Feng and B. Chen, "Production of ultrapure hydrogen from biomass gasification with air," *Chemical Engineering Science*, vol. 64, pp. 582-592, 2009.
- [37] X. Wang, B. Jin and W. Zhong, "Three-dimensional simulation of fluidized bed coal gasification," *Chemical Engineering & Processing*, vol. 48, pp. 695-705, 2009.
- [38] B. Dou, V. Dupont and P. T. Williams, "Computational Fluid Dynamics Simulation of Gas-Solid Flow during Steam Reforming of Glycerol in a Fluidized Bed Reactor," *Energy & Fuels*, vol. 22, pp. 4102-4108, 2008.
- [39] M. Ye, J. Wang, M. A. van der Hoef and J. A. M. Kuipers, "Two-fluid modeling of Geldart A particles in gas-fluidized beds," *Particuology*, vol. 6, pp. 540-548, 2008.
- [40] F. Taghipour, N. Ellis and C. Wong, "Experimental and computational study of gas-solid fluidized bed hydrodynamics," *Chemical Engineering Science*, vol. 60, pp. 6857-6867, 2005.
- [41] I. Hulme, E. Clavelle, L. van der Lee and A. Kantzas, "CFD modeling and validation of bubble properties for a bubbling fluidized bed," *Industrial and Engineering Chemistry Research*, vol. 44, pp. 4254-4266, 2005.
- [42] J. Corella, J. Toledo and G. Molina, "Biomass gasification with pure steam in fluidized bed: 12 variables that affect the effectiveness of the biomass gasifier," *International Journal of Oil, Gas and Coal Technology*, vol. 1, pp. 194-207, 2008.

- [43] A. F. Kirkels and G. P. J. Verbong, "Biomass gasification: Still promising? A 30-year global review," *Renewable and Sustainable Energy Reviews*, vol. 15, pp. 471-481, 2011.
- [44] P. Basu, "Combustion and Gasification in Fluidized Beds", Boca Raton, Taylor & Francis Group, 2006.
- [45] W. B. Hauserman, "Relating catalytic coal or biomass gasification mechanism to plant capital cost components," in *Proceeding of the 10th World Hydrogen Energy Conference*, Cocoa Beach, FL, 1994.
- [46] R. C. Timpe, W. B. Hauserman, R. W. Kulas and B. C. Young, "Hydrogen production from fossil fuels and other regionally available feedstocks," in *Proceedings of the 11th World Hydrogen Energy Conference*, Stuttgart, Germany, 1996.
- [47] J. L. Cox, A. Y. Tonkovich, D. C. Elliot, E. G. Baker and E. J. Hoffman, "Hydrogen from biomass: A fresh approach," in *Proceedings of the Second Biomass Conference of the Americas*, Portland, Oregon, 1995.
- [48] S. Lin, M. Harada, Y. Suzuki and H. Hatano, "Hydrogen production from coal by separating carbon dioxide during gasification," *Fuel*, vol. 81, pp. 2079-2085, 2002.
- [49] T. Hanaoka, T. Yoshida, S. Fujimoto, K. Kamei, M. Harada and Y. Suzuki, "Hydrogen production from woody biomass by steam gasification using a CO₂ sorbent," *Biomass and Bioenergy*, vol. 28, pp. 63-68, 2005.
- [50] S. Fujimoto, T. Yoshida, T. Hanaoka, Y. Matsumura, S. Y. Lin and T. Minowa, "A kinetic study of in situ CO₂ removal gasification of woody biomass for hydrogen production," *Biomass and Bioenergy*, vol. 31, pp. 556-562, 2007.
- [51] Y. Behjat, S. Shahhosseini and H. S. Hashemabadi, "CFD Modeling of Hydrodynamic and heat transfer in fluidized bed reactors," *International Communications in Heat and Mass Transfer*, vol. 35, pp. 357-368, 2008.

- [52] M. J. V. Goldschmidt, R. Beetstra and J. A. M. Kuipers, "Hydrodynamic modelling of dense gas-fluidised beds: comparison and validation of 3D discrete particle and continuum models," *Powder Technology*, vol. 142, pp. 23-47, 2004.
- [53] N. G. Deen, M. van Sint Annaland and J. A. M. Kuipers, "Detailed computational and experimental fluid dynamics of fluidized beds," *Applied Mathematical Modelling*, vol. 30, pp. 1459-1471, 2006.
- [54] G. A. Bokkers, M. van Sint Annaland and J. A. M. Kuipers, "Mixing and segregation in a bidisperse gas-solid fluidised bed: a numerical and experimental study," *Powder Technology*, vol. 140, pp. 176-186, 2004.
- [55] L. Shen, J. Xiao, F. Niklasson and F. Johnsson, "Biomass mixing in a fluidized bed biomass gasifier for hydrogen production," *Chemical Engineering Science*, vol. 62, pp. 636-643, 2007.
- [56] Y. Zhang, B. Jin and W. Zhong, "Experimental investigation on mixing and segregation behavior of biomass particle in fluidized bed," *Chemical Engineering & Processing*, vol. 48, pp. 745-754, 2009.
- [57] K. S. Lim, J. X. Zhu and J. R. Grace, "Hydrodynamics of gas-solid fluidization," *International Journal of Multiphase Flow*, vol. 21, pp. 141-193, 1995.
- [58] D. Harrison, J. F. Davidson and J. W. de Kock, "On the nature of aggregative and particulate fluidisation," *Transactions of the Institution of Chemical Engineers*, vol. 39, pp. 202-211, 1961.
- [59] P. M. Lv, Z. H. Xiong, J. Chang, C. Z. Wu, Y. Chen and J. X. Zhu, "An experimental study on biomass air-steam gasification in fluidized bed," *Bioresource Technology*, vol. 95, pp. 95-101, 2004.
- [60] W. P. Walawender, D. A. Hoveland and L. T. Fan, "Steam gasification of pure cellulose. 1. Uniform temperature profile," *Ind. Eng. Chem. Process Des. Dev.*, vol. 24, pp. 813-817, 1985.

- [61] N. Gao, A. Li, C. Quan and F. Gao, "Hydrogen-rich gas production from biomass steam gasification in an updraft fixed-bed gasifier combined with a porous ceramic reformer," *International Journal of Hydrogen Energy*, vol. 33, pp. 5430-5438, 2008.
- [62] B. Acharya, A. Dutta and P. Basu, "An investigation into steam gasification of biomass for hydrogen enriched gas production in presence of CaO," *International Journal of Hydrogen Energy*, vol. 35, pp. 1582-1589, 2010.
- [63] M. R. Mahishi. "Theoretical and experimental investigation of hydrogen production by gasification of biomass.", Ph.D Thesis, University of Florida, 2006.
- [64] J. Corella, M. P. Aznar, J. Delgado and E. Aldea, "Steam gasification of cellulosic waste in a fluidised bed with downstream vessels," *Industrial and Engineering Chemistry Research*, vol. 30, pp. 2252-2262, 1991.
- [65] J. Herguido, J. Corella and J. Gonzalez-Saiz, "Steam gasification of lignocellulosic residues in a fluidised bed at a small pilot scale. Effect of type of feedstock," *Industrial and Engineering Chemistry Research*, vol. 31, pp. 1274-1282, 1992.
- [66] S. Turn, C. Kinoshita, Z. Zhang, D. Ishimura and J. Zhou, "An experimental investigation of hydrogen production from biomass gasification," *International Journal of Hydrogen Energy*, vol. 23, pp. 641-648, 1998.
- [67] B. Balasubramanian, A. L. Ortiz, S. Kaytakoglu and D. P. Harrison, "Hydrogen from methane in a single-step process," *Chemical Engineering Science*, vol. 54, pp. 3543-3552, 1999.
- [68] R. W. Hughes, D. Y. Lu, E. S. Anthony and A. Macchi, "Design, process simulation and construction of an atmospheric dual fluidized bed combustion system for in situ CO₂ capture using high-temperature sorbents," *Fuel Processing Technology*, vol. 80, pp. 1523-1531, 2005.

- [69] L. Yu, J. Lu, X. Zhang and S. Zhang, "Numerical Simulation of the Bubbling Fluidized Bed Coal Gasification by Kinetic Theory of Granular Flow (KTGF)," *Fuel*, vol. 86, pp. 722-734, 2007.
- [70] O. Gryczka, S. Heinrich, N. G. Deen, M. van Sint Annaland, J. A. M. Kuipers, M. Jacob and L. Morl, "Characterization and CFD-modeling of the hydrodynamics of prismatic spouted bed apparatus," *Chemical Engineering Science*, vol. 64, pp. 3352-3375, 2009.
- [71] R. Panneerselvam, S. Savithri and G. D. Surender, "CFD Simulation of hydrodynamics of gas-liquid-solid fluidised bed reactor," *Chemical Engineering Science*, vol. 64, pp. 1119-1135, 2009.
- [72] C. Bin, W. Cong, W. Zhiwei and G. Liejin, "Investigation of gas-solid two-phase flow across circular cylinders with discrete vortex method," *Applied Thermal Engineering*, vol. 29, pp. 1457-1466, 2009.
- [73] M. A. van der Hoef, M. van Sint Annaland and J. A. M. Kuipers, "Computational fluid dynamics for dense gas-solid fluidized beds: a multi-scale modeling strategy," *Chemical Engineering Science*, vol. 59, pp. 5157-5165, 2004.
- [74] M. A. van der Hoef, M. van Sint Annaland and J. A. M. Kuipers, "Computational fluid dynamics for dense gas-solid fluidized beds: A multi-scale modeling strategy," *China Particuology*, vol. 3, pp. 69-77, 2005.
- [75] A. Boemer, H. Qi and U. Renz, "Verification of Eulerian simulation of spontaneous bubble formation in a fluidized bed," *Chemical Engineering Science*, vol. 53, pp. 1835-1846, 1998.
- [76] A. Boemer, H. Qi and U. Renz, "Eulerian simulation of bubble formation at a jet in a two-dimensional fluidized bed," *International Journal of Multiphase Flow*, vol. 23, pp. 927-944, 1997.

- [77] L. Huilin, Z. Yunhua, J. Ding, D. Gidaspow and L. Wei, "Investigation of mixing/segregation of mixture particles in gas-solid fluidized beds," *Chemical Engineering Science*, vol. 62, pp. 301-317, 2007.
- [78] S. Gerber, F. Behrendt and M. Oevermann, "An Eulerian modeling approach of wood gasification in a bubbling fluidized bed reactor using char as a bed material," *Fuel*, vol. 89, pp. 2903-2917, 2010.
- [79] D. J. Patil, M. van Sint Annaland and J. A. M. Kuipers, "Critical Comparison of hydrodynamics models for gas-solid fluidized bed-part I: bubbling gas-solid fluidized beds operated with a jet," *Chemical Engineering Science*, vol. 60, pp. 57-72, 2004.
- [80] D. J. Patil, M. van Sint Annaland and J. A. M. Kuipers, "Critical comparison of hydrodynamic models for gas-solid fluidized bed-part I: bubbling gas-solid fluidized beds operated with a jet," *Chemical Engineering Science*, vol. 60, pp. 57-72, 2004.
- [81] E. Simsek, B. Brosch, S. Wirtz, V. Scherer and F. Kruell, "Numerical simulation of grate firing systems using a coupled CFD/discrete element method (DEM)," *Powder Technology*, 2009.
- [82] M. R. Mahishi and Y. D. Goswami, "Thermodynamic optimization of biomass gasifier for hydrogen production," *International Journal of Hydrogen Energy*, vol. 32, pp. 3831-3840, 2007.
- [83] T. Cebeci, J. P. Shao, F. Kafyeke and E. Laurendeau, "Computational Fluid Dynamics for Engineering", Long Beach California, Horizons Pub. Inc. Berlin Springer, 2005.
- [84] C. J. Chen, R. Bernatz and K. D. Carlson, "The Finite Analytical Method in Flows and Heat Transfer", New York, Taylors and Francis, 2000.
- [85] J. R. Grace, "Handbook of Multiphase Systems", Washington D.C., Hemisphere, 1982.

- [86] D. Gidaspow, R. Bezburuah and J. Ding, "Hydrodynamics of circulating fluidized beds, kinetic theory approach," in 7th Engineering Foundation Conference on Fluidization, 1992, pp. 75-82.
- [87] C. K. K. Lun, S. B. Savage, D. J. Jeffrey and N. Chepuruiy, "Kinetic theories for granular flow: Inelastic particle in Couette flow and slightly inelastic particles in a general flow field," Journal of Fluid Mechanics, vol. 140, pp. 223-256, 1984.
- [88] Anonymous "Chemical reaction study using CFD," in Fluent 6.2 User's Guide, pp. (12-1)-(17-18)2003.
- [89] T. Sheppard. (2010,December 6), "Equilibria",
<http://www.blobs.org/science/article.php?article=25>.
- [90] Anonymous (2010,December/06)," "Smart" Clothes",
<http://itech.dickinson.edu/chemistry/?p=420>.
- [91] J. Smith. (2010,December/06),"Building of a heterogeneous catalysis reactor",
http://www.che.sc.edu/centers/RCS/smith/jake_smith_reactor_page.html.
- [92] J. Corella and A. Sanz, "Modeling circulating fluidized bed biomass gasifiers. A pseudo-rigorous model for stationary state," Fuel Processing Technology, vol. 86, pp. 1021-1053, 2005.
- [93] J. Gonzalez-Saiz. "Advance in biomass gasification in fluidized bed", PhD Thesis, University of Saragossa, 1988.
- [94] C. Fushimi, K. Araki, Y. Yamaguchi and A. Tsutsumi, "Effect of heating rate on steam gasification of biomass: 1. Reactivity of char," Industrial and Engineering Chemistry Research, vol. 42, pp. 3922-3928, 2003.
- [95] Y. C. Choi, X. Y. Li, T. J. Park, J. H. Kim and J. G. Lee, "Numerical study on the coal gasification characteristic in an entrained flow coal gasifier," Fuel, vol. 80, pp. 2193-2201, 2001.

- [96] B. W. Brown, L. D. Smoot, P. J. Smith and P. O. Hedman, "Measurement and prediction of entrained flow gasification process," *AICHE Journal*, vol. 34, pp. 435, 1988.
- [97] R. Govin and J. Shah, "Modeling and simulation of an entrained flow coal gasifier," *AICHE Journal*, vol. 30, pp. 79, 1984.
- [98] H. Liu and B. M. Gibbs, "Modeling NH₃ and HCN emission from biomass circulating fluidized bed gasifiers," *Fuel*, vol. 82, pp. 1591-1604, 2003.
- [99] A. Irfan and G. Dogu, "Calcination kinetics of high purity limestones," *Chemical Engineering Journal*, vol. 83, pp. 131-137, 2001.
- [100] C. R. Milne, G. R. Silci=ox, D. W. Pershing and D. A. Kirchgessner, "Calculation and sintering models for applications of high temperature short time sulfation of calcium based sorbent," *Industrial and Engineering Chemistry Research*, vol. 29, pp. 139-152, 1990.

